2023

EUTROPHICATION ON TWIN LAKES: APPLYING A PHOSPHORUS BUDGET AND SHORELINE SURVEYS TO ASSESS CURRENT & HISTORICAL LAKE HEALTH

Tyler K. LeMahieu
Michigan Technological University, tklemahi@mtu.edu

EUTROPHICATION ON TWIN LAKES: APPLYING A PHOSPHORUS BUDGET AND SHORELINE SURVEYS TO ASSESS CURRENT & HISTORICAL LAKE HEALTH

By

Tyler K. LeMahieu

A THESIS

Submitted in partial fulfillment of the requirements for the degree of

MASTER OF SCIENCE

In Environmental Engineering

MICHIGAN TECHNOLOGICAL UNIVERSITY

2023

This thesis has been approved in partial fulfillment of the requirements for the Degree of MASTER OF SCIENCE in Environmental Engineering.

Department of Civil, Environmental, and Geospatial Engineering

Thesis Co-Advisor:	*Dr. Cory McDonald*
Thesis Co-Advisor:	*Dr. Veronica Webster*
Committee Member:	*Dr. Noel Urban*
Committee Member:	*Dr. Fengjing Liu*
Committee Member:	*Mr. Robert Gubernick*
Department Chair:	*Dr. Audra Morse*

1 TABLE OF CONTENTS

Contents

2 ACKNOWLEDGEMENTS

A kind and sincere thank you to all those who helped make this work happen. Thank you, Mom, Dad, and Zach. Thank you to my dear friends and community at Michigan Tech who have so often stuck closer than a brother. Thank you to Nathaniel, Allie, Ben, Henry, Laura, Chris, Zoe, Zach, Nadia, and Ben for your help in collecting data for this project. Thank you to my advisors and committee, along with those others I've asked questions of throughout this process. Thank you to my Lord for equipping, growing, and sustaining me.

The author would like to acknowledge and thank private donors, Michigan Tech's Civil, Environmental, and Geospatial Engineering Department, and the National Science Foundation Graduate Research Fellowship Program for funding support.

This material was supported by the National Science Foundation Graduate Research Fellowship Program under Grant No. (NSF grant #2205026). Any opinions, findings, and conclusions or recommendations expressed in this material are those of the author(s) and do not necessarily reflect the views of the National Science Foundation.

3 LIST OF FIGURES

4 LIST OF TABLES

5 ABSTRACT

The Twin Lakes system, a series of lakes including Lake Gerald and Lake Roland, was historically categorized as oligotrophic but is now mesotrophic having experienced cultural eutrophication. A mass balance phosphorus budget model was constructed for the Twin Lakes system in Houghton, Co. Michigan for the 2022 stratified season. Additional spatial insights were gleaned through a survey of shoreline water quality, which corroborated the model results. The lakes currently experience substantial depletion of hypolimnetic dissolved oxygen during late summer stratification. A budget reveals approximately 22% (6.6 kg) of the current 29.5 kg total phosphorus inputs to Twin Lakes (during the stratified period) are from sources not clearly attributable to natural processes and are likely attributable to nutrient inputs from the primarily residential shoreline developments. Modeling suggests the lakes were indeed oligotrophic, and that the system would be relatively responsive to loading reductions. Substantial reductions to that "residual load" (in excess of 64%) would be required to return the system to an oligotrophic state. Shoreline surveys support the hypothesis of shoreline development sources nutrient pollution. The performed work brought to question the broad applicability of methods for using optical brightening agents (OBAs) as a tracer of septic leakage. The development of heatmaps as visual tools proved useful for understanding drivers of lake water quality spatially. The lakes show distinct regions of elevated conductivity from the largest contributing tributary, whose watershed bisects a state highway corridor. This suggests road salt contamination to Twin Lakes. This work serves as a case study examination of eutrophication and phosphorus budget for a naturally low productivity system of lakes in series in the Great Lakes region.

6 INTRODUCTION

6.1 Twin Lakes History & Background

Lake Gerald and Lake Roland ("Twin Lakes") are in Elm River Township within Houghton County in Michigan's Upper Peninsula (see figure 6-1). The area of Lake Roland is 111 hectares and Lake Gerald is 148 hectares, each with a maximum depth of approximately 12.2 meters. The southwest lobe of Lake Gerald is a 33-hectare basin referred to as Little Lake Gerald with a maximum depth of about 6.2 meters. The lakes are connected by a small navigable channel. Twin Lakes is an important cultural and recreational resource. Twin Lakes State Park is located on the shore of Lake Roland. The 2744.1-hectare watershed is primarily forested (Figure 6-2). The system drains out of Lake Roland via the Misery River, and lake levels are regulated at the lake's outlet by a rail-weir system; the lake surface elevation ranges between 361.63 and 362.11 meters AMSL (Wright, 2015).

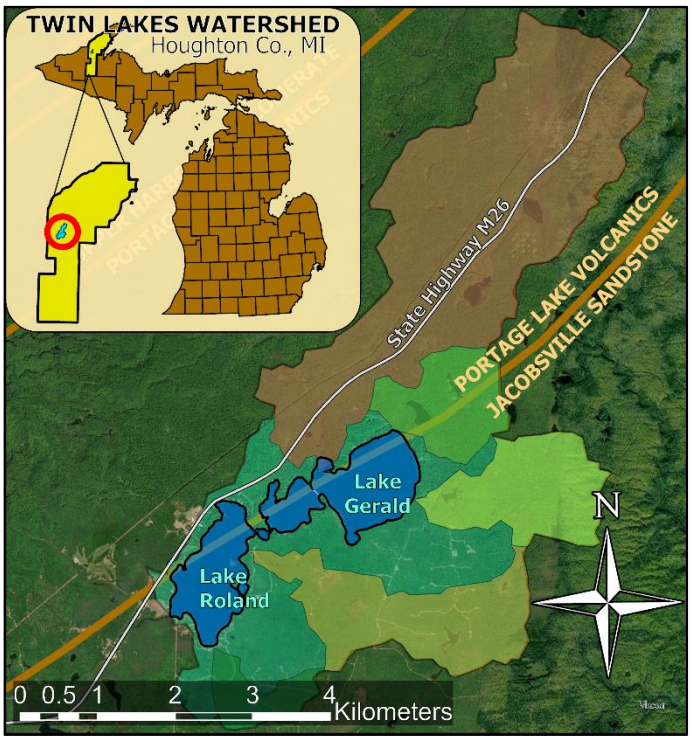

Figure 6-1: Watersheds and bedrock geology map of the Twin Lakes area (EGLE, 2022a; MDNR, 2022).

The lakes formed following glacial retreat over the junction of two geologic formations: The primarily basaltic Portage Lake Volcanics and Jacobsville Sandstone formations (see

figure 6-1) (Madison, 2019; MDNR, 2022). The bedrock material and glacial till overlying bedrock are both low in primary nutrients and the area was historically, and is today heavily forested (Madison, 2019; NLCD, 2016). The area saw substantial logging in the early 1900s, giving way to the state park's establishment sometime before 1931 (Madison, 2019; NETRONLINE, 2022). Recreational development of the area with seasonal homes and cabins increased in the 1940s through the 1960s, with further development continuing today (Madison, 2019).

Limnologically, Twin Lakes is a temperate dimictic system, meaning the lakes completely mix twice per year – once during fall cooling and once during spring warming (Chapra, 2008). During summer stratification, a mixed warm-water layer (epilimnion) forms over top of the bottom cold-water layer (hypolimnion), divided by a depth at which no mixing occurs and a sharp temperature gradient is observed (thermocline) (Chapra, 2008). Prior to 1970, the Twin Lakes system was documented as oligotrophic, meaning low in biological productivity and characterized by low nutrients levels, clear water, and sparse vegetation (Madison, 2019, 2022). In these systems algal blooms, dissolved oxygen (DO) deficits, and fish kills are not to be expected (Chapra, 2008; Schlesinger & Bernhardt, 2013). Additionally, in temperate cold-water oligotrophic lakes, a relatively oxygenated hypolimnion creates a cool sanctuary for cold-water fish in the summer months (Chapra, 2008; EGLE, 2006; Schlesinger & Bernhardt, 2013). Since 1970, however, the lakes have become mesotrophic (moderately productive) through the process of eutrophication. As a natural process in the lifecycle of a lake, eutrophication can take place over thousands of years (Chapra, 2008). Cultural eutrophication, or the

rapid acceleration of this process by anthropogenic influence, is common in lakes around the world today and is a likely cause for the change in water quality at Twin Lakes (Chapra, 2008; Schlesinger & Bernhardt, 2013).

Evidence for eutrophication is provided by the historical fisheries management of the lake. The lakes have been managed as a two-story fishery in the past, with rainbow trout, walleye, splake, and lake trout being stocked by the DNR; however, the rainbow trout and splake populations have not been sustained recently, in part due to declining water quality in the lakes, and the lake trout have persisted only with annual winter adult stocking (Madison, 2019, 2022). Since the early 2000s, heavy aquatic vegetation growth (*Chara* and *Elodea*) has been documented throughout the lakes, and isolated fish-kills have been observed in bays and coves (Madison, 2019, 2022). The lakes do still support a high-quality warm-water panfish fishery, as was documented in the first survey of the lake in 1925 (Madison, 2019). Previous water quality data on the lakes is sparse, but additional 2006 data from the USGS Michigan Water Science Center showed significant DO depletion in the hypolimnion, moderate nutrient levels in the lake, and elevated phosphorus levels in the hypolimnion indicating sediment phosphorus release (internal loading), all symptoms of eutrophication (Chapra, 2008; USGS, 2006).

Typical causes of cultural eutrophication include nutrient-rich agricultural runoff, industrial activity and discharges, increased erosion, lawn fertilizers, and nutrient-containing wastewater discharges which include human waste, detergents, food material, etc. (Boardman, Danesh-Yazdi, Foufoula-Georgiou, Dolph, & Finlay, 2019; McCrackin

et al., 2018). The Twin Lakes watershed contains no agriculture or industry, ruling out those influences. Less than 5% of the watershed is developed (see figure 6-2), though this development is generally clustered on the shores of the lakes. Most of these developments have some cleared areas, mown lawns, and a cottage/cabin/house present. This makes erosion, lawn fertilizers, and waste discharges likely pertinent factors in the eutrophication of the lakes. Areas of shoreline are still being cleared for development and most existing developments have lawns with little or no buffer at the shoreline (though lawn care practices certainly vary). Lake Roland (at 14.9 developments/km of shoreline) is generally more developed than Lake Gerald (13.1 developments/km). On Lake Gerald, the Little Lake Gerald (the furthest downstream basin) is the most developed individual basin (17.1 developments/km) while big Lake Gerald (10.5 developments/km) is far less developed than the rest of the lake system. Appendix A shows where developments are located on the lakes in greater detail.

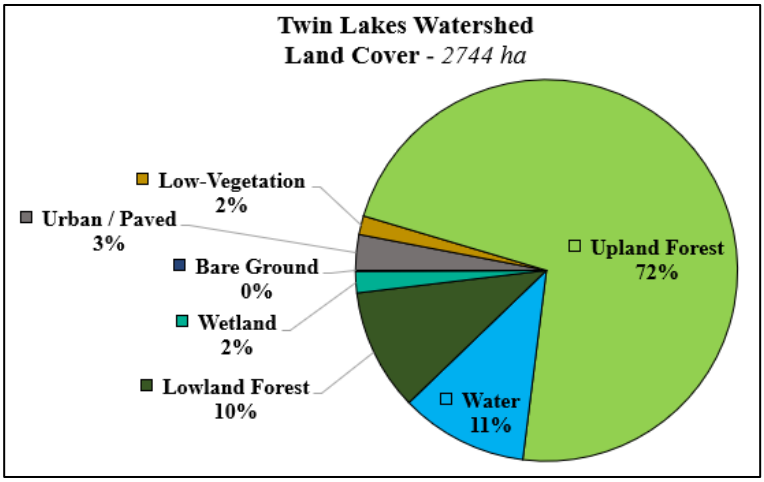

Figure 6-2: Broad landcover of Twin Lakes watershed (NLCD, 2016).

For Twin Lakes in particular, failing or poorly maintained septic tanks are worthy of consideration as a nutrient source. Typical modern septic tank installations have a service life of 15-40 years with proper maintenance (Dersch, 2017; EPA, 2022; Graham, 2022).

No sewer service is present near Twin Lakes and almost all residences and cabins likely have a septic systems; therefore, any septic tanks installed with development before ~1983 are likely past service life. Additionally, older tank installations were likely placed nearer to shorelines than current installations, and septic tanks and drain fields are commonly not maintained making premature failure likely (Graham, 2022). Based on Western UP health department data, at least 9 septic systems are located in low-lying near lake zones (Wright, 2015). The Natural Resource Conservation Service (NRCS) Web Soil Survey (WSS) septic field absorption fields suitability layer ranks all soils at Twin Lakes as "Very Limited," (NRCS, 2022). This indicates that soil features are present which impede effective septic leachate sorption which, "cannot be overcome without major soil reclamation, special design, or expensive installation procedures," and that "poor performance and high maintenance," can be expected for these systems (NRCS, 2022).

Twin Lakes, as a naturally low-nutrient lake system with a recent history of development which includes no agriculture, makes an interesting candidate for study. Sources of eutrophication are limited and the relatively undeveloped nature of the watershed provides an excellent opportunity for assessing pre-development lake conditions. Further, the future of the lakes has very real implications for management decisions and lake users, making examination of Twin Lakes metabolism timely. Study of Twin Lakes might serve as a good case study, applicable to other forested lakes in the region or lakes in series.

6.2 Project Goals

This work aims to understand the current water quality in Twin Lakes, to identify stressors to the system, and to provide insight and direction for stakeholders and managers of the lakes. The work seeks to produce a seasonal water and phosphorus budget identifying and quantifying phosphorus sources and sinks. The research also involves collection of shoreline survey data to identify spatial variation in the lakes and likely nutrient loading sources. The study attempts to describe and understand the Twin Lakes system more fully, enabling effective holistic management into the future for recreational use, fishery management, residential interest, lake health, and community development.

Specific project goals include the following:

1) Characterize current and historical nutrient loading to the system

2) Identify any significant current sources of nutrient pollution

3) Establish a phosphorus loading goal to return the lakes to historical oligotrophic status

4) Provide applied management insight for lake managers and stakeholders

7 METHODS

7.1 Data Sources & Processing:

7.1.1 Elevation Data:

Topographic data for the Twin Lakes area were obtained from the US Geological Survey (USGS) and Michigan's Department of Environment, Great Lakes, and Energy (EGLE). One-third arc-second digital elevation model (DEM) files for the entire Misery River watershed and surrounding area were obtained from the National Map GIS Data Delivery Application (USGS, 2022). For a large portion of the Twin Lakes watershed, 2-foot resolution LIDAR was provided by EGLE staff as a DEM (Hanson, 2022).

Accurate bathymetric data (1-foot contours) were obtained from the Navionics® corporation online maps (Garmin, 2022). These maps are created by collection of data from recreational users of Navionics® GPS-enabled depth finder systems which send back locations and depths to the Navionics® corporation. Verbal permission from Navionics® was granted to use their publicly available online maps for this work, but no spatial source data was provided. Therefore, the online contours were gathered by printing the webpage to PDFs at the highest resolution available in the internet browser until all the lake system had been covered. These PDFs were mosaiced in Adobe Photoshop, and the contour lines were extracted to a PNG format. These PNG contour lines were imported and georeferenced in ArcGIS Pro and subsequently converted to vector line segments. These line segments were manually checked and corrected for short circuits and errors. Each line segment was assigned its appropriate depth as an attribute before conversion to a point layer. This pseudo-point-cloud was used to generate a DEM

surface for the lakebed bathymetry. Contours were generated from this DEM and backchecked to the Navionics® map contours image to verify the efficacy of this data processing method. The DEM was then converted to metric depths for further analysis. Circa 1937 bathymetric maps of the Twin Lakes system were available in PDF form from the Michigan Department of Natural Resources (MDNR), which were additionally used for general reference (MDNR, 1937).

A depth-area-volume relationship for each lake was constructed for 1-meter intervals by generation of a shelled polygon contour map for each lake in ArcGIS Pro. The average area (m^2) between each shell was multiplied by the depth distance between each shell (1 meter, except 0.192 meters between 12- & 12.192-meter depths at the lake bottom) to obtain the volume in each depth segment. This relationship was used to verify later analyses of the water budget, and to define lake volumes, the layers of each lake, and the Twin Lakes system overall. Appendix B contains a bathymetric map of Twin Lakes and depth-area-volume relationships for the lakes.

7.1.2 Land Use, Soils, Geology, & Groundwater:

Land use & cover for the Twin Lakes watershed and surrounding area was obtained from the 2019 USGS National Land Cover Database (NLCD) to 30-meter resolution in raster format (NLCD, 2016). Soils data were obtained in vector polygon form for the Twin Lakes watershed and surrounding area from the National Soil Conservation Service (NRCS) Web Soil Survey (NRCS, 2022). Soil data included soil type, hydrologic classification, texture, and designated “Septic Tank Absorption Fields” suitability class

among other features, and are described and discussed where appropriate. Quaternary Geology maps and Glacial Land Systems maps were obtained from EGLE's open GIS data portal, and Bedrock Geology maps were obtained from MDNR's open GIS data portal (EGLE, 2022a; MDNR, 2022). The land substrate is composed of glacial till and alluvium overlying the bedrock boundary of Jacobsville Sandstone to the south and east with the Portage Lake Volcanics to the north and west of the lakes.

Approximate groundwater depths surrounding the lakes were acquired through local well logs obtained from EGLE's online Water Well Viewer mapping tool (EGLE, 2022b). All area well logs were downloaded and a point layer was created to best represent each well's location. Sometimes the online mapper point was used, while other times the point was placed elsewhere manually due to the well log narrative or visibility of the wellhead. The static water depth was subtracted from the LIDAR elevation at the point to provide a groundwater elevation. Using linear interpolation between each well log point (n=78), a groundwater elevation raster was produced. This is used for general reference only and is only applicable near the lakes' shore.

7.1.3 Parcel Ownership, Septic, & Development History:

The Elm River Township property ownership records are maintained by Houghton Co. through a third-party firm who, with permission from Houghton Co., provided the parcel GIS layer for this work (Coleman, 2022). Septic records, which are maintained separately by the Western UP Health Department, were not obtained. Rather, septic systems of note were identified with data from a 2015 hydrologic study by OHM consultants, which

provided locations of near-shore and low-lying septic systems on the Twin Lakes parcels (Wright, 2015). The developmental history of the Twin Lakes shoreline was obtained by examination of historical imagery from 1938-2020 via the "Historic Aerials" website viewer (NETRONLINE, 2022). In a GIS layer, polygons were drawn to capture the regions of newly developed shoreline between each aerial image date.

7.1.4 Additional Site-Specific Data Sources:

Historical water quality data for Twin Lakes is generally sparse. Monitoring by USGS occurred twice in 2006 (April & August) recording temperature, DO, pH, and conductivity through the water column at the deepest point of Lake Roland (USGS, 2006). A limnology course at Michigan Technological University visited "Twin Lakes Bog" for laboratory exercises intermittently from 1979 through 2002, collecting some variable combination of temperature, DO, pH, and conductivity through the water column during the September-October period (Urban, 2022). Based on examination of depth sampled, stratification depth, and narrative descriptions in this data "Twin Lakes Bog" is almost certainly Little Lake Gerald.

Other groups having studied the lakes include the MDNR and OHM Advisors (on behalf of the Houghton County Drain Commissioner). Fisheries studies have been conducted historically by the MDNR and a summary of the history of the Twin Lakes fishery proved useful for bounding baseline conditions on the lakes and the early designation of the lakes as oligotrophic (Madison, 2019). The OHM "Lake Level Study for Twin Lakes," sought to identify typical water levels for the lakes based on landscape hydrology

and to provide alternative analysis and hydrologic modeling for various lake-level control options (Wright, 2015). This report (and the subsequent adoption of its recommendations) provides useful insight into the system's hydrology and the impact and consideration for nearshore structures (e.g. septic drain fields).

Also noteworthy is the narrative accounts of local residents heard during the field work for this study. While onsite, many long-time residents and local workers provided perspectives and historical accounts into the fishery, management of lake levels, recreation, development, vegetation, and water quality of the Twin Lakes system. These accounts came from individuals who cared for the lakes deeply and wanted to see them maintained at their best for a wide variety of values collectively. These perspectives, gained from many years spent on Twin Lakes, helped to corroborate and inform the observations and conclusions from both the 2022 field season and the other data sources applied to this work.

7.2 Stream Gauging & Water Budget:

7.2.1 Stream Gauging

Stream gauges were installed both at the direct outlet of Twin Lakes under the Emily Lake Road bridge (south end of Twin Lakes on figure 7-1), and on the largest inflowing tributary where it crosses highway M-26 (north of Twin Lakes on figure 7-1). Both gauging locations are on the Misery River and were maintained from May 4 (M-26 site) and May 17 (outlet bridge site) through November 3, 2022. The gauging stations consisted of water level loggers (Hobo U-20) recording temperature and pressure at ten-minute intervals. The locations of these gauges were recorded via GPS (Garmin Astro 320) and visited every 1 to 3 weeks to offload data and measure flow and depth directly (15 visits).

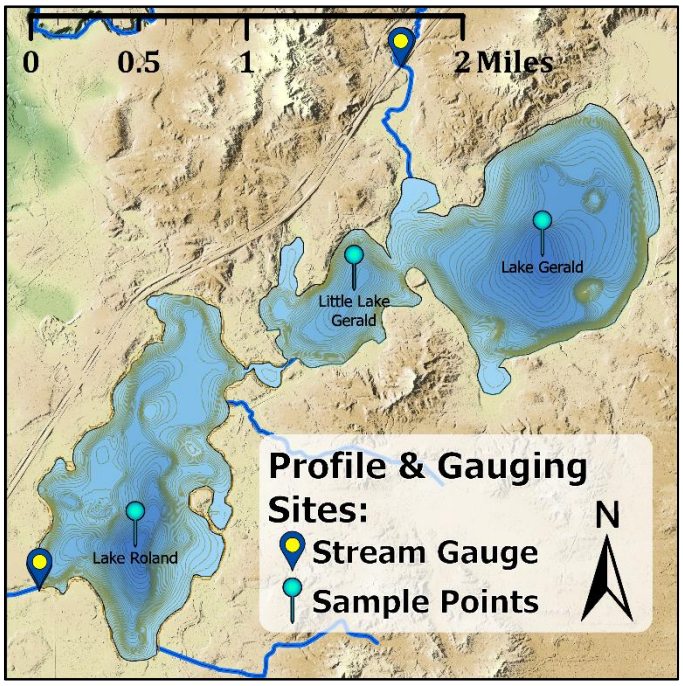

Figure 7-1: Sites of stream gauging & sampling, and lake profiles & at-depth sampling

Flow measurement was measured using a pygmy flowmeter (Rickly brand) and current meter digitizer (Aqua CMD 102-003). The following standard method of flow measurement was utilized when flow was sufficient to turn pygmy flow meter in crossing outlets. Flow velocity was recorded at between five and seven locations in the crossing, noting water depth, lateral location of test (distance from river-right), time of

measurement (40 to 100 s), number of pygmy flow meter rotations, and CMD output velocity (m/s). The average velocity between measurement at 20% and 80% of depth was applied to that proportional area of the cross section (Turnipseed, 2010). The flow for each section of the cross-section was summed to provide total flow. During low-flow conditions, this method was not always possible, and the specific alternative methods are noted for each site below.

The gauge of the Misery River inlet was located at the crossing of the Misery River with highway M-26, directly upstream of the wetland complex through which the Misery River flows, about 650 m before meeting Lake Gerald properly. A staff gauge was placed at the outlet of the bottomless concrete box culvert at the crossing, with the zero-point level to the streambed, and the submerged level logger set in a wire cage recording at the zero-depth point. The level logger in the air was affixed to the trunk of a nearby tree, which was above any water elevation experienced and recorded ambient atmospheric pressure and temperature. Survey involved recording the length of the culvert at the invert, and elevations of the following (via optical level): culvert outlet opening cross section, submerged level logger (base of staff gauge), various control points. The water depth and discharge values from site visits were used to construct a stage-discharge relationship, which provided a continuous record discharge (10-minute interval). The submerged level logger malfunctioned from 8/23/22 to 9/10/22, resulting in a data gap. Due to no notable rain events during this period and bounding low-flow conditions, an 18-day period of sustained low flow from early August was substituted for this period.

During low-flow conditions at the M-26 culvert, flow was measured at a constriction in the channel about 10 m downstream of culvert outlet (remnants of an abandoned beaver dam). Cross-sectional geometry of channel was recorded, and velocity measured with the pygmy flow meter throughout the cross-section, noting location of each measurement in the cross-section. Area-weighted average of flow velocity was calculated and applied to the respective area of the constriction cross-section and summed. Essentially the same methodology as described above was employed, but in a small and irregular cross-section which disallowed velocity measurement at 20% and 80% of depth. During two occasions of CMD malfunction, flow was measured by determining and averaging three cross-sectional areas in the constricted region. A light floating object (i.e. leaf or scrap of flagging) was floated from the first through third cross-section (~3.5 m) and timed. This was repeated several times at a number of starting locations (varying distance from right bank). The average velocity was applied to the average cross-sectional area of the study reach. When these measurements were compared to the otherwise determined gauging relationship, it provided flow results corroborative to the other methods.

Rather than a stage-discharge relationship, gauging of the lakes' outflow down the Misery River utilized depth over the engineered outlet weir structure present to determine flow. The following equation for discharge (*Q*) over a rectangular broad-crested weir was applied (Mays, 2019; Sturm, 2001; USDA, 2022):

$$Q = \frac{2}{3} C_v C_d \sqrt{\frac{2}{3} g} * L * {H_1}^{\frac{3}{2}} \qquad (7.2A)$$

where C_v is an approach velocity coefficient (taken as 1 with negligible approach velocity in lake; head approximately equals effective head), C_d is a coefficient of discharge (0.848 for a broad-crest), g is the gravitational constant, L is the length of the weir crest perpendicular to flow, and H_1 is the hydraulic head above the weir crest upstream of the weir. Notably, H_1 was dependent both on water elevation recorded and number of "logs" present at a given point time.

The weir consisted of a concrete pad with three independent 17cm-square steel "logs" or "rails" which could be raised or lowered independently to change the weir height and control lake outflow. These logs were moved regularly throughout the season in response to lake levels. The number of logs present was noted upon each site visit, and changes to the weir height could be noted through abrupt change in the level logger record. The weir equations were verified for accuracy by field measurement of flow. The water depth observed at each level logger installed was also noted during site visits. The wetland and beaver complex downstream of the weir was often backwatered, therefore a backwater correction to the weir equation was applied where applicable. This corrected discharge (Q_s) was applied when water level downstream of the weir surpassed the weir crest (with downstream head of H_2) as follows (USDA, 2022):

$$Q_s = Q * \left(1 - \left(\frac{H_2}{H_1}\right)^{1.5}\right)^{0.385} \qquad (7.2B)$$

A level logger was placed to record head over the weir 2 meters upstream of the weir (into the lake) at the base of the structure's concrete wingwall. Another level logger was placed in a cage with a staff gauge at the outlet of the bridge structure, measuring

downstream depth. The logger was located at the zero point of the gauge, which was flush with the riverbed. The level logger in the air was affixed to the top of the staff gauge cage, which was above any 2022 water elevation experienced. Survey of the site included measurement of the width of the weir opening, width of the bridge perpendicular to flow, length (in direction of flow) of weir crest, length of the bridge invert, and elevations of the following with optical level: bridge outlet opening cross section, weir base, weir crest (for all three set depths), each submerged level logger, and control points.

During low flow conditions, it was common that no water would crest the weir. The weir would leak variably between the logs; however, this flow could not be measured while the downstream backwater submerged these leaks (which was typical). Additionally, during high flow conditions water could flow around the weir logs over part of the concrete structure. The presence, absence, and apparent degree of these leakages were noted on site visits. When the leak was above the downstream water level, the volume-time method was performed with a 5-gallon bucket (5 trials) on July 18. The leakage was assumed constant at 0.002 CMS (measured on 7/18) during the course of the year; this leakage correction was insignificant during periods of notable flow, but provided a more realistic non-zero outflow during low-flow periods. The leak rate appeared variable throughout the season, but due to limited ability to quantify this leak a single leakage rate correction was utilized. The 7/18 leak appeared visually to be greater than some visits and lesser than others, so was deemed acceptable. Other leakage correction methods were

considered relating to head at the weir or observed flow but did not provide consistently better results than the singular correction method, so were not utilized (see appendix C).

7.2.2 Water Budget

A water budget was constructed for each lake using gauged inflows and outflows according to:

$$\frac{dV}{dt} = Q_{in} - Q_{out} + P - E \qquad (7.2C)$$

where *V* is water volume, and *dt* is a ten-minute timestep throughout all calculations. Q_{in} is flow into the lake, Q_{out} is flow out of a given lake, P is precipitation directly falling on the lake surface, and E is evaporation off the lake surface.

The inflowing Misery River gauge was used as the basis for overland and streamflow contribution per unit area at a given time. Inflow to each lake (Q_{in}) was calculated according to:

$$Q_{in} = Q_{WS} + Q_{US} \qquad (7.2D)$$

where Q_{US} is the inflow from the directly upstream lake (if present). Q_{WS} is inflow from overland and streamflow scaled according to the Misery River inlet gauge flow (Q_{misery}) by:

$$Q_{WS} = Q_{misery} * \frac{A_{WS} - A_{US-WS}}{A_{misery}} \qquad (7.2E)$$

with A_{WS} the total drainage area of the lake and A_{US-WS} the drainage area contributing directly to the lake(s) upstream of the lake in question. A_{misery} is the area of the Misery River watershed above the inlet gauge. The upstream lakes' flows (Q_{US}) were not gauged

(i.e. from Lake Gerald to Little Lake Gerald and from Little Lake Gerald to Lake Roland) but were assumed to be between the higher lake's inflow and outflow weir discharge (Q_{out-LR}) at any given point. Thus the inflow for Little Lake Gerald (and outflow for Lake Gerald) is taken as:

$$Q_{US-LL} = (Q_{misery} * x_{LL}) + (Q_{out-LR} * (1 - x_{LL})) = Q_{out-LG} \qquad (7.2F)$$

where $x_{LL}$is a correction factor between 0 and 1. Similarly for the inflow of Lake Roland and outflow of Little Lake Gerald is:

$$Q_{US-LR} = (Q_{US-LL} * x_{LR}) + (Q_{weir} * (1 - x_{LR})) \ = Q_{out-LL} \qquad (7.2G)$$

with x_{LL} being a correction factor between 0 and 1. The water budget was constructed in MS Excel, and the Data Analysis GRG Nonlinear Solver tool was applied to vary x_{LL} and x_{LR} such that the volume-weighted percent change in each lake volume was minimized. Notably also, the outflow of Lake Roland (Q_{out-LR}) is directly measured from the weir gauging station. From the resulting change in lake volume per the water budget, an expected depth change was determined according to bathymetry data (-0.15 m) and compared to the observed change in depth (-0.12 m) to verify applicability of this optimization approach to the whole budget. The optimized values of *x* were 0.754 and 0.973 for Lake Gerald and Little Lake Gerald outflows respectively; this makes sense intuitively, with Lake Gerald's outflow being ~75% influenced by the very proximal inflow, and the relatively small volume of Little Lake Gerald and more broad connection to Lake Gerald leading its outflow to maintain ~97% of its character from Lake Gerald. Lake Roland is hydrologically connected to the other lakes, causing the outflow rate to influence exchange within lakes, but is also distal by two narrow channel contractions with a pond between these contractions, buffering the response of any drawdown or

newly added impedance. Additionally, due to the outlet weir, the flow out of Lake Roland is often very near zero, making the flow between the lakes logically more closely related to that expected from the Misery River.

Daily precipitation depth was taken as the average recorded depth at National Weather Service (NWS) monitoring stations in Chassell, MI (20.1 km west-southwest of site) and Pelkie, MI (20.1 km east-southeast of site). Precipitation (*P*) was taken as the daily precipitation divided up evenly into 10-minute time segments. This is a simplification of the rainfall hyetograph for each event but enables calculation at the ten-minute timestep in accordance with streamflow data and accurately represents precipitation contribution each day. Care should be taken to not apply the model to specific sub-daily fluctuations in water level, but one may note that it still provides more insight into these sub-daily variations than it would if built on a daily timestep.

Evaporation (*E)* was calculated according to the combined energy and aerodynamic method according to (Mays, 2019; Mosner & Aulenbach, 2003):

$$E = \left(\frac{\Delta}{\Delta+\gamma}\right) E_r + \left(\frac{\gamma}{\Delta+\gamma}\right) E_a \qquad (7.2H)$$

where E_r is the energy method determined evaporation rate, E_a is the aerodynamic method determined evaporation rate, γ is the psychrometric constant (66.8 Pa/ºC), and Δ is the gradient of saturated vapor pressure for a given air temperature (T_α) and saturated vapor pressure (e_{as}) according to:

$$\Delta = \frac{4098 e_{as}}{(237.3+T_\alpha)^2} \qquad (7.2I)$$

$$e_{as} = 611e^{\frac{17.27T_\alpha}{237.3+T_\alpha}} \quad (7.2J)$$

The energy method determined evaporation rate (E_r) is calculated according to:

$$E_r = \frac{R_n}{l_v \rho_w} \quad (7.2K)$$

where ρ_w is density of water (taken as 999.1 kg/m^3 for average lake surface temperature), R_n is the net radiative flux, and l_v is the latent heat of vaporization. The net radiative flux was taken as 60% (approximate average Houghton County cloud cover) of the hourly solar normal value obtained for each month at the Twin Lakes latitude (46.9º N) from a solar atlas reference (SOLARGIS, 2023). l_v (joules) is taken as:

$$l_v = 2.501 * 10^6 - 2370 * \mathrm{T}_\alpha \quad (7.2L)$$

The aerodynamic method determined evaporation rate (E_a) is calculated according to:

$$E_a = B(e_{as} - e_a) \quad (7.2M)$$

where e_a is the vapor pressure and *B* is the vapor transfer coefficient. The vapor pressure is determined by:

$$e_a = R_h e_{as} \quad (7.2N)$$

where R_h is relative humidity, which was obtained as a daily average for Twin Lakes via Weather Underground historical dataset (Wunderground, 2022). *B* is determined according to:

$$B = \frac{0.102u_2}{\left[\ln\left(\frac{z_2}{z_0}\right)\right]^2} \quad (7.2O)$$

where u_2 is wind speed (m/s) as measured at instrument height z_2 (1 meter for dataset). z_0 is the roughness height of the water surface, taken as 0.03 cm. Wind speed was obtained as a daily average from the NWS weather station at the Houghton County

Memorial Airport (CMX) located 21 miles north of Twin Lakes (NOAA, 2022). The CMX wind speeds were considered comparable to what would be experienced at Twin Lakes due to comparable open fetch distances between the two sites (both approximately 800-1200 meters for west and northwest winds).

Notably, groundwater flows are excluded from equation 7.2C – this was due to lack of data available to parameterize groundwater movement and a satisfactory balance achieved without groundwater incorporation. Well logs were examined to try to understand the groundwater hydrology of the area, but coverage and accuracy was insufficient to provide any consistent or clear picture of the groundwater surrounding Twin Lakes (see section 7.1.2). Initially, the groundwater component of the water budget was to be calculated as the residual of the water budget as presented in this section; however, upon constructing the water budget, the residual was essentially zero. Therefore, groundwater movement was excluded from the water budget.

7.3 Water Sampling:

For all water sampling, sample bottles, caps, and in-line filtration devices were washed in a 10% HCl solution overnight, and subsequently rinsed twice with distilled water and three times with Milli-Q water before air-drying. Bottles were capped and only handled with gloved hands from that point onward. Fresh latex gloves were worn during all field sample collection as well. All samples were immediately bagged and placed in a closed and iced cooler immediately following collection as described below. Samples were transported and delivered to the lab for storage in a freezer (unless otherwise noted). All sample analyses were performed by the AQUA lab at Michigan Technological University's (MTU's) Great Lakes Research Center (GLRC) within the specified holding time. Stream and lake profile samples were collected at the locations noted in figure 7-1.

7.3.1 Stream Samples

Total phosphorus (TP) sampling occurred on 15 dates at the Misery River inlet to Twin Lakes (M26 culvert) and on 14 of those 15 dates at the lakes' outlet (Emily Lake Road bridge). At the M26 culvert, TP samples were taken from the centerline of the stream, at mid-depth in the plane of the culvert outlet. At the outlet bridge, during periods of high flow TP samples were collected similarly at the midpoint and mid-depth of the bridge outlet. During periods of low flow when little or no water was cresting the outlet weir and the Misery River was backwatered to the weir, TP samples were taken from leaks between weir logs or from the overtopping water. This was aimed at capturing TP concentrations of the water leaving the lakes, rather than water influenced by stagnation in the backwater ponding beneath the lakes' outlet. Care was taken to not disturb

sediment before sample collection occurred in every case. TP samples (40 mL minimum) were collected as whole water samples and submitted to the AQUA lab. There, samples were processed first by digestion with a reagent containing potassium persulfate, sodium hydroxide, and boric acid (beginning alkaline and becoming acidic) before analysis of orthophosphate with a SEAL Analytical AQ2 Discrete Analyzer. All TP samples results returned were above detection limits (>1.2 μg/L).

7.3.2 Lake Profile Sampling

At the deepest point of each lake, profiles and water samples were collected on 9 dates. A sonde profile of temperature, dissolved oxygen (DO), pH, and conductivity was collected at each site with a YSI EXO-2 wired sonde and data collector at 1-meter increments. Water samples were collected to be analyzed for soluble reactive phosphorus (SRP), TP, total nitrogen (TN), and total organic carbon (TOC) at depths corresponding to mid-epilimnion, mid-hypolimnion, 0.5m above lakebed on each lake (near-lakebed). A chlorophyll *a* sample from the surface water was also collected at each lake. In later sampling visits, exact samples collected were modified to meet refined research goals. A GPS point of each realized anchor point was collected in-field (Garmin Astro 320). Figure 7-1 shows the sampling locations on each lake and table 7-1 details which procedures were completed specifically on each sampling date.

Table 7-1: Water sampling and measurements performed on Twin Lakes field visits on each lake

Sample	Depth	17-May	7-Jun	6-Jul	18-Jul	2-Aug	23-Aug	27-Sep	4-Oct	19-Oct
Sonde Profile	Throughout Column	x	x	x	x	x	x	x	x	x
Chlorophyll	Surface	x	x	x	x	x	x	-	-	-
TP	**Epilimnion**	x	x	x	x	x	x	x	x	x
	Thermocline / Mid depth	-	-	-	-	-	-	-	x*	x
	Hypolimnion	x	x	x	x	x	x	x	x	x
	Lower Hypolimnino	-	-	-	-	-	x*	-	-	-
	Near-lakebed	x	x	x	x	x	x	-	x	-
TOC	**Epilimnion**	x	x	x	x	x	x	-	x	x
	Hypolimnion	x	x	x	x	x	x	-	x	x
	Near-lakebed	x	x	x	x	x	x	-	-	-
TN	**Epilimnion**	x	x	x	x	x	x	-	x	x
	Hypolimnion	x	x	x	x	x	x	-	x	x
	Near-lakebed	x	x	x	x	x	x	-	-	-
SRP	**Epilimnion**	-	x	x	x	x	x	-	x	x
	Hypolimnion	-	x	x	x	x	x	-	x	x
	Near-lakebed	-	x	x	x	x	x	-	x	-

*Little Lake Gerald excluded

Water samples at depth were collected with a Geotech Geopump peristaltic pump with the intake at the depth of interest. The pump was allowed to run for twice the residence time of the 4.8mm-diameter hose (15-meter length) at a given depth to ensure water collected was entirely from the target location in the water column. The clear hosing was not covered but was kept in the shade as much as possible during sunny days. In all sample collections, the hose was discharged to minimize turbulence and distance to the collection bottle without any contact between the hose and bottle. A small head space was left to prevent bottle damage during freezing.

TP samples (40 mL minimum) were collected as whole water samples and submitted to the AQUA lab. There, samples were processed first by digestion with a reagent containing potassium persulfate, sodium hydroxide, and boric acid (beginning alkaline and becoming acidic) before analysis of orthophosphate with a SEAL Analytical AQ2 Discrete Analyzer. TOC & TN samples were collected together (40mL minimum) as whole water samples before analysis simultaneously with a Shimadzu TOC-LCPH

analyzer with TNM-L by the AQUA lab. All TP and TOC & TN samples results returned were within detection limits.

SRP samples were collected at-depth and filtered upon collection with an in-line 47mm 0.45 um cellulose filter (5 mL minimum). A fresh filter was used and the filter holder thoroughly rinsed with milli-Q water between each SRP sample. The samples were analyzed for orthophosphate with a SEAL Analytical AQ2 Discrete Analyzer by the AQUA lab. SRP levels were very low and generally were returned below or near detection limits by this instrument (<1.2 μg/L).

Chlorophyll *a* sampling involved sample water volume being pumped from the surface of the water column (~5 cm below surface) with a Geotech Geopump peristaltic pump. Pumped water was filtered in the field with an in-line 47 mm 0.25-micron glass filter retaining chlorophyll. The filtered volume was recorded (~150 mL in every case) and discarded. The glass filter was folded over and placed immediately in tin foil and a labelled plastic bag before placement in the cooler. Chlorophyll-a samples were measured by the AQUA lab fluorometrically with a Turner 10-AU Fluorometer, using a blue mercury vapor lamp (excitation filter of 436 nm and emission filter of 680 nm). Data were returned as μg/L chlorophyll *a*.

7.3.3 Shoreline Surveys

Shoreline sampling occurred on three dates (6/6, 7/6, & 8/2) in 2022, during each of which 20 sites spread throughout the Twin Lakes System were visited. A total of 40 points along the shoreline and two mid-lake points (deepest points of Lake Gerald and Lake Roland) were sampled according to the following shoreline sampling procedure. Site selection was adaptive between sampling events and sought to representatively capture variable shoreline conditions among development types, development age, undeveloped shoreline types, known septic conditions, and unique features (i.e. tributary inlets, etc.) while giving a picture spread evenly among the three lakes. Figure 7-2 shows the sites sampled over these three dates. Table 7-2 shows the resulting breakdown of site types and quantity of sampling visits.

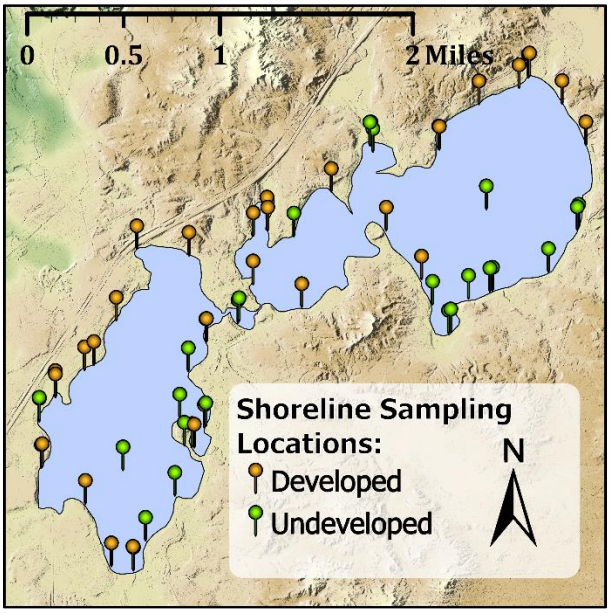

Figure 7-2: Shoreline survey sampling locations – 60 sampling events over 42 sites

Table 7-2: Breakdown of types and number of visits to shoreline sites during 2022 shoreline surveys

		Number of Sites				Total Visit Count
		Total Sites	Visited Once	Visited Twice	Visited Thrice	
Developed Sites *by Development Period*	~Pre-1960	12	*9*	*3*	*0*	15
	~1960-2000	9	*4*	*5*	*0*	14
	~Post-2000	3	*1*	*2*	*0*	5
	Total:	**24**	***14***	***10***	***0***	**34**
Undeveloped Sites *by Land Type*	Open Water	2	*2*	*0*	*0*	2
	Wetland / Swamp	3	*0*	*2*	*1*	7
	Upland	13	*9*	*4*	*0*	17
	Total:	**18**	***11***	***6***	***1***	**26**
	GRAND TOTAL	**42**	***25***	***16***	***1***	**60**

The timing of each shoreline sampling date was early in the week and aimed to capture period of high summer use specifically to observe any septic signal. For example, the Wednesday, July 6 sampling date aimed to see any effects from the period of heavy occupation corresponding to the Independence Day holiday. Combined coordination of borrowed equipment along with field help limited flexibility in scheduling work. As a result, limited variability of weather existed during these shoreline samples. The weather during each sampling event was cool and foggy giving way to mostly clear or sunny and breezy conditions during the day. Timing of visits to specific sites within the day was varied using different starting points and moving clockwise vs. counterclockwise on each day.

At each shoreline sampling site measurements were taken of temperature, depth, pH, conductivity, DO, SRP, Dissolved organic carbon (DOC), nitrate + nitrite, dissolved

nitrogen (DN), and fluorescence in the range of optical brightening agents (OBAs). OBAs are found in laundry detergents and their presence in surface waters, while not a concern themselves, is indicative of human wastewater contamination (Dubber & Gill, 2017; Kramer, Canonica, Hoigné, & Kaschig, 1996). Multiple methods for OBA detection have been published which have seen limited application (Cao, Griffith, & Weisberg, 2009; Stanford & Jourdonnais, 1985). Section 8.2.2 discusses these methods further. At least one picture was taken of the shoreline at each site. Any notable features of the site were recorded in narrative format (i.e. aquatic vegetation quantity and type, degree of development, retaining walls, land use / land cover of site, buffer strips, outbuildings, etc.). Sampling occurred within 5 meters of the shoreline and between 0.15 and 0.82 meters of lake depth (excluding two mid-lake points). A GPS point of each site visited was collected in-field (Garmin Astro 320).

Temperature, DO, pH, and conductivity were collected at each site with a YSI EXO-2 wired sonde and data collector at a depth of ~0.15 meters. Depth at each shoreline site was measured with a portable staff gauge or measuring tape. Water samples were collected with a Geotech Geopump peristaltic pump with an intake approximately 0.15 meters above the lakebed. The pump was allowed to run for twice the residence time of the 4.8 mm-diameter hose (15-meter length) at a given depth to ensure water collected was entirely from the target site and depth. The clear hosing was not covered but was kept in the shade as much as possible during sunny days. For all sample collection, the hose was discharged to minimize turbulence and distance to the collection bottle without any contact between the hose and bottle. A small head space was left to prevent bottle

damage during freezing. Samples were immediately placed on ice in a covered cooler after collection.

SRP, DOC & DN, and nitrate + nitrite samples were collected at-depth and filtered upon collection with an in-line 47 mm 0.45 um cellulose filter (50 mL minimum). A fresh filter was used and the filter holder thoroughly rinsed with milli-Q water between each sample taken. The SRP samples were analyzed for orthophosphate with a SEAL Analytical AQ2 Discrete Analyzer by the AQUA lab. SRP levels were very low and often were returned at or near detection limits by this instrument. DOC & DN measurement was performed by simultaneous TOC & TN analysis of the filtered samples with a Shimadzu TOC-LCPH analyzer with TNM-L by the AQUA lab. All DOC & DN samples results returned were within detection limits. Nitrate + nitrite was analyzed with a SEAL Analytical AQ2 Discrete Analyzer by the AQUA lab. Nitrate + nitrite levels were low and were generally returned below or near detection limits (<15 μg/L).

OBA sample collection, storage, and preparation were performed by the researcher, while analysis was performed by the AQUA lab. To test for OBAs, fluorescence samples (40 mL minimum) were collected as whole water samples and immediately wrapped in aluminum foil upon collection to prevent ultraviolet degradation of the OBA compounds (Burres, 2011; Dixon, 2009; Kramer et al., 1996). Samples were stored on ice in the field but not allowed to freeze; rather, samples were brought back to the lab for storage at 1º C for no longer than 7 days before analysis. The fluorescence of these samples was analyzed with a Turner 10-AU Fluorometer equipped with the Turner Optical Brighteners

Module (Turner Part #7200-047-W, measuring at 350/80 nm excitation and 445/15 nm emission). Average florescence of milli-Q water blanks was subtracted from the sample florescence returned for each sample set. Also submitted with each set of samples was a set of three standards of a known OBA-containing substance (Tide liquid laundry detergent - original); standard solutions were prepared by dilution in milli-Q water to concentrations of 500, 50, and 1 ppm Tide detergent. The returned fluorescence values of the standard solutions were neatly linear to detergent concentration ($\geq$0.9997 R^2 for n=3 each & 0.9993 R^2 for all n=9) across a range which bounded the returned florescence values of the environmental samples. Naturally occurring organic matter can fluoresce at the examined wavelengths as well, complicating analysis (Cao et al., 2009; Dubber & Gill, 2017; Kramer et al., 1996); therefore, florescence values were normalized to site DOC concentrations (OBA:DOC ratio) for interpretation (Jourdonnais, 1986; Stanford & Jourdonnais, 1985). Further examination and discussion of this methodology, and alternative approaches are explored in section 8.2.2.

Data was processed statistically in MS Excel and spatially in ArcGIS Pro. Statistical differences between subsets of data were assessed by 95% confidence intervals first with normality assumed, and second with natural log transformed data. For each metric (DOC, SRP, DN, conductivity, and OBA:DOC), Lake Gerald was compared to Lake Roland and developed sites were compared with undeveloped sites (on each lake individually, and as a whole lake system). Data were spatially processed to create heat maps of each species. The ArcGIS Pro “Topo to Raster” tool was applied using collected data points, with the lake perimeter as a boundary, to create an interpolated concentration gradient of each

species along the shoreline. Similarly, the “Spline with Barriers” tool was applied to each species’ dataset, with the lakes area as the boundary, to create an interpolated gradient of each species concentration across the whole lake surface.

7.3.4 Erie-Ontario Mine Drainage

Various former mine sites were visited in December 2022 to confirm their presence or absence (Diggings, 2022). At the singular mine of note (discussed further below), conductivity measurements (Hach HQ40d) were taken 1) in the cistern water, 2) in the surface drainage ~15m downstream of the cistern, and 3) in the directly neighboring surface drainage of similar size, not draining from the observed mine site.

7.4 Total Phosphorus Model & Budget

7.4.1 2-Box Model Framework

TP was modeled in the Twin Lakes system using a 2-box mass balance framework for each lake during the 2022 stratified period. The model considered the concentration of TP in a distinct and completely mixed epilimnetic upper box (P_{epi}) and the concentration of TP in a distinct and completely mixed hypolimnetic lower box (P_{hyp}). Lake Gerald, with Little Lake Gerald included, was modeled as one 2-box system in series with Lake Roland as a second 2-box system. This model framework is in general accord with the 2-box model framework presented in *Surface Water Quality Modeling* (Chapra, 2008). A differential equation describing mass transport on TP is applied to each box. Change in hypolimnetic TP (P_{hyp}) in the lower box is modeled according to:

$$\frac{dP_{hyp}}{dt} = \frac{+/-Epilimnetic\ Diffusion+/-Internal\ Load\ \&\ Burial+Epilimnetic\ Settling}{V_h} \quad (7.4A)$$

Where:

$$Epilimnetic\ Diffusion = \left(\boldsymbol{V_t} * A_t * \left(P_{epi} - P_{hyp}\right)\right)$$

$$Internal\ Load\ \&\ Burial = \left(\boldsymbol{v_b} * A_t\right)$$

$$Epilimnetic\ Settling = \left(\boldsymbol{v_s} * A_t * P_{epi}\right)$$

The $Epilimnetic\ Diffusion$ is controlled by the vertical mixing coefficient (V_t) and the TP concentration gradient between the boxes, and refers to diffusive transport across the interface with the upper box, or the thermocline area (A_t). The $Internal\ Load\ \&\ Burial$ is controlled by the net burial rate (v_b) and refers to the net exchange of TP at the sediment surface (area approximated by A_t) from either gravitational burial or sediment P release during period of low DO. The $Epilimnetic\ Settling$ is controlled by epilimnetic TP and the settling rate (v_s) and refers to gravitational settling of TP across A_t. The mass

of TP is made a concentration by dividing by the hypolimnetic volume (V_h). Change in epilimnetic TP mass (P_{epi}) in the upper box is modeled according to:

$$\frac{dP_{epi}}{dt} = \frac{+External\ Load - D/S\ Transport +/- Hypolimnetic\ Diffusion - Settling}{V_e} \quad (7.4B)$$

Where:
$External\ Load = W_{ext}$
$D/S\ Transport = (Q_{out} * P_{epi})$
$Hypolimnetic\ Diffusion = (\boldsymbol{V_t} * A_t * (P_{hyp} - P_{epi}))$
$Settling = (\boldsymbol{v_s} * A_t * P_{epi})$

The $Hypolimnetic\ Diffusion$, similar to epilimnetic diffusion above, is controlled by V_t and the TP concentration gradient between the boxes and refers to diffusive transport across A_t. The $Settling$ term again is controlled by P_{epi} and the v_s and refers to gravitational settling across A_t. The $D/S\ Transport$ term is controlled by P_{epi} and the flowrate out of the lake (Q_{out}) and includes TP leaving the system to the next lower lake or the Misery River. The mass of TP is made a concentration by dividing by the hypolimnetic volume (V_e). The $External\ Load$ (W_{ext}) refers to epilimnetic TP inputs which is defined by:

$$W_{ext} = U/S\ Lake\ Load + Direct\ Watershed\ Load + Atmospheric\ Load + Residual\ Load \quad (7.4C)$$

Where:
$U/S\ Lake\ Load = (Q_{out-U/S} * P_{epi-U/S})$
$Direct\ Watershed\ Load = ((Q_{Misery} * \frac{A_{WS}}{A_{Misery}}) * P_{Misery})$
$Atmospheric\ Load = (\boldsymbol{P_{atm}} * SA)$
$Residual\ Load = (\boldsymbol{W_{ant}} * Per)$

The $U/S\ Lake\ Load$, where applicable, refers to TP flowing into the lake from the above lake, and is a function of the outflow of the upper lake ($Q_{out-U/S}$) and the epilimnetic TP concentration in the lake ($P_{epi-U/S}$). The $Direct\ Watershed\ Load$ is the TP loading

from tributaries and overland flow to the lake and is based on the TP concentration in the Misery River at a given time (P_{Misery}) and flow which is scaled directly by the area of the contributing watershed (A_{WS}) according to the area of the Misery River watershed (A_{Misery}) and the flow it produces (Q_{Misery}) at a given time (with the watershed area draining through any above lake(s) excluded from A_{WS}). The $Atmospheric\ Load$ is controlled by the lake surface area (SA) and a constant rate of atmospheric deposition (P_{atm}), and includes TP in the atmosphere falling to the lake surface. The $Residual\ Load$ is controlled by the shoreline length (Per) and a constant loading rate per unit length of shoreline (W_{ant}), and includes primarily the TP load from any anthropogenic sources along with any error in the other component processes. Figure 7-3 presents this model framework graphically.

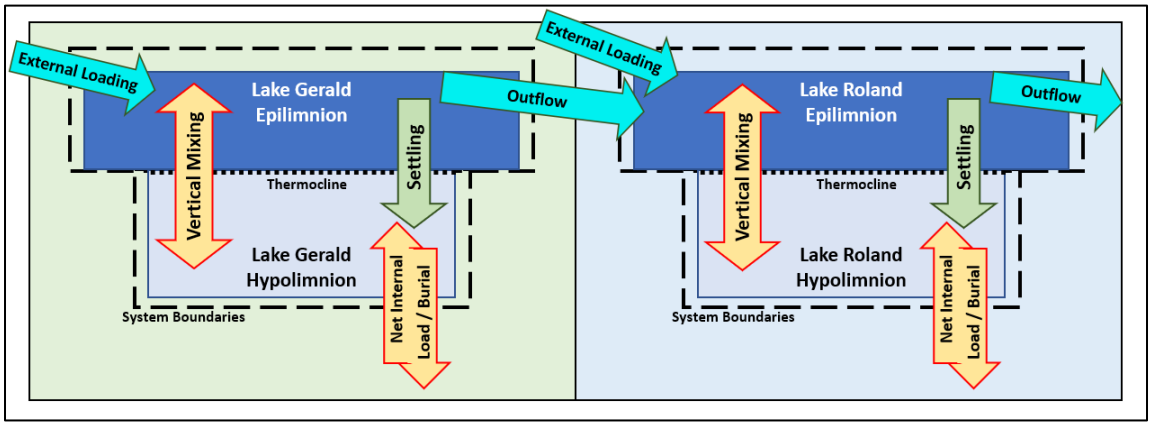

Figure 7-3: Conceptual coupled 2-box mass balance models of total phosphorus in Twin Lakes.

The component constants and parameters composing equations 7.4A-C are tabulated and described in greater detail in appendix D. Most values are observed in the field or measured via GIS, while estimated and optimized values (values bolded in definitions of equations 7.4A-C) are discussed further in section 7.4.3. The model was constructed in

MATLAB R2021a using the ODE45 function for solving non-stiff differential equations (MathWorks, 2022a). The model operates on a 10-minute timestep to match stream gauging data frequency, though conclusions are drawn from the output at only a daily or longer interval (generally seasonally). The code for the model and component functions can be shared upon request of the author.

7.4.2 Model Period & Initial Conditions

The model period was selected to match the stratified period of the lakes as closely as possible, utilizing as much field-collected data as possible. Of the nine on-lake field visits with temperature profiles, the lake was sufficiently stratified for six of them (June 7 through September 27).

Table 7-3: 2022 temperature profiles (ºC) throughout Twin Lakes; red corresponds to the warmest waters, and green to the coolest

Date:	17-May	7-Jun	6-Jul	18-Jul	2-Aug	23-Aug	27-Sep	4-Oct	19-Oct
Depth (m)	**Lake Gerald**								
0	13.23	17.34	21.03	25.15	22.39	23.24	15.67	15.11	8.99
1	13.10	17.65	20.89	25.08	22.23	23.15	15.69	15.11	9.05
2	12.41	17.33	20.74	23.32	22.02	22.96	15.69	15.11	9.04
3	11.87	16.07	20.65	22.29	21.96	22.47	15.69	15.08	9.05
4	10.92	15.62	20.57	21.64	21.92	22.15	15.69	14.87	9.05
5	8.60	15.04	19.50	20.48	21.40	21.34	15.69	14.77	9.09
6	7.80	12.92	18.59	16.55	18.43	19.54	15.67	14.72	9.09
7	7.10	9.95	12.80	12.33	13.52	14.87	15.66	14.70	9.00
8	6.90	8.20	9.94	10.30	10.98	11.79	15.63	14.43	8.99
9	6.79	7.94	9.27	9.62	10.03	10.56	15.15	14.43	8.97
10	6.72	7.73	9.08	9.38	9.78	10.08	10.50	11.10	8.92
11	6.64	7.66	8.80	9.05	9.50	9.90	10.17	10.70	8.87
~11.5	6.53		8.00	9.04	9.46				
Depth (m)	**Little Lake Gerald**								
0	14.71	18.39	21.68	25.20	22.90	23.23	15.26	14.84	7.84
1	14.26	18.25	21.51	25.17	22.72	23.09	15.30	14.84	7.85
2	12.94	17.16	21.05	23.59	22.48	23.03	15.31	14.50	7.86
3	9.10	16.33	20.78	22.17	22.10	22.48	15.31	14.74	7.89
4	7.52	13.38	19.07	18.65	20.20	21.05	15.32	14.53	7.88
5	6.79	8.49	12.20	13.11	14.18	16.63	15.32	14.41	7.88
6	6.50	7.71	9.91	10.97	12.01	13.55	15.32	14.31	7.89
~6.4	6.43	7.61	9.53	10.52	11.50	13.23	15.33	14.29	8.04
Depth (m)	**Lake Roland**								
0	14.05	18.30	21.78	25.36	22.52	23.10	15.15	14.46	7.90
1	13.87	18.26	21.40	25.22	22.34	23.09	15.17	14.42	7.91
2	13.65	18.13	21.34	23.00	22.22	22.66	15.17	14.35	7.91
3	13.56	16.62	20.85	21.76	21.89	22.10	15.16	14.27	7.91
4	9.50	15.77	20.15	20.36	21.21	21.33	15.15	14.16	7.91
5	8.49	13.07	18.14	17.42	18.57	20.00	15.14	14.09	7.91
6	7.80	10.06	13.23	13.32	14.35	16.00	15.13	14.05	7.91
7	7.43	8.20	9.96	10.07	10.32	11.26	15.13	13.88	7.91
8	7.20	7.77	8.42	8.65	8.73	9.55	13.00	13.74	7.91
9	6.99	7.44	8.11	8.00	8.27	8.65	9.22	11.14	7.90
10	6.84	7.25	7.64	7.69	7.92	8.29	8.46	9.19	7.90
11	6.78	7.15	7.49	7.61	7.80	8.04	8.23	8.32	7.87
~11.75	6.72	7.07	7.53	7.46	7.75	7.93	8.17	8.23	7.86

Those dates were selected as the start and end dates of the model given uncertainty surrounding changes before or after those dates. Earlier than June 7 (i.e. the May 17 visit), the lakes were beginning to stratify, but had a less distinct and stable thermocline

which was higher in the water column. Notably, fall mixing began very near to September 27 based on the first cold-weather days and nights leading up to that date, with Little Lake Gerald having turned over just before that visit. Lake Gerald began to mix then, but Lake Roland remained largely stratified. This made September 27 an excellent end-date given it represented the very beginnings of fall mixing, yet to a large extent preserving the final character of the truly stratified season. The hypolimnetic TP plot in figure 8-2 demonstrates this, with peak TP levels reached on the September 27 visit, and rapidly decreasing on following visits. The changed volumes of the epilimnions and hypolimnion were considered while determining the mass of TP present on this date, though the model results were relatively insensitive to that minor adjustment. Table 7-3 shows the temperature profiles of the lakes throughout the season.

Initial model TP conditions were assumed equal to measured TP on June 7 in each modeled segment. The initial TP concentration in the epilimnion and hypolimnion of Lake Gerald as modeled was taken as a volume-weighted average between concentrations measured in the big Lake Gerald basin, and in Little Lake Gerald. The hypolimnetic Lake Roland TP initial concentration was as measured on that date (this was the only metric available for this layer). The epilimnetic Lake Roland initial concentration was taken as an average between the TP concentration sampled at the deep point of the lake and the concentration sampled at the lake's outflow (also epilimnetic water on the same day). Taking average values where possible was helpful in removing sample variability resulting from small sample sizes (one sample per site per visit). This was particularly helpful for Lake Roland initial conditions. The would-be initial TP

concentration in Lake Roland, using only the single mid-lake measurements, would have been high enough to create substantial difficulty in fitting the model with reasonable optimized parameter values (optimization addressed elsewhere). Figure 7-4 shows these average values for the Lake Roland epilimnion. Lake Gerald and Little Lake Gerald can also be reasonably grouped because 1) the channel separating the basin is large enough that some mixing may occur, and 2) they share generally similar water chemistry (see shoreline survey discussion). This weighted averaging of TP in those basins is consistent with Lake Gerald and Little Lake Gerald being grouped for consideration in the model.

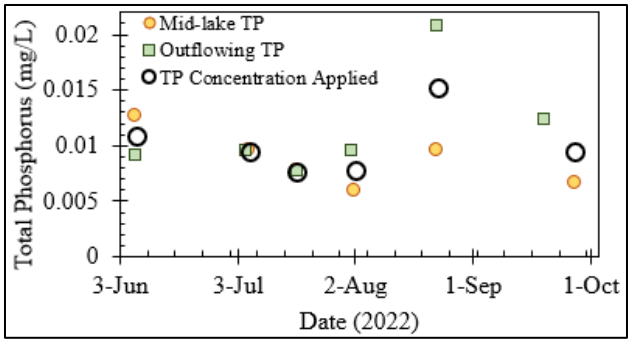

Figure 7-4: Lake Roland epilimnetic TP measurements, and averaging in model framework

7.4.3 Parameter Selection & Optimization

Most model parameters are derived from field observations or measurement using GIS. The values obtained from literature or calibrated are discussed here. These parameters include P_{atm}, V_t, v_s, v_b, and W_{ant} and are addressed in that order. Appendix D summarizes all contributing parameters and the means by which they were selected or obtained.

Estimates of atmospheric loading rates are variable with location and have sparse coverage in literature (Redfield, 2002). Atmospheric deposition is primarily from local to regional land sources – P is carried with particles on the wind and deposited downwind

(Boehme, 2012; Camarero & Catalan, 2012; Redfield, 2002; Tipping et al., 2014). The P_{atm} value utilized came by averaging values from two reasonable sources. The first was 3.35E-4 mg/m^2/d and was the average loading rate value from the 4 most representative sites (Shagawa Lake, Minnesota; northern inland forested sites; Narrow Lake, Alberta; & forested central Ontario lakes) listed among a long set of lakes (Redfield, 2002; Tipping et al., 2014). Seasonal variation of these values was not presented or included for this work. These lakes were in remote forested regions without major pollutant sources nearby upwind. Due to the Twin Lakes system's inland nature and forested surroundings void of any large developments, these values (among the lowest loading rates in the list) are reasonable. Alternatively though, Twin Lakes is downwind of Lake Superior on three sides (including the prevailing wind). The surface of Lake Superior will not contribute to atmospheric P loads transported to Twin Lakes, as the board land surface would for lakes located further inland. Therefore, a second loading rate considered was 2.55E-4 mg/m^2/d, as applied in a phosphorus budget for Lake Superior (Chapra & Sonzogni, 1979). Due to little land area surrounding Twin Lakes (before reaching Lake Superior), but the land type fitting the description of those forested sites, a value averaging these two options was utilized – 2.95E-4 mg/m^2/d for P_{atm}.

The diffusive mixing, represented by V_t, between the hypolimnion and epilimnion of each lake was determined by fitting a second MATLAB model to temperature measurements in the lake during the stratified period. Heat transfer to the hypolimnion was utilized as a tracer for diffusion; figure 7-5 shows this framework graphically.

Change in average hypolimnetic temperature (T_h) per unit time was modeled according to:

$$\frac{dT_h}{dt} = \frac{V_t A_t (T_e - T_h)}{V_h} \qquad (7.4D)$$

With heat transfer across A_t to the hypolimnetic water (volume V_h) controlled by a diffusion transfer coefficient (V_t) and the difference in T_h and the average temperature of the epilimnetic water (T_e) at a given time.

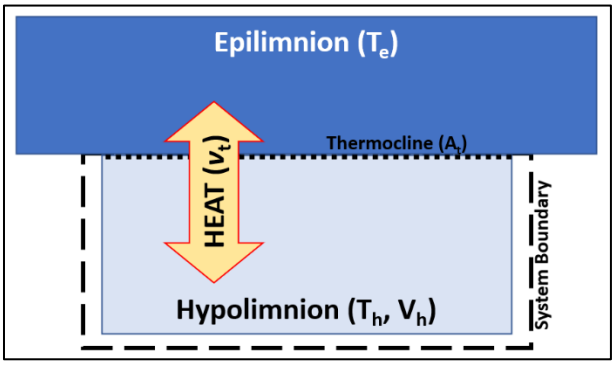

Figure 7-5: Box model of thermal transfer across the thermocline.

The stratified period of June 7 through September 27 was utilized for this model, and it was carried out on the hypolimnion of each lake separately, including Little Lake Gerald. The differential equation was assessed using the ODE45 function in MATLAB (MathWorks, 2022a). The average temperature of the epilimnion and hypolimnion on the June 7 field visit was taken as the initial condition. The value of $V_t$was allowed to vary between 0 and 2 m/d, a very large range which is conservative and unrestrictive. V_t was optimized using the simulated annealing (simulannealbnd) function in the Global Optimization Toolbox under default settings (MathWorks, 2022b). Performance of fit was assessed by calculating the root mean square error (RMSE) between modeled and observed average layer temperature values for days with lake profiles taken (n=6). The model output V_t for Lake Roland was utilized directly in the TP model (0.0055 m/d). For Lake Gerald in the TP model, a lake volume-weighted average V_t value (0.0143 m/d) was taken between the modeled values of V_t for Lake Gerald and Little Lake Gerald (0.0139

and 0.0165 m/d respectively), which have separate basins and had separate temperature profiles and layer volumes.

A similar optimization methodology to that employed for determining V_t was utilized within the TP model to obtain v_s, v_b, and W_{ant}. A single value for both v_s and v_b were determined independently for both lakes (i.e. v_{b-LG} & v_{s-LG} for Lake Gerald, and v_{s-LR} & v_{b-LR} for Lake Roland). One W_{ant} value was considered for the whole system, but was adjusted by the shoreline development density of each lake (yielding W_{ant-LG} & W_{ant-LR} for Lake Gerald and Roland respectively) according to:

$$W_{ant-LG} = W_{ant} * \frac{\rho_{LG}}{\rho_{TL}} \qquad (7.4E)$$

$$W_{ant-LR} = W_{ant} * \frac{\rho_{LR}}{\rho_{TL}} \qquad (7.4F)$$

where development density (number of developments per km shoreline) for Lake Gerald, Lake Roland, and Twin Lakes overall is given by ρ_{LG}, ρ_{LR}, and ρ_{TL} respectively. These five parameters (v_{b-LG}, v_{s-LG}, v_{s-LR}, v_{b-LR}, and W_{ant}) were optimized simultaneously using simulated annealing (simulannealbnd) function in the Global Optimization Toolbox (MathWorks, 2022b). The initial "temperature" setting in the simulated annealing optimization algorithm was adjusted from 100 (default) to 10,000 to avoid local minima for W_{ant}.

The values of v_s and v_b were bound by extremes found in a host of scientific literature. The value of v_s was generally bounded by 0.01 and 0.06 m/d but was allowed to vary between 0.01 and 0.1 m/d (Chapra & Sonzogni, 1979; Snodgrass & Dillon, 1983;

Sperling, 1992; Zhang, Liu, & Guo, 2016). The value of v_b was generally bound by -0.05 and 0.05 m/d, but was allowed to vary between -0.05 and 0.5 m/d (Albright, 2022; James, 2017a, 2017b; Larson et al., 2020; Malecki, White, & Reddy, 2004; Orihel et al., 2017). There was no literature values found for a shoreline-specific residual loading rate (i.e. W_{ant}), so a wide range of values was allowed. W_{ant} was allowed to vary between 0 mg TP/km shoreline/day and 15,000 mg TP/km shoreline/day (from no influence, to that which would unreasonably dominate the nutrient budget).

Model fit was determined similarly to the vertical mixing model. The normalized RMSE (NRMSE) was calculated for the difference in modeled and measured TP concentrations for each day with measurements in the model period (n=6), and for each lake (Lake Gerald and Lake Roland) and each layer (epilimnion and hypolimnion). This resulted in 24 total observations for use in calibration. Measured concentrations for each layer of each lake were taken by the same method as addressed above for initial conditions. Average values were taken where applicable to remove variability from small sample size. One example MATLAB model output is shown in figure 7-6, illustrating the time between observed points, and the model

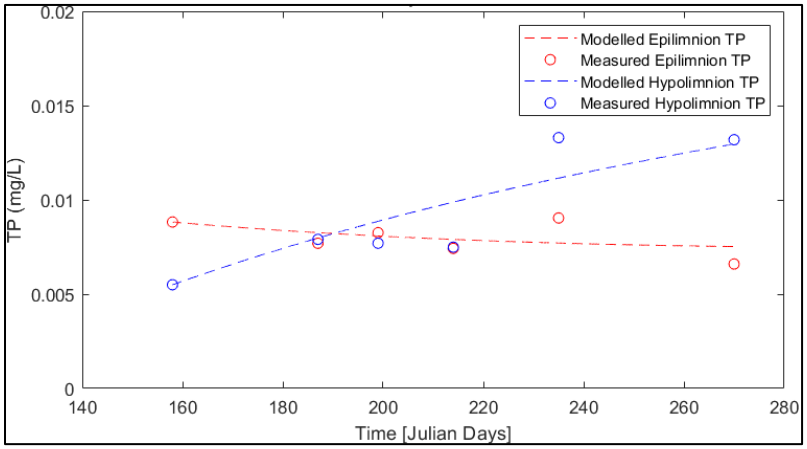

Figure 7-6: Sample model output for Lake Gerald; distance between TP modeled (lines) and measured (points) served as the basis for assessment of model performance and fit

output shown as lines, and fit to observed points.

Simulated annealing produced inconsistent values for each parameter depending on the model run. Therefore, 200 independent model executions were performed and the results logged. Linear relationships between the three parameters on each lake (v_s, v_b, and W_{ant}) emerged, which is logical given the system is not fully constrained (5 unknowns and 4 differential equations). A more complete comparison of these model outputs can be found in appendix E. The optimized parameter values converge, however, at the lowest error executions. The average parameter values from the best 10 model executions were utilized for the accepted model. Figure 7-7 shows the convergence of each parameter to a "best" value for n=200 executions. These "best" converging values all fell in a range reasonable for the parameter, so were accepted.

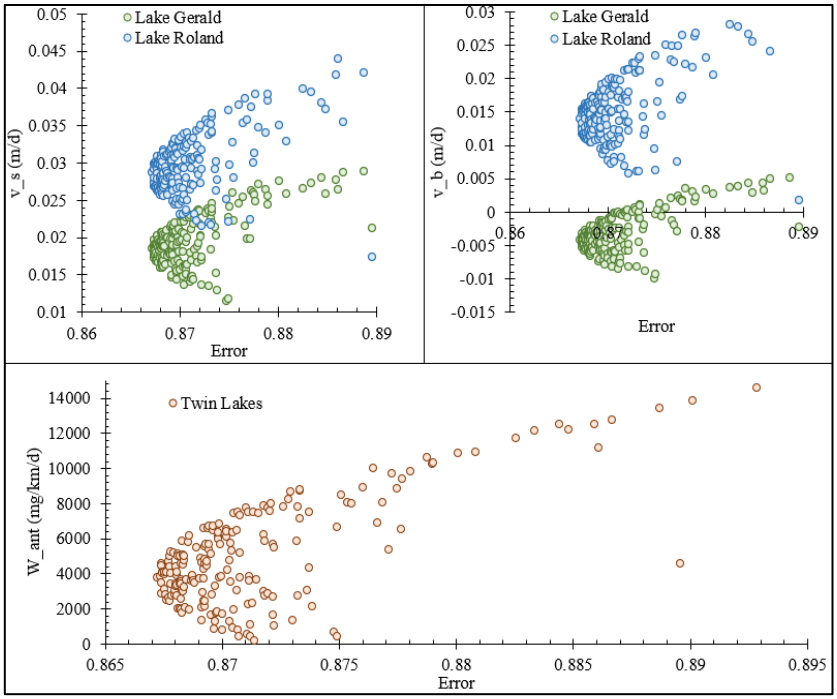

Figure 7-7: Parameter optimization output for settling rates, burial rates, and residual loading rate over 200 independent model runs

Final model fit, calibrated to observed TP concentrations in the water column, had a NRMSE of 0.8674 comparing model output against n=24 observations (n=20, if the 4

observations corresponding to the start point for the model are removed). This final model fit, and associated results are presented in section 8.4.

7.4.4 Model Validation, Application, & Sensitivity Analysis

Due to data collection occurring over just one year with small samples and the same model year used for analysis, there was no in-lake validation dataset for comparison. Rather, other comparisons to known (pseudo-validation) data were utilized. One such comparison was between model-predicted TP concentrations flowing out of Twin Lakes and measured TP outflowing concentrations at the Misery River outflow. One other application-based test, though less quantitative, came by comparison of the model's long-term predictions to the potential history of Twin Lakes. The latter involved setting a pre-development TP concentration for the lakes and assuming a timeframe of loading increase until present, while aligning the result with known historical markers for the lakes. This application is addressed in greater detail in section 7.4.5.

Outflowing TP concentrations were collected on 14 dates in 2022 at the Misery River outlet of Lake Roland. Linear interpolation between these sampling times (which reasonably assumes slow linear change in Lake Roland mixed layer TP) was utilized to construct a TP mass load exiting Twin Lakes for the full model period. A flow-concentration relationship was not utilized, because flow was dependent most directly on human operation of the outlet weir (though this was influenced by watershed conditions), and because TP concentration was dependent on epilimnetic lake TP more directly than by the influence of storm-forced watershed processes. This mass flow was largely driven

by the system hydrology, given very little outflowing water for much of the season. Figure 7-8 shows these results on log-scale to highlight the differences throughout the model period, rather than just during the period of high flow. The total error in outflowing TP sums to 0.35 kg (excess exported by model) over the course of the model period. This could correlate to up to a 5.3% decrease in the residual load if corrected; however, this considered relatively minor given potential error in the interpolative approach for the "true" value of TP export utilized. This is particularly true during two large rain events in the early season, when the largest flows of the model period were observed. During those periods, one TP measurement, which is higher than the model prediction for that period, essentially sets the outflowing TP concentration for the duration of the high flow events. This served as acceptable validation of model performance given data collection constraints.

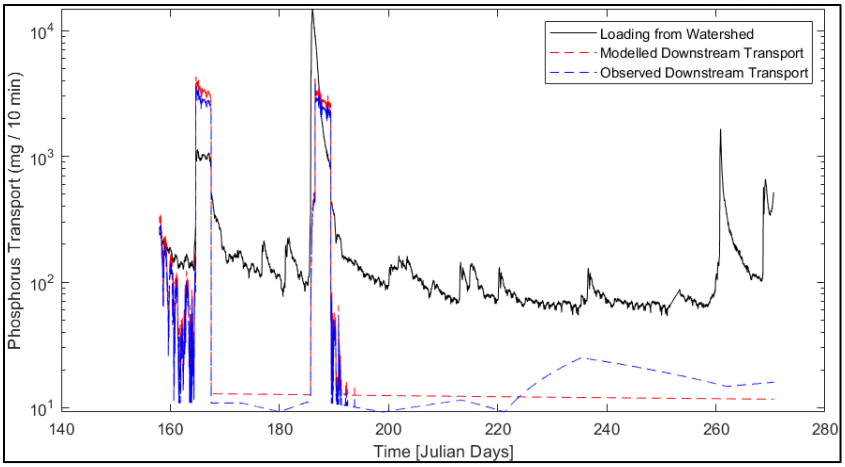

Figure 7-8: Log-scaled comparison of gauge-measured TP outputs compared to model predicted TP outputs on Twin Lakes

For sensitivity analysis of the model, the variability of calibrated parameters between model executions was considered (see section 7.4.3 & figure 7-7). Notably, the model was most sensitive to the "residual load" estimation, with a very large range of values accepted in one model iteration or another. The "settling" and "internal load & burial"

terms for both Lake Gerald and Lake Roland had relatively precise and non-overlapping calibrations which fell neatly in the range of acceptable values. A direct relationship existed between these parameters (see appendix E), but parameter estimates converged at the lowest error model outputs.

7.4.5 Model Forecast & Case-Scenarios

The results of the model were utilized to provide a coarse predictive tool for lake future health and potential response to changes in future TP loading. This forecast model was carried out on the scale of all of Twin Lakes (rather than lake by lake in series). The lakes are truly very connected and changes to Lake Gerald will be felt in Lake Roland in subsequent years (though less-so in vice versa). Generalizing to the whole system of common stakeholders appears more apt from a management perspective and aims to prevent leaning on this predictive tool beyond its design intent. That being the case, generalization about potential differences between each lake's response can and are made in discussion.

The model forecast was accomplished by applying the 2022 constructed TP budget to the lakes as a whole each year moving forward to simulate changes to overall system TP concentration.

Several "what-if" scenarios are considered alongside this for specific modifications to the lake TP budget (i.e. immediate 50% residual load reduction, 75% residual load reduction carried out over next 10 years, etc.). The initial condition (year of 2022) was taken to be the volume-weighted averages of the mean TP concentrations modeled in the epilimnion

and hypolimnion of both Lake Gerald and Lake Roland during the model period (i.e. stratified period, which is of greatest concern). A steady state was assumed during the rest of the year; essentially, this assumes that pre-development conditions prevail during that period. This may not be a good assumption, given the possibility of continued excess loading throughout the year; however, it is likely that excess loads would at least decrease for this period. Further, no data collection of hydrology or nutrient concentrations was complete to parameterize the nutrient budget over the remaining year and speculation dominates creating a budget for a full year. Directly scaling the modeled budget to a full year (both considering and not considering scaling internal load and/or residual load) resulted in unreasonable predictions (e.g. immediate dramatic increase in lake TP concentration). Therefore, the budget was applied as modeled. The results are validated by comparison against historical knowledge of the lakes, which is discussed at greater length in sections 8.4.2 and 8.5.3. Change in mass of TP (P) annually was determined according to:

$$\frac{dP}{dt} = -(P * F_r) + [\theta * (-B + W_{int})] + W_{ant} + W_{ext} + W_{atm} \qquad (7.4G)$$

where outflowing TP is controlled by the system's flushing rate (F_r), external watershed loads (W_{ext}) and atmospheric loads (W_{atm}) remain constant, and the residual load (W_{ant}) is manipulated based on the scenario tested. Internal loading (W_{int}) and burial (B) terms are scaled according to the mass of TP present in the lakes in a given year (P_i) by a correction factor (θ) defined as:

$$\theta = \frac{P_i}{P_{2022}} \qquad (7.4H)$$

where P_{2022} refers to the mass of TP in 2022. This correction seeks to conservatively recognize that loading reductions will result in decreased burial and (in particular) internal loading, but on a delay. The mass balance defined above is carried out on an annual timestep. Further, the steady state result of the 100% residual load reduction scenario was taken as the starting point for a historical hindcast. This hindcast, starting at development on the lakes and assuming a steady rate of increased TP loading, provides validation for this approach and interesting insight into the potential history of the lakes. This is discussed at great length later.

8 RESULTS & DISCUSSION:

8.1 Lake Profiles, Metabolism, & Management Implications

8.1.1 2022 Profile Measurements

Lake profiles reveal the Twin Lakes system to be a series of three basins which stratify distinctly. Table 7-3 shows the temperature profiles for each of the nine profile-measurement visits to the lakes. Both Lake Roland and (big) Lake Gerald stratified at 6 m in depth, and Little Lake Gerald (the smaller intermediate basin), stratified at 4 m in depth. Dissolved oxygen profiles provided helpful insight into the lake metabolism, with substantial DO depletion occurring in the hypolimnions of each basin, with the downstream basins experiencing greater symptoms. DO depletion began to reach into the epilimnion of each lake, though most prominently in Lake Roland (table 8-1). Complete conductivity and pH profiles were also collected on these dates. These profiles

Table 8-1: 2022 Twin Lakes dissolved oxygen profiles (mg O_2/L)

Date:	17-May	7-Jun	6-Jul	18-Jul	2-Aug	23-Aug	27-Sep	4-Oct	19-Oct
Depth (m)	Lake Gerald								
0	10.23	9.19	8.49	8.08	8.16	8.34	8.79	9.64	10.83
1	10.26	9.21	8.52	8.17	8.15	8.36	8.83	9.67	10.78
2	10.29	9.21	8.51	8.50	8.15	8.36	8.84	9.67	10.77
3	10.32	9.25	8.49	8.37	8.11	8.25	8.86	9.64	10.76
4	10.17	9.15	8.46	8.05	8.04	8.06	8.86	9.45	10.76
5	9.90	8.99	7.40	7.09	7.34	7.21	8.86	9.29	10.75
6	9.70	8.39	6.97	4.17	3.70	3.60	8.87	9.24	10.75
7	9.39	7.62	4.30	2.06	0.82	0.38	8.87	9.19	10.75
8	9.29	6.57	2.93	1.31	0.43	0.29	8.87	8.98	10.75
9	9.21	6.20	2.13	0.89	0.35	0.26	8.27	8.41	10.76
10	9.14	5.95	1.91	0.71	0.32	0.24	0.80	0.88	10.77
11	8.74	1.10	0.80	0.27	0.27	0.20	0.40	0.47	10.51
~11.5	1.30		0.46	0.24	0.29				
Depth (m)	Little Lake Gerald								
0	9.82	9.45	8.21	7.98	8.07	8.27	8.71	9.75	10.96
1	9.85	9.47	8.23	8.00	8.07	8.29	8.82	9.76	10.94
2	10.02	9.65	8.25	8.16	8.05	8.28	8.84	9.76	10.92
3	9.90	9.40	8.13	8.03	7.92	8.16	8.86	9.71	10.90
4	9.30	8.91	7.18	5.85	5.20	6.35	8.87	9.63	10.89
5	8.39	4.81	2.13	0.76	0.72	0.72	8.87	9.53	10.88
6	6.62	2.45	0.64	0.37	0.46	0.28	8.84	8.92	10.86
~6.4	2.05	0.70	0.37	0.27	0.30	0.22	6.90	1.60	7.00
Depth (m)	Lake Roland								
0	9.76	9.28	8.14	8.05	7.79	8.13	8.60	9.83	11.17
1	9.78	9.27	8.14	8.16	7.94	8.13	8.77	9.87	11.16
2	9.78	9.27	8.13	8.17	7.88	8.08	8.81	9.88	11.16
3	9.75	8.90	7.83	6.90	7.40	7.44	8.86	9.84	11.15
4	9.50	8.57	7.02	5.07	6.10	6.50	8.87	9.69	11.15
5	9.38	7.83	5.25	2.58	1.42	4.26	8.87	9.67	11.14
6	9.25	7.17	3.36	1.53	0.42	0.80	8.87	9.69	11.14
7	9.22	6.97	3.52	1.99	0.59	0.43	8.86	9.30	11.13
8	9.19	6.78	3.41	1.69	0.36	0.36	2.72	9.01	11.13
9	9.02	6.44	2.99	0.77	0.30	0.32	1.10	2.84	11.13
10	8.61	6.29	2.02	0.31	0.28	0.30	0.56	0.98	11.13
11	8.25	5.86	0.51	0.26	0.27	0.28	0.43	0.62	11.12
~11.75	0.60	0.60	0.33	0.22	0.22	0.24	0.36	0.50	4.95

are less directly relevant to discussion here but included in appendix F alongside larger versions of tables 7-3 and 8-1.

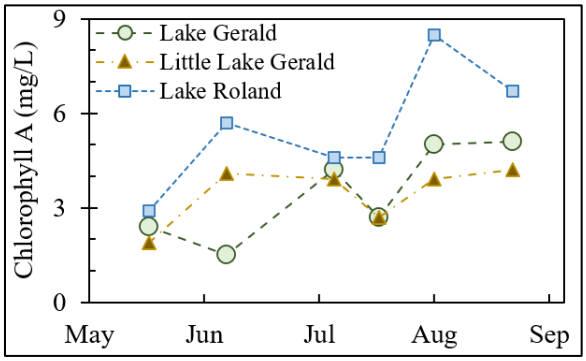

Figure 8-1: 2022 Chlorophyll *a* in Twin Lakes

TP, TOC, TN, and Chlorophyll *a* levels had variable trends during the 2022 monitored season (figures 8-1 & 8-2). Chlorophyll *a* levels climbed into the later summer, indicating increased algal growth (see figure 8-1). TOC, TN, and epilimnetic TP levels remained relatively constant throughout the measurement period. Hypolimnetic and lakebed TP levels climbed during stratification, which is expected from epilimnetic settling and sediment release during periods of low DO. Lake Gerald and Little Lake Gerald observations were typically very similar with a few notable exceptions (i.e. late season hypolimnetic TP) discusses elsewhere. Lake Gerald and Lake Roland generally showed distinct water chemistry (discussed in section 8.3).

Twin Lakes indeed is P-limited based on observed data, indicated by an N:P ratio of greater than 7.2 (Chapra, 2008). The ratio of N to P for any given sample site and instance was 32.8 on average and ranged from 11.9 to 76.9 (for n=66, equally distributed between three basins).

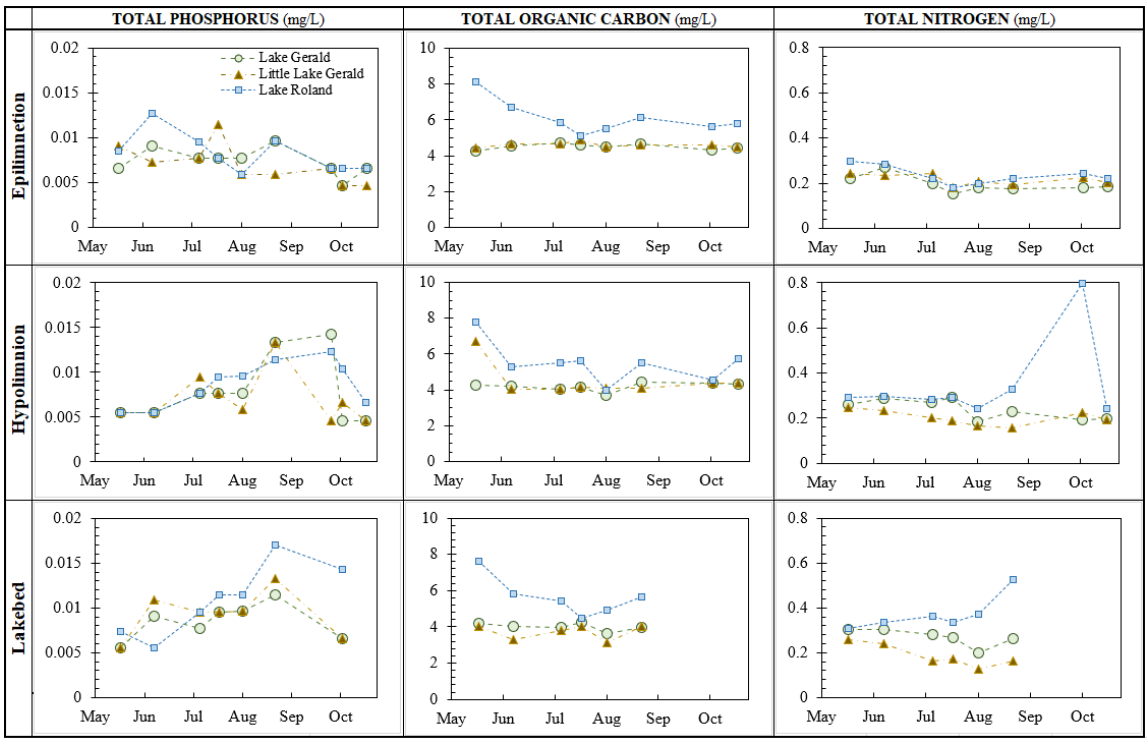

Figure 8-2: Profiles of total phosphorus, total organic carbon, and total nitrogen at three depths in Twin Lakes during the 2022 season; all units are mg / L of the specified species

8.1.2 Historical Profiles

The 2006 USGS profiles reveal similar temperature and DO profile conditions to what was observed in the 2022 season, dating DO depletion at least back that far (figure 8-3). Data from the 1980s through early 2000s from the laboratory courses are inconsistent both in dates of samples, and the amount and type of samples taken. The measurements may have some inaccuracy due to variability and inexperience

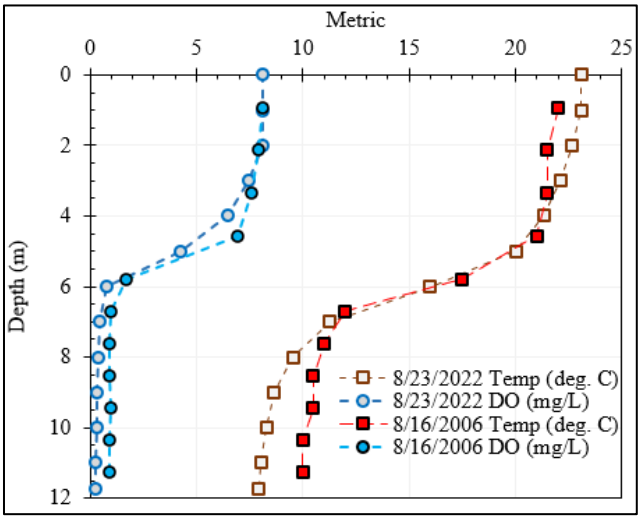

Figure 8-3: August 2006 USGS Lake Roland Profiles compared to August 2023 (USGS, 2006)

of samplers and unknown equipment limitations associated with the nature of a lab course (table 8-2). Thus, these metrics should be taken as generally insightful, rather than specifically accurate.

Laboratory course sampling clearly did not occur at the deep point of the lake, but a thermocline at ~4 meters is still present while stratified (table 8-2). DO depletion in Little Lake Gerald seems to date back to at least the early 1990s, though the earliest sampling years (1979 onward) appeared to be generally after fall turnover, so conclusions cannot be drawn for the 1980s. Similarly, Little Lake Gerald trends should not necessarily be translated directly to the state of Lake Gerald and Lake Roland. Section 8.5.3 discusses the possible history of Twin Lakes water quality in greater detail based on these data, other historical observations, and the phosphorus budget model results.

Table 8-2: Michigan Tech laboratory course dissolved oxygen and temperature profiles for Little Lake Gerald spanning 1979 to 2004; depths at nearest 0.5-meter (Urban, 2022)

Temperature (C)														
Depth (m)	16-Sep-91	17-Sep-90	18-Sep-92	20-Sep-91	20-Sep-04	21-Sep-90	21-Sep-92	29-Sep-80	30-Sep-02	8-Oct-92	11-Oct-79	12-Oct-81	13-Oct-92	22-Oct-81
0.0	18	17	15	13.4	18	14.9	16	12	14.8	11.2	9.5	10.3	9.3	6.5
1.0	18	16	16	13.3	18	14.5	15	11.9	14.2	11.2	9.5	10	9.2	6.2
2.0	17.9	15.5	16	13.3	17.5	14.5	14.8	11.7	14.1	11.2	10	9.7	9.2	6.1
3.0	17	15.2	15	13.2	17	14.5	14.8	11.5	14.1	11.2	10	9.2	9.2	6
4.0	11.9	12.5	14.2	13.1	15.5	13.1	14.2	11.1	13	11.2	9.5	8.8	9.2	6
4.5		10.5		9.2		11.5								
5.0	9.1	10.5	12		11		12.5		13	11.2		8.3	9.5	6
5.5	8.8	10												
Dissolved Oxygen (mg/L)														
Depth (m)	16-Sep-91	17-Sep-90	18-Sep-92	20-Sep-91	20-Sep-04	21-Sep-90	21-Sep-92	29-Sep-80	30-Sep-02	8-Oct-92	11-Oct-79	12-Oct-81	13-Oct-92	22-Oct-81
0.0		6.835	7.33		7.12	7.19	7.35	6.6	5.581	8.16	8.22	9.35		
1.0		6.247	7.37		6.87	7.16	7.32	6.53	5.59	8.03	8.11	9.51		7.8
2.0		5.727	7.24		6.57	6.93	7.35	6.44	5.378	8.05	8.25	9.18		7.75
3.0		6.1	6.26		6.23	7.16	6.92	6.32		8.01	8.08	9.07		5.65
4.0		0	1.66		1.82	7.09	6.38	6		7.79	8	8.82		
4.5			1.68				5.01			7.72				
5.0		0			0				4.823			8.43		

8.1.3 Trophic State & Trends Among Lakes

Trophic status of lakes exists on a continuum, without hard and fast cutoffs between trophic designations. For example, two classifications are presented below (tables 8-3 and 8-4) from two texts on lake ecology and modeling (Chapra, 2008; Schlesinger & Bernhardt, 2013).

Table 8-4: Trophic state classification of lakes adapted from Chapra (2008)

Parameter	Oligotrophic	Mesotrophic	Eutrophic
Total Phosphorus	< 10 ug/L	10 - 20 ug/L	> 20 ug/L
Chlorophyll a	< 4 ug/L	4 - 10 ug/L	> 10 ug/L
Secchi Depth	> 4 m	2 - 4 m	< 2 m
Hypolimnetic O_2 Sat.	> 80%	10 - 80%	< 10%

Table 8-3: Trophic state classification of lakes adapted from Schlesinger and Bernhardt (2013)

Parameter	Oligotrophic	Mesotrophic	Eutrophic
Total Phosphorus	< 7.5 ug/L	5 - 30 ug/L	> 20 ug/L
Total Nitrogen	< 400 ug/L	250 - 600 ug/L	> 500 ug/L
Total Org. Carbon	< 3 mg/L	1 - 5 mg/L	> 5 mg/L
Chlorophyll *a*	< 3 ug/L	2 - 15 ug/L	10 - 500 ug/L

These systems of classification suggest moderate differences in classification by different measurements taken in Twin Lakes throughout the 2022 field season. The results of each system for Twin Lakes are presented in tables 8-5 and 8-6, taking the average and range of values observed in the epilimnion and / or hypolimnion (as applicable). Notably, wherever the average fall in either the oligotrophic or eutrophic classifications, the range of values observed has notable overlap with mesotrophic range (minimum oxygen saturation excluded). Thus, each lake falls best into the mesotrophic category, all component metrics considered; that being said, Lake Gerald and Little Lake Gerald remain nearer oligotrophic than Lake Roland (which leans nearer to eutrophic).

Table 8-5: Twin Lakes 2022 trophic classification by mean and range of each metric per Chapra (2008). Note color-scheme corresponds to table 8-3.

Lake	Total Phosphorus Average *(Range)* [ug/L]	Chlorophyll *a* Average *(Range)* [ug/L]	Minimum Hypolimnetic Oxygen Saturation [%]
Lake Gerald	8.72 *(5.5-14.3)*	3.73 *(1.5-5.1)*	2.2%
Little Lake Gerald	7.32 *(5.5-13.3)*	3.45 *(1.9-4.2)*	2.2%
Lake Roland	10.0 *(5.5-17.0)*	6.02 *(4.6-8.5)*	1.9%

Table 8-6: Twin Lakes 2022 trophic classification by mean and range of each metric per Schlesinger and Bernhardt (2013). Note color-scheme corresponds to table 8-4.

Lake	Total Phosphorus *(Range)* [ug/L]	Total Nitrogen *(Range)* [ug/L]	Total Organic Carbon *(Range)* [mg/L]	Chlorophyll *a* *(Range)* [ug/L]
Lake Gerald	8.72 *(5.5-14.3)*	217 *(127-304)*	4.28 *(3.11-6.68)*	3.7 *(1.5-5.1)*
Little Lake Gerald	7.32 *(5.5-13.3)*	209 *(158-249)*	4.54 *(4.01-6.68)*	3.5 *(1.9-4.2)*
Lake Roland	10.0 *(5.5-17.0)*	313 *(178-796)*	5.75 *(3.95-8.11)*	6.0 *(4.6-8.5)*

The body of profile data demonstrates Little Lake Gerald and Lake Gerald function very similarly, though they stratify as separate basins and flow is generally from (big) Lake Gerald to Little Lake Gerald. Figures 8-1 and 8-2 show TOC, TP, Chlorophyll *a*, and TN tracking at very similar levels in both the epilimnion and hypolimnion in big and Little Lake Gerald (though to a lesser extent in TN). The range of the measured parameters also places these lakes in similar trophic classifications. This supports their grouping as one body for the phosphorus mass balance model. This makes sense given their locational proximity, and the relatively short residence time of Little Lake Gerald (~159 days). Little Lake Gerald retains much of the character of Lake Gerald proper.

Lake Roland, on the other hand, appears quite distinct among the three basins. Figures 8-1 and 8-2 reveal generally higher TOC, TP, Chlorophyll *a*, and TN levels in Lake Roland. Lake Roland also has some hydrologic differences among the lakes which set it

apart; namely, Lake Roland has a more intermittent outflow and a larger evaporative component to regular water losses making it function as a sink of sorts (discussed in section 8.3). Trophic designations, as noted above, point to Lake Roland having notably higher productivity than Lake Gerald. These factors support the two-system nutrient budget model with distinct parameters between Lake Gerald and Lake Roland. Lake Roland may naturally have higher productivity within the Twin Lakes system (making eutrophication symptoms more readily noticeable), or it may simply be more susceptible to eutrophication (which is now observable as the process occurs).

Both Little Lake Gerald's similarity to Lake Gerald proper, and the distinct nature of Lake Roland were visibly noticeable by the researcher given a summer of regular and detailed observation on the lake (i.e. subjective impressions of apparent water clarity, beach quality, algal / plant growth, filtration difficulty, etc.).

8.1.4 Fishery Management Implications

Notable DO depletion was observed throughout Twin Lakes during 2022 (see table 8-1). An oligotrophic system, as Twin Lakes was historically characterized, would not be expected to experience this degree of DO depletion (Chapra, 2008; Schlesinger & Bernhardt, 2013). The hypolimnion of each lake became anaerobic (<1 mg/L) and was near anoxic (<0.2 mg/L) during the 2022 season. Sometimes this deficit extended upward into the bottom of the epilimnion (most prominently in Lake Roland) which is highly uncommon in a low productivity system (see figure 8-4). Formerly successful stocking of cold-water fish (early 1980s) indicates these species historically had a zone of water

which was both cold and oxygenated in which they could pass the summer months, and therefore oxygen depletion must not have been historically present to near the same degree (Madison, 2019, 2022).

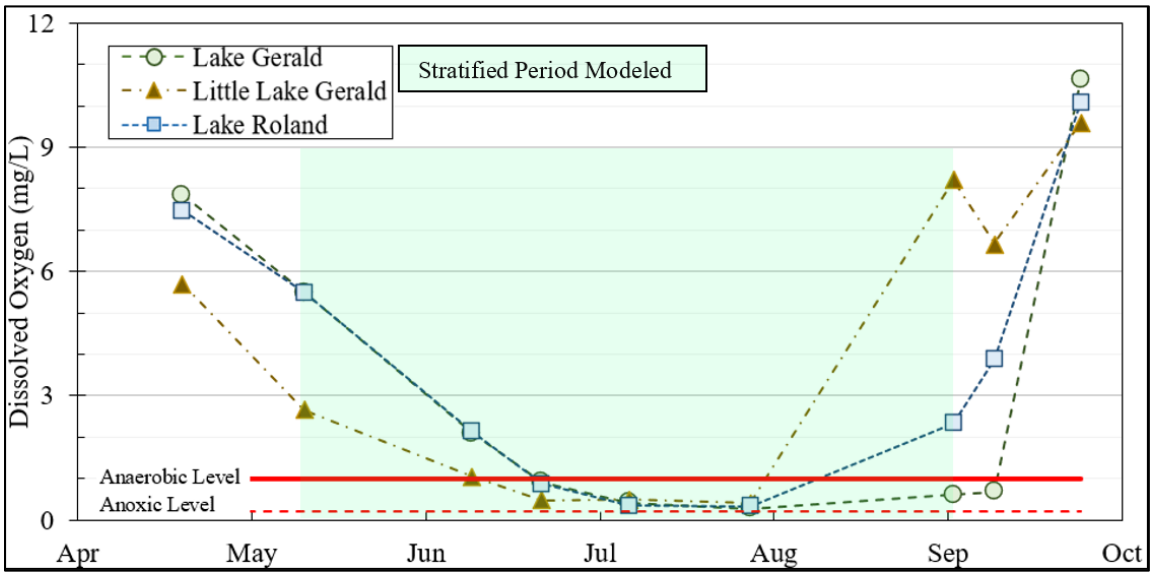

Figure 8-4: 2022 average hypolimnetic (lower water column) dissolved oxygen in Twin Lakes

A DO deficit has very real implications for the fishery of these temperate dimictic lakes. During stratification, the epilimnion is mixed and oxygenated by wind and warmed by the air and sun, but the hypolimnion does not mix with other water, so remains relatively cold and has no fresh oxygen input (Chapra, 2008). The hypolimnions of oligotrophic systems, being cool refugia with relatively oxygenated water (see table 8-3) typically provide both the low temperatures and substantial oxygen cold-water fish need (Chapra, 2008; EGLE, 2006; Wisconsin, 2022). Mesotrophic and eutrophic systems may encounter increasing DO depletion (see table 8-3) and are less commonly supportive of cold-water fish species (Brungs & Jones, 1977; Chapra, 2008; Wisconsin, 2022).

Cold-water fish including rainbow trout, splake, and lake trout have been historically stocked on Twin Lakes, though only winter lake trout stocking (to support ice fishing) is maintained at present (Madison, 2019). Rainbow trout and splake stocking ceased on Twin Lakes due to low survival, which was very likely due to low hypolimnetic DO observed as early as the early 1990s (Madison, 2019, 2022). Further, recent localized fish kills of warm-water species anecdotally support that oxygen depletion may be increasing and impacting more than just cold-water species (Madison, 2019, 2022). The observed DO dynamics in Twin Lakes suggest that both eutrophication is occurring, and any continued cold-water species stocking efforts will increasingly have low survival. The warm-water fishery will be likely less impacted, as those fish live in the warmer more-oxygenated top waters; however, localized fish kills may become more common.

8.2 Shoreline Surveys & Revealed Drivers of Lake Metabolism

Shoreline surveys sought to explore the drivers of shoreline and overall lake water chemistry, and to perhaps identify specific sources of nutrient pollution. The survey approach employs conductivity and nutrient analyses as tracers for potential contamination in the lakes. The results are not conclusive in showing specific pollution sources but provide limited support for the hypothesis.

8.2.1 Spatial Patterns in Water Quality

Heat maps (figure 8-5 below) provide interesting insight into drivers of water quality in Twin Lakes. DOC is notably higher on Lake Roland than Lake Gerald, but with the largest hotspots clearly related to tributary mouths. Similarly, SRP hotspots appear linked to tributaries. This is consistent with the lakes being P-limited, as delivered SRP is likely to be consumed quickly in the lakes. The DN signal is variable, but also shows the largest hotspots at tributary mouths.

The heat map for nitrate + nitrite (figure 8-5) reveals sparing detection, but interestingly the sites with detection are not associated with tributaries as in the case of the other nutrients. This is notable given nitrate + nitrite generally is negligible in natural systems and is linked to nutrient pollution sources (i.e. fertilizers, sanitary sewage, etc.) (ATSDR, 2016; CDC, 2023; EPA, 2015; Reckhow, 1981). As noted above, 12 of the 17 sites with nitrate + nitrite detection occurs on shoreline with some development. Mean detected nitrate + nitrite levels were similar between those 12 developed sites and the 5 undeveloped sites (33.8 μg/L and 33.6 μg/L respectively).

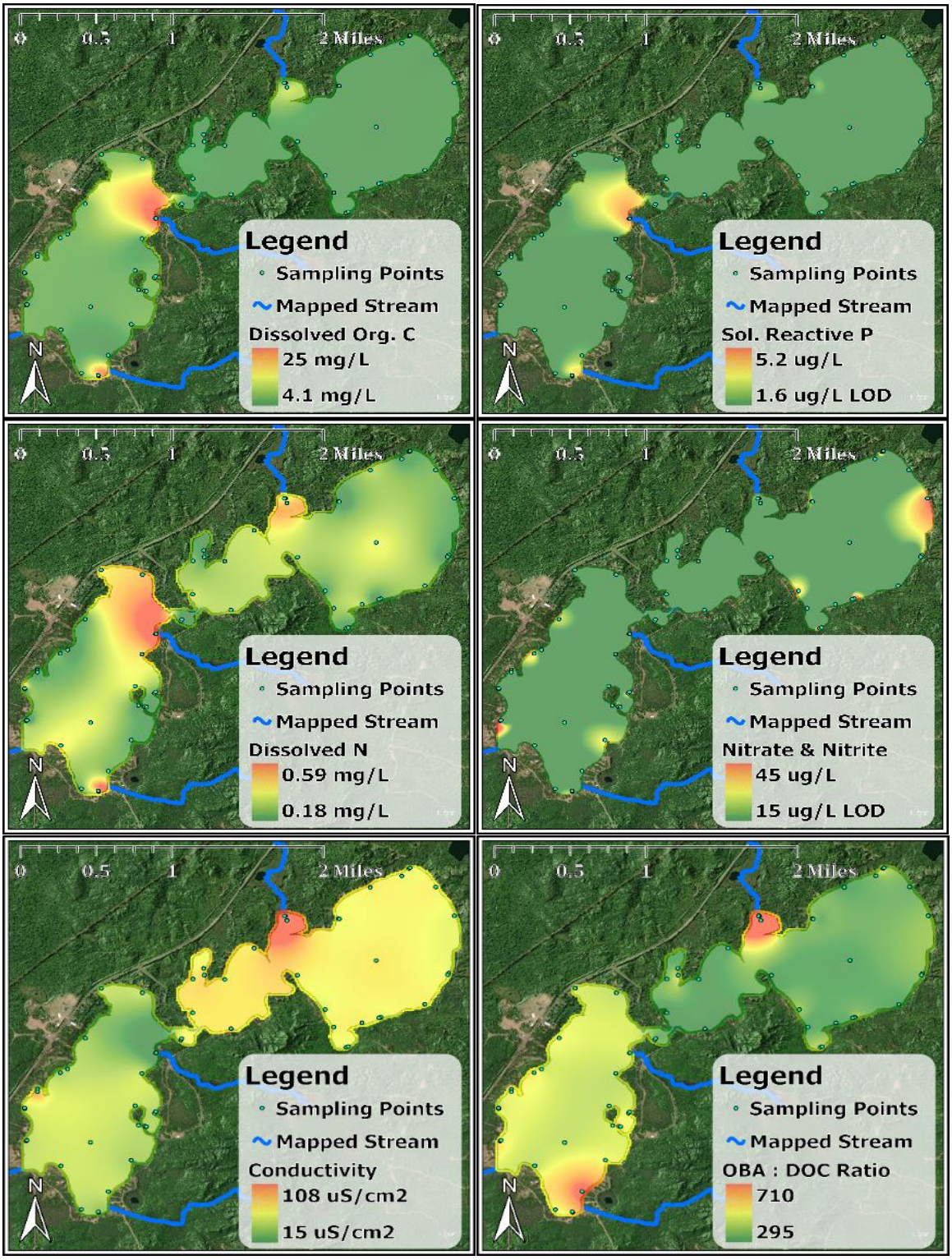

Figure 8-5: Heat maps of dissolved organic carbon (C)*, soluble reactive phosphorus (P), dissolved nitrogen (N), nitrate & nitrite, conductivity*, and the OBA:DOC ratio* from shoreline measurements. Asterisks* indicate statistically significant differences between Lake Gerald & Lake Roland

Figure 8-5 also reveals conductivity as notably higher on Lake Gerald than Lake Roland, with a prominent hotspot at the mouth of the Misery River to the lakes. The mouth of the second largest tributary (on Lake Roland) produces a notable cool-spot on the map. The landcover of these two sub-watersheds is similar (see figure 8-7), except the Misery River is cut north to south by highway M-26. One likely explanation for the elevated conductivity on Lake Gerald is road salt application, which can be retained in soil and elevate receiving water conductivity (Battifarano, 2020; S. Chapra, Dove, & Rockwell, 2009; Kelly, Findlay, Hamilton, Lovett, & Weathers, 2019; McGuire & Judd, 2020). Previous mining activity in the upper Misery River watershed presents a less likely, but alternative explanation (explored at greater length in section 8.5.1). Another explanation worth considering is distinct geology and water flow paths in the Misery River watershed given the Misery River watershed overlies a different bedrock than much of the rest of the Twin Lakes watershed per figure 6-1. This may have some merit, but does not explain the isolated and significant nature of the signal at the Misery River outlet and soils data provides some contradiction to this hypothesis (see section 8.2.2 for a more full discussion).

Figure 8-5 also shows a notably stronger OBA:DOC signal on Lake Roland than Lake Gerald. Section 8.2.2 addresses this in greater detail.

Statistical examination similarly revealed significant differences between Lake Gerald and Lake Roland, but not between developed and undeveloped shoreline sites. No statistical difference ($\alpha=0.05$) for any measured parameter was shown between developed

and undeveloped sites on either Lake Gerald, Lake Roland, or the two lakes taken together. Observations of DOC, conductivity, and the OBA:DOC ratio were significantly different between Lake Roland and Lake Gerald. DOC and the OBA:DOC ratio were greater on Lake Roland, and conductivity was greater on Lake Gerald. No statistical difference was observed between Lake Roland and Lake Gerald for DN. The confidence intervals for tested site groupings are presented in appendix G.

SRP and nitrate + nitrite were excluded from this confidence interval analysis due to a small number of samples with detectable levels (n=12 for SRP, and n=17 for nitrate + nitrite). An insufficient number of detected samples were present to provide robust confidence intervals for subsets of the data. Nitrate + nitrite detections only occurred on the 6/6/22 sampling date; therein, detections more often occurred at developed sites (12 of 17 sites with detectable levels) and had higher mean levels on Lake Gerald (38.3 μg/L for n=8) compared to Lake Roland (29.2 μg/L for n=9). SRP detections were spread between the three shoreline sampling dates and occurred similarly at developed sites compared to undeveloped sites (6 of 10 detection sites were developed). SRP detections were dominated by tributary mouth sites (shown and discussed below). SRP and nitrate + nitrite samples are qualitatively useful, but do not provide direct statistical support for specific patterns in water quality.

8.2.2 Optical Brighteners Results

Being that septic leakage involves slow transport in and dilution by shallow groundwater, it can be very difficult to detect (Dubber & Gill, 2017; Kramer et al., 1996). Similarly,

the transient nature of wastewater flows with facilities usage can make detection spotty. The methodology implemented here has had limited application elsewhere. It assumes laundry detergent OBAs are conservative in groundwater and travel contemporaneously with other septic materials including grey water and fecal matter, generally a good assumption. Because organic matter (OM) can also fluoresce in the same wavelength range as OBAs, the fluorescence signal was normalized to the DOC present at the site (Curtis, 2012; Jourdonnais, 1986; Stanford & Jourdonnais, 1985). This yields an OBA:DOC ratio, which theoretically should remain below a certain threshold except where OBAs are present. This threshold is determined by either A) analysis of a suite of standard solutions containing known quantities of specific OM and OBAs (Stanford & Jourdonnais, 1985), or B) comparison against a local sample which can be considered an undisturbed reference condition (Curtis, 2012; Jourdonnais, 1986; Koopal, 2022). Option A is analytically intensive, requires expensive materials, and requires OM standards which may or may not be representative of OM for the Twin Lakes area; therefore, option B was attempted.

As noted above, there was a statistically significant difference between Lake Roland and Lake Gerald OBA:DOC concentrations, but not between developed and undeveloped sites. The 95% confidence intervals for OBA:DOC on the undeveloped sites fully encompass the confidence intervals of the developed sites. This presents a challenge to setting a threshold for septic contamination. A previous study used a ratio of 380 RFU/mg C/L, which would classify only 22 of 60 observations as uncontaminated (almost all on the less-developed Lake Gerald, and indiscriminate of shoreline

development) (Jourdonnais, 1986; Stanford & Jourdonnais, 1985). Consistently over three visits, the highest OBA:DOC ratios occurred at the mouth of the Misery River, which would otherwise be one of the best candidates to be a reference site. This is for two reasons: 1) The watershed contains essentially no development which would house septic systems, and certainly no septic systems are present near that shoreline, and 2) the site location would not be expected to be influenced by shoreline seepage elsewhere in the lake, because it is in an isolated and undeveloped cove which will flow out to the lake in net from the river's outflow. These factors combine to prevent the establishment of a threshold OBA:DOC value which would indicate septic contamination.

The fluorescence signal does not seem to linearly increase with DOC concentration. If that were the case, one would expect this normalization approach to remove any correlation of the fluorescence signal to DOC (according to the ratio OBA/DOC directly). The critical Pearson's correlation coefficient (r-crit), above which would indicate relationship between DOC and OBA:DOC, is 0.2542 (assuming normality of data and n=60, α=0.05, & 2-tails). The Pearson's r value comparing OBA:DOC to DOC is 0.8372, indicating a very significant relationship (alternatively: $p=0.011 < 0.05$ by ANOVA). It appears that DOC concentration still generally drives the OBA:DOC ratio in the methodology employed. This calls the usefulness of this method to question for at least some circumstances and sites.

Alternative methods of DOC normalization were attempted including OBA:Log(DOC), $OBA:DOC^2$, and $OBA:DOC^{0.5}$. Each of these approaches yielded a still-significant

relationship between DOC and the normalization result (see appendix H). The ratio of $OBA:DOC^n$ was also attempted, where n was varied (Excel Data Analysis GRG Nonlinear solver) to minimize the Pearson's correlation coefficient (Excel CORREL function) between OBA values and $OBA:DOC^n$ values. The resulting value of n was 1.178, and yielded an r value of -2.43E-8 (alternatively: $p=0.9999 >> 0.05$ by ANOVA), meaning the normalized ratio was no longer influenced by DOC. This method was discarded as well though, because the highest normalized values still corresponded to very undeveloped sites, and no significant difference between developed and undeveloped sites was present throughout the dataset. This analysis suggests insufficient statistical backing for the methodology as employed for Twin Lakes.

This examination helps elucidate some of the factors which may enable the method to be successful or not. In the first published application of this method by another group, where a threshold OBA:DOC of 380 was proposed, the environmental DOC concentrations were notably lower (0.16 – 6.61 mg C/L) than on Twin Lakes (4.15 – 24.89 mg C/L), and standards were prepared with water from a nearby bog spiked with pure OBAs (Stanford & Jourdonnais, 1985). A subsequent study applied the same threshold to a different nearby lake with similarly low DOC, assuming comparable conditions (Jourdonnais, 1986). A more recent study with different equipment used the highest value of any "reference" site (with presumed low background levels) to set a threshold ratio of 22.7; notably, this lake also had lower DOC levels than Twin Lakes (generally ~2 mg C/L with maximum of 7.58 mg C/L) (Curtis, 2012; Koopal, 2022).

Another method of septic detection using UV light exposure was considered and may have merit for future work (Cao et al., 2009; Dubber & Gill, 2017). This approach had highly successful lab calibration, but was applied at miniscule level of dissolved organic matter (DOM) (<1 μg C/L) relative to what was observed on Twin Lakes (4.15 – 24.89 mg C/L) (Cao et al., 2009; Dubber & Gill, 2017). The study had mixed success in identifying OBAs presence positively in sanitary sewer streams which could be expected to have relatively high levels of OBAs (Cao et al., 2009; Dubber & Gill, 2017). This method was not employed due to calibration at conditions not representative of natural systems and mixed results in another application, but it may be worth considering for lake applications if the OBA:DOC ratio methodology cannot be generally applied. Further work on these methodologies is likely required for their successful application on lakes with typical DOC levels above 2-4 mg C/L.

Considering the OBA:DOC heat map conceptually may still provide some useful insight. Figure 8-5 shows a generally higher OBA:DOC ratio on Lake Roland, and apparent hot spots at the inflow of the Misery River to Lake Gerald and just north of the southern-most tributary to Lake Roland. The methodology employed would anticipate DOC hotspots being knocked down and new "warmer" areas to emerge identifying locations of leaking septic systems. Curiously, this does not happen at the Misery River mouth on Lake Gerald, but does happen at the mouth of the next larger tributary on Lake Roland. This may be due to different types of OM present and delivered by each tributary. It may also be that there is some impact of conductivity or water age to this metric (discussed below). More notably, a hotspot appears on the south end of Lake Roland in figure 8-5's

OBA:DOC map which was not present in the DOC map. A small tributary (80 ha watershed by figure 8-8) had a notably high DOC signal in figure 8-5, but that signal is reduced with OBA:DOC normalization. Just north of that tributary though, an OBA:DOC hotspot forms. That site was a very sandy-shored location near a number of residences which were developed between 1998 and 2009. One sample instance is not sufficient to conclusively prove septic leakage, but that area may be worthy of further examination. Further, the age of these developments makes them relatively low-risk candidates for leakage relative to the rest of the lake; this may indicate substantially more widespread leakage, with any particular leak having low odds of detection. On the other hand, it could be an artifact of a methodology which requires more rigorous development. Taken in light of the other portions of shoreline surveys, the results do not refute, and may limitedly support the hypothesis of leaking septic systems on Twin Lakes.

An interesting relationship is apparent between the OBA:DOC ratio (& similarly with only DOC) and conductivity at shoreline survey sites. Figure 8-6 shows a strong relationship between OBA:DOC and conductivity, as well as between DOC and conductivity (slightly less strong) when visual outliers are removed. These outliers generally were sites with particularly high DOC levels, like tributary inlets (see figure 8-5). This relationship is greatly disrupted by the outlying points. The source of this correlation is not fully clear, but may be related to time of water spent in the Twin Lakes system; moving downstream in the Twin Lakes chain, the DOC tends to increase and conductivity tends to decrease (discussed in section 8.3); therefore, the perceived relationship may simply be a function of coincident trends in the lakes. This would make

outlying values at specific sites to be expected. Alternatively, this may demonstrate different flow paths between the lakes. More substantial groundwater contribution could result in higher conductivity and lower DOC relative to overland and surface flow. The outliers would be expected to be dominantly tributaries in that case; about half the outliers are at tributary mouths, and not all tributary mouth measurements were outliers. If hydrologic sources were distinct between the lakes though, further gauging and water quality testing on different tributaries would be ideal to elucidate underlying processes. The land areas directly contributing to each lake overlay somewhat different bedrock geologies, which would lend to this theory (see figure 6-1); however, the groundwater table depth in the land area contributing to Lake Roland is comparable or higher than that contributing to Lake Gerald, which would lend slightly to a higher fraction groundwater in waters contributing to Lake Roland (and expected lower DOC and higher conductivity), which is the apparent opposite of what is seen on the lakes (NRCS, 2022). Additionally, if geology

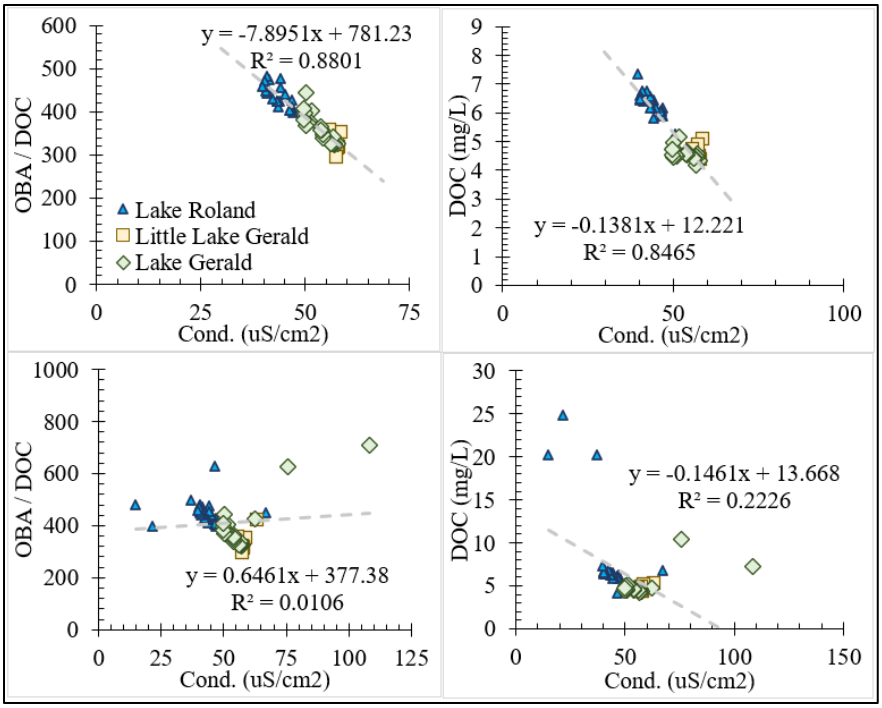

Figure 8-6: Conductivity trending with DOC and the OBA:DOC ratio at shoreline survey sites with n=9 outliers corresponding to 6 shoreline sites removed (top plots) and outliers retained (bottom plots).

were the only driver of the conductivity signal, a hot spot in the farthest north corner of Lake Gerald (at a drainage outlet per figure 6-1) might be expected because that drainage largely overlies the same geologic formation, but this is not seen in figure 8-5.

8.2.3 Shoreline Survey Conclusions & Limitations

Elevated conductivity in the Misery River points to likely road salt contamination which is not present in the other tributaries to Twin Lakes. Further work could confirm road salt as the source of this elevated conductivity (i.e. looking for increased conductivity moving down the watershed or measuring salts directly, rather than using conductivity as a proxy). The lake water column experienced conductivity levels with mean of 46.5 $\mu S/cm^2$ and a range 30.4 - 81.6 $\mu S/cm^2$. Monitoring the rate of conductivity increase may prove valuable to understand the risk truly posed by this contamination into the future. Further examination of the Erie-Ontario Mine (discussed later) would be wise to eliminate the mine as a potential source of elevated conductivity.

Nutrient pollution is likely occurring on Twin Lakes from residential sources, but no specific identified point source stems from these analyses. Nitrate + nitrite signals generally located near developed sites provide some limited backing for residential nutrient pollution which may include fertilizer runoff, septic leakage, or yard waste disposal and decomposition. Similarly, OBA:DOC trends, though messy, may indicate some level of leaking septic systems. Indeed, septic systems leaks are likely present based on historical infrastructure data. In a 2015 lake level study, OHM Advisers noted at least 8 low-lying or near-shore septic systems on Twin Lakes, with many more septic

systems present (Wright, 2015). The operating life of a modern septic system is ~15-40 years (assuming regular pumping & inspection every ~3-5 years), making any system installed before 1983 due for replacement (Dersch, 2017; EPA, 2022). Most occupied lots on Twin Lakes were developed before 1983 aerial imagery, with a significant number developed even before 1943 (NETRONLINE, 2022). Additionally, the Natural Resource Conservation Service rates all soils surrounding Twin Lakes "Very Limited" for septic drain fields meaning they can expect "poor performance and high maintenance," (NRCS, 2022). It is further likely that many of the existing septic tanks are not serviced regularly. The Spreadsheet Tool for Estimating Pollutant Loads (STEPL) produced by the US Environmental Protection Agency (EPA) estimates that leaking septic tanks have capacity to produce substantial quantities of TP deliverable to the lakes (examined at greater length in section 8.4.1) (TetraTech, 2018). Shoreline survey evidence for residential nutrient pollution is not overly quantitative, but qualitatively supports the hypothesis based on historical infrastructure records and site conditions. This is further substantiated by the modeled "residual load" discussed in detail in section 8.4.

Tributaries have an outsized impact on shoreline water quality near their outlets, making watershed management critically linked to Twin Lakes water quality. Figure 8-5 shows DOC, SRP, and DN hotspots clearly linked to stream mouths. Conductivity in figure 8-5 similarly seems to act as a tracer for the two largest inflowing tributaries, with a high conductivity inflow resulting in higher conductivity on Lake Gerald and a low conductivity inflow at the head of Lake Roland seeming to dilute the conductivity of the water it receives from Lake Gerald. Tributaries contribute about 23% of the P load

(discussed in section 8.4), making them a notable loading source. Therefore, effective nutrient management in watersheds contributing to Twin Lakes is essential to restoring and maintaining a healthy system. Twin Lakes' contributing sub-watersheds contain no agriculture and are primarily upland forest (see figure 8-7), with logging as the main disturbance on the broad landscape. Therefore, maintenance of best management practices (BMPs) by logging operations would likely limit sediment and nutrient delivery to runoff, streams, and eventually the lakes. Appendix I contains a more detailed breakdown of NLCD land cover for this area.

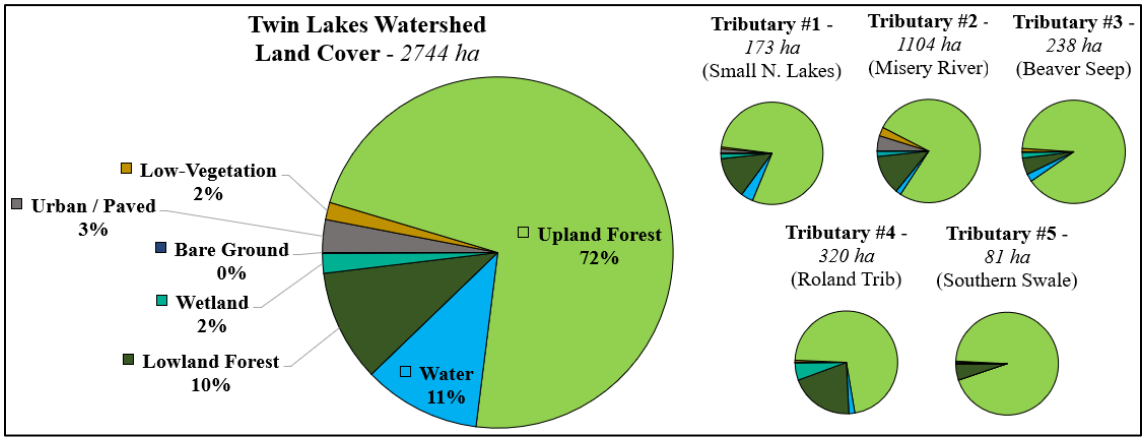

Figure 8-7: Land cover of Twin Lakes watershed by generalized categories of the NLCD (NLCD, 2016). Tributaries are numbered by their outlet to Twin Lakes north to south.

It makes sense that tributary influence alone would show up so clearly on the shoreline survey heat maps (figure 8-5), though it is not the only notable nutrient loading source. This is because all other loads (i.e. atmospheric deposition, anthropogenic loads, & internal loads) would be expected to be non-point loads either dispersed across the lake area or along the shorelines. Large residential pollutant sources may or may not show up

as hotspots as well. Tributaries are large contributors though, with only a distinct few main entrance points to Twin Lakes, making their conspicuous presence in the heat maps logical.

The nutrient budget model assumes that all streamflow delivery and nutrient loading (P in particular) can be scaled directly by watershed area to the Misery River, which was gauged and sampled at M-26 upstream of the lakes. If that assumption is incorrect, it would impact understanding of the results. Figure 8-5 seems to show "hotter" spots from the second largest tributary compared to the Misery River with respect to SRP, DOC, and DN. This may mean that this other tributary contributed disproportionately more nutrients; however, the Misery River mouth sampled during shoreline samples is downstream of a large wetland-pond complex which is hydrologically connected to the lakes and likely moderates nutrient levels before the lake-proper. The Misery River ponds are conceptually included in Lake Gerald in the model, because the gauging station is upstream of them at M-26. This is unlike the second largest tributary, which discharges distinctly at the Twin Lakes shoreline. The TP samples taken on the upstream Misery River gauge were notably higher (6.6 to 33.4 μg/L with mean of 12.4 μg/L and n=15) than those on Lake Gerald (5.5 to 14.3 μg/L with mean of 7.9 μg/L and n=28), supporting this assessment. Further, no other tributaries sampled (the rest of which were very small) exhibit this disproportionate hotspot. Therefore, the loading rate measured at the Misery River gauging station is taken as the most reliable metric available. Any error here would be rolled into the "residual load" of the nutrient budget. Given greater resources, or in

future work, gauging or paired TP samples with both the Misery River and that next largest tributary would be ideal.

Shoreline surveys provide utility in the diagnosis of lake conditions with notable limitations. Shoreline surveys were not intended to quantitatively construct a model of the lake, but do provide general ranges on shoreline water quality metrics on Twin Lakes. They also provide useful visual tools which supplement the understanding of the lake set forth by the formal nutrient budget. Low levels of SRP and nitrate + nitrite in particular limit the interpretation possible of those data. 60 visits across 42 sites was a relatively small sampling of shoreline conditions, and conditions may vary notably from those seen on the three days of shoreline survey. Weather conditions may also impact the results – each shoreline survey day was during a relatively dry period with cloudy/foggy morning conditions giving way to sunny afternoon skies. Specifically, waste indicators (like OBAs in this case), have been shown to have variable signals with different hydrologic conditions (Nshimyimana et al., 2018; Verhougstraete, Martin, Kendall, Hyndman, & Rose, 2015). Conditions following notable rain could provide an alternative and useful picture of nutrient conditions and sources along the shores of Twin Lakes.

The use of OBAs as a septic tracer in this work is also notably limited. Similarly to the other metrics, small number of sites (relative to total shoreline) and limited ability to capture all shoreline variability certainly render the method as applied challenging on its face. Further, the resulting inability to set a baseline condition consistent with application in other instances poses a challenge to the utility of the method. Further work to

understand how DOC and OBA fluorescence across a range of environmental conditions is merited. In particular, application to environments not low in DOC and across a large range of DOC types may need further investigation. More rigorous testing of a natural systems-applied UV exposure application to OBA detection would be warranted as an alternative method for OBA-based septic tracer taction.

8.3 System Hydrology & Implications for Lake Health

The Twin Lakes system acts as a "drainage" lake system with surface water runoff largely driving flow through the system (WI-DNR, 2022). Very low baseflow conditions were present through the bulk of the 170-day gauged season with often near-zero flow at the lakes' outlet. Almost all Lake Roland outflow (~98.2% of total gauged outflow volume) was during spring runoff or following distinct rain events. This is consistent with previous observations of sustained low summer flow before the installation of the current weir structure on Emily Lake Rd. (Wright, 2015); this is likely due to a combination of relatively high evaporation (compared to lake volume) on Lake Roland over Lake Gerald and operation of the weir to maintain a goal water level during the summer season when the lake would be expected to be low. The lakes' area of 221.4 hectares is 8.07% of the total watershed area including the lakes (2744.1 hectares). Several distinct drainages are present entering Twin Lakes, with the Misery River being the only named drainage and the largest (38.2%

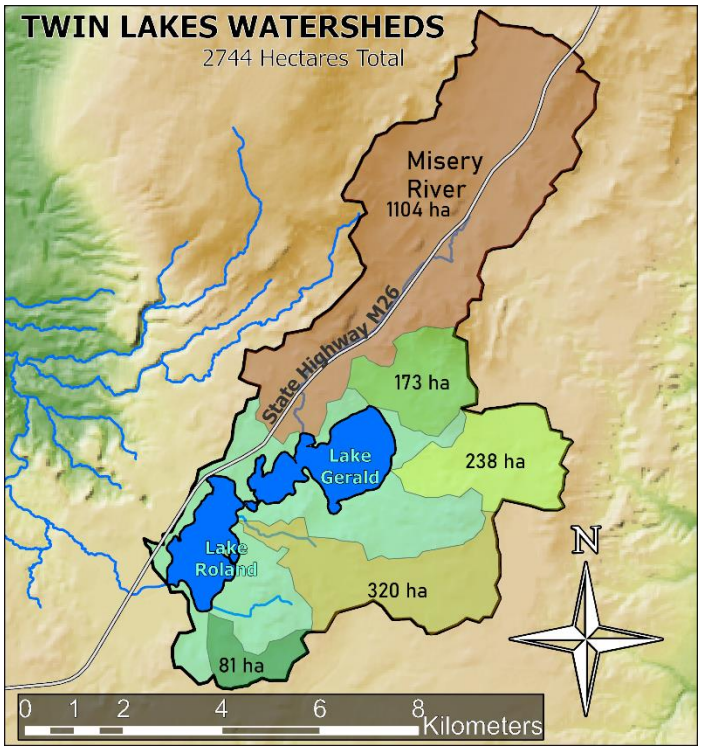

Figure 8-8: Twin Lakes watershed including largest five contributing subbasins

of watershed area). Figure 8-8 shows the five largest distinct drainages, while Table 8-7 summarizes some hydrologic characteristics of the Twin Lakes system.

Table 8-7: Hydrologic characteristics of Twin Lakes system.

Parameter	Big Lake Gerald	Little Lake Gerald	Lake Gerald	Lake Roland	TWIN LAKES
Base Inflow (m^3/hr)	75	67	75	94	106
Average Inflow (m^3/hr)	277	311	289	411	389
Base Outflow (m^3/hr)	63	67	67	7	7
Average Outflow (m^3/hr)	299	312	312	397	397
Lake Volume (m^3)	6,956,409	1,185,118	8,141,527	4,701,701	12,843,227
Surface Area (m^2)	1,147,641	327,898	1,475,539	1,112,688	2,588,227
Residence Time (days)	970	159	1129	493	1622
Epilimnetic Residence Time (days)	726	121	847	428	1275
Flushing Rate (/year)	0.376	2.303	0.323	0.740	0.225

The lake levels varied by as much 0.34 meters during the gauged season minimum (361.93 m on 9/16) to maximum (362.27 m on 5/27). Very broadly, significant inflow and outflow was observed in the lakes during spring melt, followed by low baseflow conditions through most of the stratified period. Late summer and fall once again saw increased rainfall and streamflow, refilling the lakes to a degree. One large storm event occurred July 4th into July 5th, which produced significant flow of the same order as spring and fall events. The outflow weir system was effective in controlling water levels – indeed, the weirs had all three logs in place for most of the stratified period maintaining relatively constant water levels. During spring melt, late season increased rainfall, and after large storms the water level would quickly rise on the lakes and typically one (but sometimes two) logs would be lifted, which would create a very large outflow and quickly return water levels to near their previous level. Figure 8-9 shows the components of the 2022 water budget for all of Twin Lakes broadly.

Recall, no groundwater flow in or out of the lakes was considered (see section 7.2.2) because the water budget balanced well without groundwater and data was not available. Error in evaporation estimation, for example, could obscure a groundwater flow out of Lake Roland which would result in the low outflow observed, which would confound the proposed sink effect here.

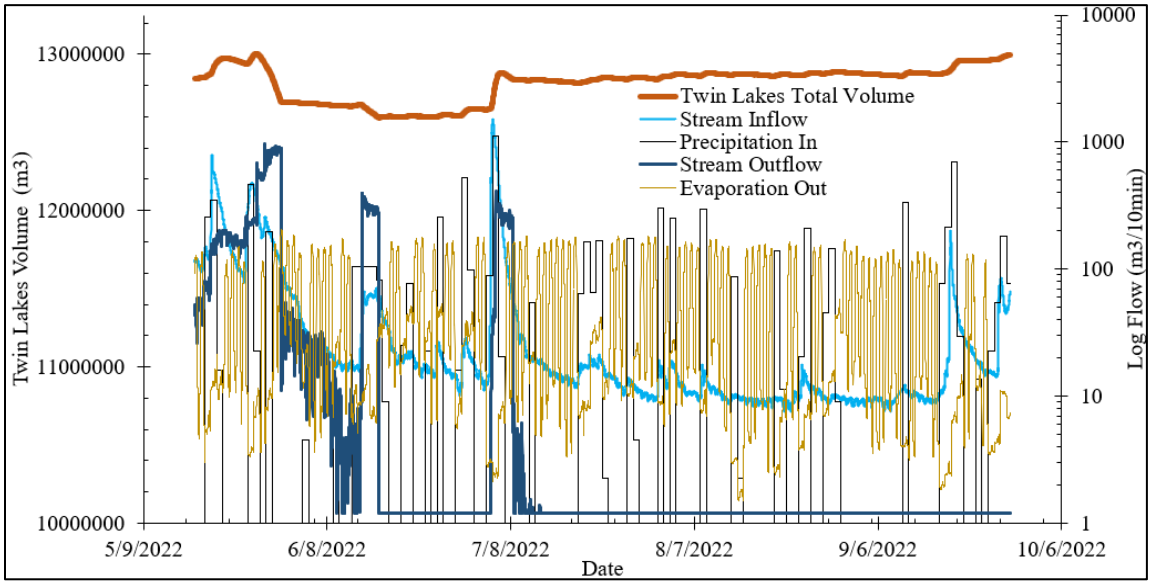

Figure 8-9: Twin Lakes volume (left axis) with inflows and outflows (right axis) for 2022 gauged season

TP sampling at the Misery River inflow gauge revealed a significant correlation between streamflow and TP concentration ($p<0.05$ see figure 8-10). This relationship was applied through the whole gauged season to all inflow. No sampling occurred on other smaller drainages to verify that this relationship holds in the other portions of the watershed. Shoreline sampling results imply that this assumption may or may not be accurate (see figure 8-5), as discussed in section 8.2. TP sampling at the lake outlet revealed no such

significant correlation in flow and phosphorus concentration. Linear interpolation was applied between sampling dates to build a continuous record of outflowing phosphorus concentrations. This makes sense given that the phosphorus dynamics in the lake feeding the outflow would control outflowing TP, rather than watershed hydrology as in the inflow.

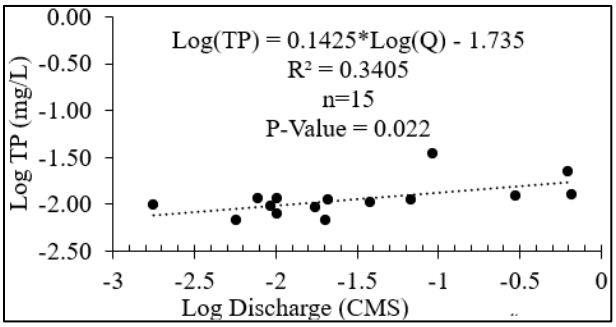

Figure 8-10: Flow-Concentration relationship for total phosphorus (TP) in the Misery River.

Interestingly, as the lowest lake in the system, Lake Roland seems to act as a sink of sorts, with substantial evaporation and very little outflow to match what it gains from upstream. This would point to an expected increase in nutrient concentrations and resulting productivity in Lake Roland relative to the other lakes. This is supported by both the shoreline survey and lake profiles water sampling performed. During profile sampling, chlorophyll *a*, TP, TOC, and TN concentrations were consistently higher in Lake Roland than either Lake Gerald or Little Lake Gerald (see figures 8-1 & 8-2). Similarly, during shoreline surveys, DOC and optical brightener signals were notably higher in sites on Lake Roland. Sample filtration was not timed but took noticeably longer on Lake Roland, often requiring multiple filters to obtain required sample volumes, which was never necessary on Lake Gerald. Conductivity, however, decreased in Lake Roland. Conductivity appears to be elevated in Lake Gerald due to high conductivity at the Misery River outlet, but then diluted in Lake Roland by the low-conductivity inflow from other tributaries (see figure 8-5). This is important to

understanding any eutrophication in the Twin Lakes system because the impacts of any eutrophication will likely be seen more quickly and more dramatically on Lake Roland if it acts as a sink for the watershed. Phosphorus will accumulate in Lake Roland without being flushed as quickly as in the upper lakes, accelerating productivity in the lake disproportionately to the other lakes. This is further supported by the greater symptoms of eutrophication already observed on Lake Roland including faster and greater DO depletion and higher productivity as indicated by Chlorophyll *a* concentrations.

8.4 Nutrient Budget & The Role of Phosphorus

8.4.1 Stratified Period 2022 Phosphorus Budget

For the 2022 stratified season, the two-box model of Lake Gerald and Lake Roland in series yields results consistent with a historically oligotrophic system. The budget shows watershed loading, internal sediment loads, atmospheric deposition, and the calculated "residual load" are all important components of the current overall sources of P to the lakes. Figure 8-11 shows the overall modeled P budget for Twin Lakes. During the stratified period, total P inputs to the lakes exceeded outputs, which is to be expected for this period as residential presence increases, DO depletion enables hypolimnetic P release, P is bound by growing aquatic life, and lower summer lake outflows remove less P. Larger outflow magnitudes and decreased loads during the fall through spring period would be expected to see outputs exceed inputs and more closely balance the nutrient budget. Atmospheric deposition, often a relatively small contributor to overall P budgets, is the largest single contributor to Twin Lakes as modeled, though it remains relatively low in overall magnitude (compare to Han, Bosch, and Allan (2011);

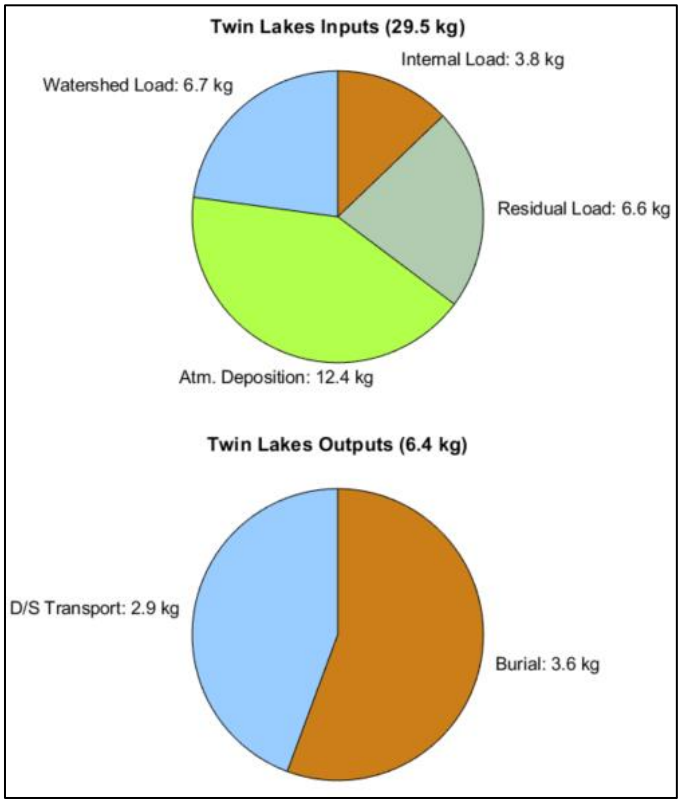

Figure 8-11: Total phosphorus inputs and outputs to the Twin Lakes system as modeled for the 2022 stratified season

Hoverson (2008); James, Barko, Eakin, and Sorge (2002); & Pelletier and Welch (1987)). This supports the historical classification of Twin Lakes as oligotrophic. Further, the relatively low loading rates observed here demonstrate potential for disruption by minor changes to the system. For example, *X* kg of added P loading would be a relatively larger fractional increase to TP in Twin Lakes relative to another lake with larger overall P budget, and would thus be expected to have disproportionately large impacts.

Examining the TP budgets of Lake Gerald and Lake Roland individually demonstrates interesting differences between the lakes (figure 8-12). Notably, the internal load and burial components of the budget are inverse processes; both burial of particulate P and release of P during anoxic periods is likely occurring in the hypolimnions of both lakes. The net flux at the sediment surface is considered for the model; thus, Lake Gerald is modeled with net P release from sediments and Lake Roland is modeled with net P burial in the sediment. This makes sense given a larger hypolimnion and hypolimnetic lakebed alongside lower overall TP levels in Lake Gerald; consequently, less hypolimnetic P is present for sedimentation and similar sediment P is available for release over a larger area experiencing similar oxygen depletion (see table 8-1). The result is Lake Gerald exhibiting a net internal load while Lake Roland experiences a net burial of P in the hypolimnion. Due to a larger directly contributing watershed area and lake surface area in Lake Gerald (1994 ha watershed & 114.8 ha surface area) compared to Lake Roland (749 ha watershed excluding Lake Gerald drainage area & 111.3 ha surface area) along with net internal loading, Lake Gerald experiences greater overall P loading than Lake Roland (19.3 kg and 13.2 kg respectively), yet retains more low-productivity character than Lake

Roland (see section 8.1). This may seem counterintuitive, but Lake Gerald is a much larger lake (8.14E6 m^3) than Lake Roland (4.70E6 m^3) and does not experience the same "sink" effect that Lake Roland does (see section 8.3). These factors combine to increase productivity in Lake Roland more than in Lake Gerald.

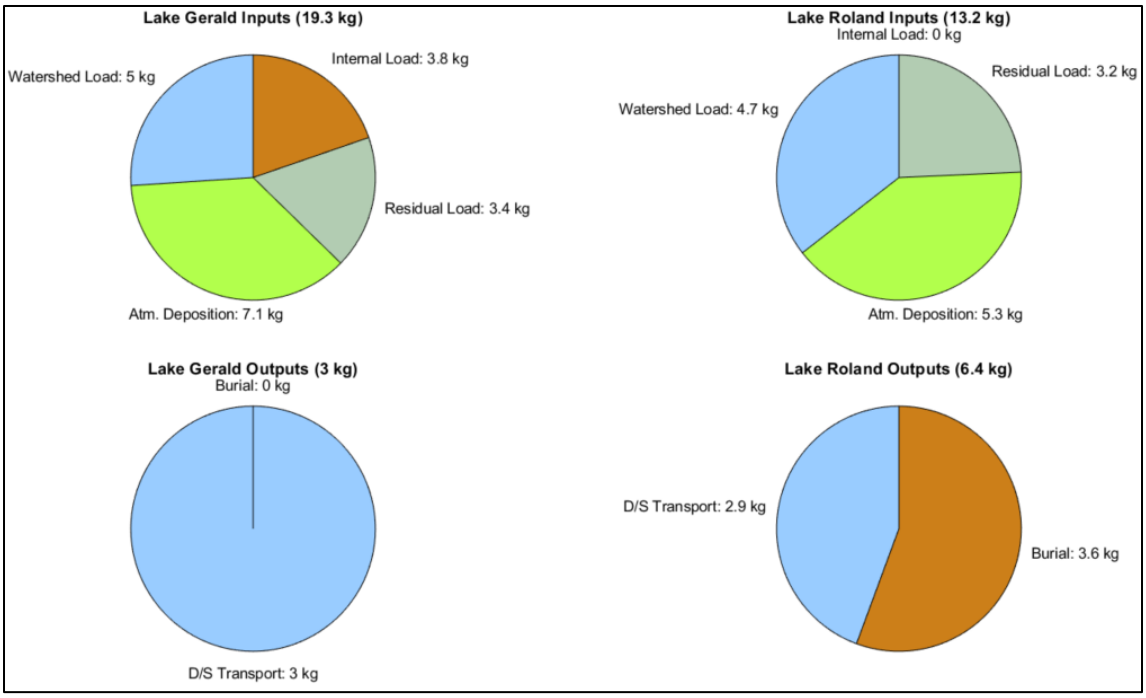

Figure 8-12: Total phosphorus inputs and outputs to both Lake Gerald and Lake Roland as modeled for the 2022 stratified season

The residual load is a calibrated parameter (see section 7.4.3), which accounts for error in the other model components with the otherwise excluded anthropogenic load to the system. The latter was assumed to dominate the residual load, so the residual loading rate was taken as a function of overall shoreline length and developed shoreline density on the lakes. Lake Gerald's overall residual load is marginally higher than on Lake Roland due to a longer shoreline (8.18 km vs. 6.83 km receptively) despite a lower development density (13.1 vs. 14.9 developments/km respectively). The loading rates applied to each

lake are similar, with Lake Roland's (4,185 mg P/km shoreline/day) higher than Lake Gerald's (3,679 mg P/km shoreline/day), which is direct function of shoreline development density. The magnitude of the residual load is certainly within a reasonable range of possibility for anthropogenic sources. Considering the potential septic load alone, the Spreadsheet Tool for Estimating Pollutant Loads (STEPL) produced by the US Environmental Protection Agency (EPA) can be employed to provide an upward bound on the amount of total phosphorus possibly delivered to the lakes (TetraTech, 2018). Assuming one septic tank per developed site with 2.43 persons/development, a 100% septic failure rate (but no direct waste outfalls to the lakes), and a mid-range septic overcharge rate (70 gal/person/day), the developments surrounding the Twin Lakes system have the capacity to produce 354 kg of deliverable TP during the 112-day stratified period. If only 2% of developments have leaking septic systems (~4 residences), under these assumptions, a TP load of 7.1 kg is estimated for the stratified season, alone exceeding the estimated residual load.

Table 8-8 contains a tabulated nutrient budget for 1) each modeled lake layer 2) Lake Gerald and Lake Roland individually, and 3) for Twin Lakes overall. Note that due to the lakes operating in series with overlapping watersheds and flow between the lakes, the mass of TP associated with the overall Twin Lakes budget in any component is not necessarily the sum of component processes on each lake. A positive "net exchange" indicates accumulation (positive change in storage) in that pool during the model period, which is seen throughout the lakes for the stratified period. This net accumulation through the stratified season was observed with sampling as well. Data was not collected

or modeled for the non-stratified period, but net export would be expected for fall through spring. Appendix J contains alternative conceptualizations of the nutrient budget components demonstrating overall magnitude for each component process and each lake.

Table 8-8: Tabulated total phosphorus budget for Twin Lakes with budget components of each modeled lake segment for stratified 2022 season

LAKE GERALD	
Epilimnetic Nutrient Budget (kg):	
Watershed Loading	5.02
Atmospheric Deposition	7.06
Anthropogenic Loading	3.39
Total Inputs:	**15.46**
Diffusion	**2.24**
Downstream Transport	2.97
Settling	13.67
Total Outputs:	**16.65**
NET EXCHANGE:	***1.05***
Hypolimnetic Nutrient Budget (kg):	
Settling	13.67
Internal Load	3.79
Total Inputs:	**13.67**
Diffusion	**-2.24**
Burial	0.00
Total Outputs:	**0.00**
NET EXCHANGE:	***11.43***
Total Nutrient Budget (kg):	
Watershed Loading	5.02
Atmospheric Deposition	7.06
Internal Load	3.79
Residual Loading	3.39
Total Inputs	**19.26**
Downstream Transport	-2.97
Burial	0.00
Total Outputs	**-2.97**
NET EXCHANGE:	**16.28**

LAKE ROLAND	
Epilimnetic Nutrient Budget (kg):	
Watershed Loading	4.71
Atmospheric Deposition	5.32
Anthropogenic Loading	3.22
Total Inputs:	**13.25**
Diffusion	**-0.09**
Downstream Transport	2.86
Settling	7.85
Total Outputs:	**10.70**
NET EXCHANGE:	***2.45***
Hypolimnetic Nutrient Budget (kg):	
Settling	7.85
Internal Load	0.00
Total Inputs:	**7.85**
Diffusion	**0.09**
Burial	3.59
Total Outputs:	**3.59**
NET EXCHANGE:	***4.35***
Total Nutrient Budget (kg):	
Watershed Loading	4.71
Atmospheric Deposition	5.32
Internal Load	0.00
Residual Loading	3.22
Total Inputs:	**13.25**
Downstream Transport	-2.86
Burial	-3.59
Total Outputs:	**-6.44**
NET EXCHANGE:	**6.81**

TOTAL TWIN LAKES	
Epilimnetic Nutrient Budget (kg):	
Watershed Loading	6.75
Atmospheric Deposition	12.38
Anthropogenic Loading	6.61
Total Inputs:	**25.74**
Diffusion	**2.15**
Downstream Transport	2.86
Settling	21.52
Total Outputs:	**24.38**
NET EXCHANGE:	**3.51**
Hypolimnetic Nutrient Budget (kg):	
Settling	21.52
Internal Load	3.79
Total Inputs:	**21.52**
Diffusion	**-2.15**
Burial	3.59
Total Outputs:	**3.59**
NET EXCHANGE:	**15.79**
Total Nutrient Budget (kg):	
Watershed Loading	6.75
Atmospheric Deposition	12.38
Internal Load	3.79
Residual Loading	6.61
Total Inputs:	**29.53**
Downstream Transport	-2.86
Burial	-3.59
Total Outputs:	**-6.44**
NET EXCHANGE:	**23.09**

Note: Diffusion is an internal process, with a positive value corresponding to net movement from the hypolimnion to the epilimnion.

8.4.2 Discussion of Validation & Sensitivity Analysis Implications

Final model fit to this small number of data points (n=20 when excluding initial conditions) is quite good visually (figure 8-13). This, combined with a low NRMSE and

optimized parameters which fell well within the reasonable literature range led to the acceptance of the model output (see section 7.4.3). Here, the implications of the model fit, validation, and sensitivity analysis are addressed.

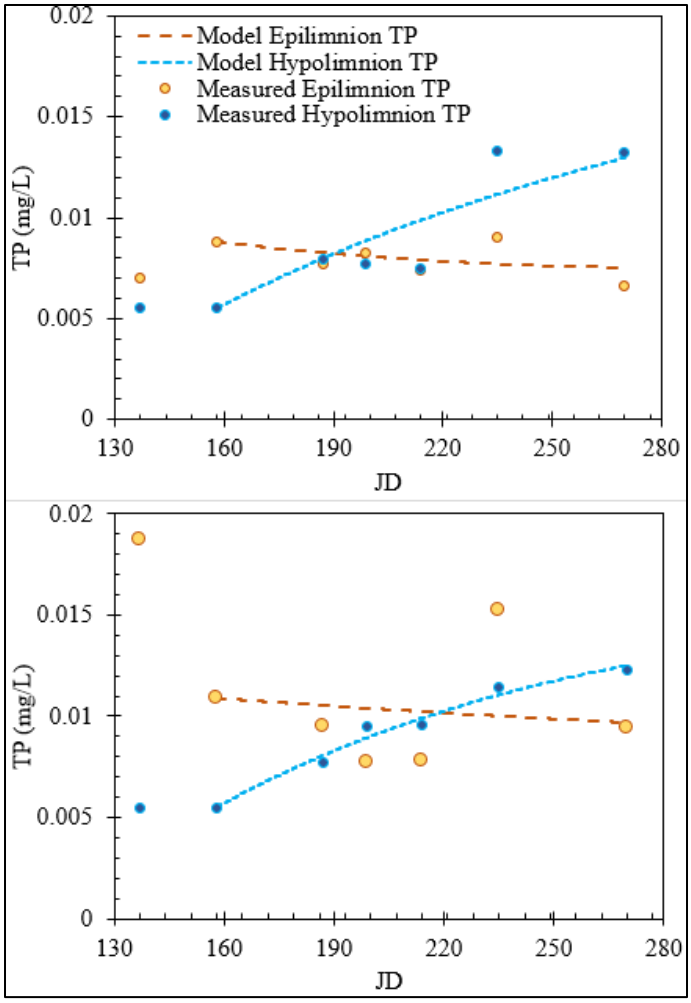

Figure 8-13: Calibrated model output for Lake Gerald (top) and Lake Roland (bottom) showing modeled total phosphorus (TP) concentrations and observed TP levels in each layer of each lake by Julian day (JD).

Validation (again, without a true validation dataset) for this calibration is provided by A) comparison of model-predicted outflowing TP mass against measured outflowing TP mass (examined in section 7.4.4), and B) model forecast (application) agreement with historical accounts of water quality in the lakes. The former provides good corroboration for the model, perhaps pointing to an overestimation of TP outflow and underestimation of the residual loading of as much as 0.35 kg. The latter is discussed here.

The model forecast is built upon the methodology outlined in section 7.4.5 and provides evidence to support the validation of the phosphorus model as presented. If the nutrient

budget for 2022 was assumed to be constant year to year for Twin Lakes, the overall average TP concentration to be expected throughout the lakes would be 8.98 µg/L at steady state (per equation 7.4G). In 2022, an average overall TP concentration of 9.06 µg/L was experienced throughout Twin Lakes, indicating the lakes are near steady state if no change in loading were to occur. When residual load was assumed to be eliminated (assuming that portion were equal to anthropogenic loading), the steady state TP concentration reached throughout the lakes is 6.67 µg/L, well below the 7.5 µg/L threshold taken to indicate oligotrophic levels (Schlesinger & Bernhardt, 2013). This indicates that the model, as calibrated, substantiates early documentation of Twin Lakes as oligotrophic and supports the historical viability of cold-water fish stocks as maintained as early as ~1980. This model forecast approach, and its coherence with the past and possible future is discussed at greater length in section 8.5.3.

The conclusions resulting from the model depend upon general acceptance of the residual load value as presented, which is discussed and justified here. The residual load is taken as the general best estimate of anthropogenic loading but may be either high or low depending on error in other model components. Figure 7-7 presents the model output being least sensitive to the calibration of the residual load, meaning it is most subject to error, which makes sense given it incorporates the error and uncertainty of other model components. For example, the residual load would increase if the model were adjusted to better fit the outflowing TP as used for validation (see section 7.4.4). Alternatively, the residual load would decrease if watershed loading were higher than employed due to disproportionately large loading from a watershed other than the Misery River. That said,

watershed loading was measured directly, there is relative confidence in the atmospheric deposition rate, and the internal load is likely conservatively high if in error; therefore, the residual load is likely near-accurate, or a slight underestimation of the anthropogenic load exerted by development along Twin Lakes. This is substantiated by the distribution of the model estimation residual load (see figure 7-7), which indicates the residual load tailing high. That is to say, relative to the best estimate presented, an inflated residual load is more likely than a deflated one. Similarly, model validation would tend toward the residual load estimation being low if it were in error (i.e. a 10.9% increase in residual load would be expected if compensating the 0.35 kg deficit in outflowing TP seen in section 7.4.4). Alternatively, this assumption of the residual load as the best estimate is supported by the model forecast which places current TP levels experienced on Twin Lakes near what would be expected at steady state for the current loading. The forecast further suggests that removal of the residual load would return the lakes to a steady-state TP level which is well-within the oligotrophic range, consistent with historical classification of the lakes.

8.4.3 Implications & Limitations

The TP budget model presented for Twin Lakes provides insight into the current and historical status of the lakes, and appears a relatively accurate representation of TP moving through the system. Relatively low TP loading rates, with a very low atmospheric deposition rate being the largest single contributing load, support the historical classification of the lakes as oligotrophic. Model forecasting, assuming removal of the residual load (taken as development-sourced), yields a background TP level in Twin

Lakes of 6.67 µg/L, well below the 7.5 µg/L level taken as oligotrophic (Schlesinger & Bernhardt, 2013). This supports the system being impacted relatively easily by any changes in P loads from development. The assumption of the residual load, as calibrated, to equal the anthropogenic loading associated with shoreline development is likely a good one, and is more likely to underestimate anthropogenic loading than overestimate it. Those anthropogenic sources of nutrients may include fertilizers, increased sediment delivery in runoff, yard waste dumping and decomposition, or leaking septic systems. Further, the residual load as anthropogenic can be shown reasonable by considering potential septic load alone. The EPA's STEPL model estimates ~354 kg of TP reaching the lakes during the model period is every septic system failed, and 7.1 kg (exceeding the model residual load) reaching the lake is only 2% of septic tanks failed (see section 8.4.1) (TetraTech, 2018). Similarly, the residual load (at 22% of total loading) is notably less than predicted by Purdue's quick and dirty "Long-Term Hydrological Impact Analysis" (L-THIA) model, which estimated around 90% of P loading from residential developments; thus, the magnitude of the residual load is very reasonably attributable shoreline development (Engel, 2016). This indicates control of TP loading from shoreline developments is likely both the most impactful and practically achievable measure for any attempts to return lake productivity to oligotrophic levels.

The TP budget presented is not without limitation, however. Use of TP as the metric for lake productivity is problematic on its face, in that, SRP is the species utilized for biologic uptake while TP could theoretically pass through Twin Lakes remaining biologically unavailable (Chapra, 2008; Fox, LaPerriere, & Carlson, 1979; Schlesinger &

Bernhardt, 2013). SRP, however, was generally not detectable in the waters (see sections 8.1.1 and 8.2.1), which is consistent with the lakes being P-limited (i.e. SRP is being used as it becomes available). Therefore, TP is used to track and assess metabolism as a best-(though flawed-) metric. Vegetative impacts and cycling of TP were not considered in the model either. Aquatic macrophytes, which were observed at high levels in some areas of the lake during the late stratified period, utilize P from the water while growing then re-introduce P to the water upon their senescence. Incorporation of an aquatic macrophyte pool to the TP model would require substantially more sophisticated sampling methodology, but could improve output and provide much more insight into the impacts of productivity on lake users (i.e. vegetation quantities impact boaters and lake aesthetics). The assumed values for atmospheric deposition and bounds (though not approached) on settling rates and internal load & burial rates are limiting so far as the accuracy of literature examined. While the values used were best estimates, direct measure of atmospheric deposition would improve model certainty. Similarly, settling and internal load / burial rates vary widely, so direct measure of these values would prove valuable. The results are also limited by the assumption of the Misery River watershed as representative of the whole Twin Lakes watershed. The Misery River watershed is only ~40.4% of the non-lake area draining to Twin Lakes, so variation in it relative to the other contributing areas could propagate relatively substantial error. More broad-scale gauging efforts could reduce this uncertainty. The model is similarly limited by a relatively small sample set for calibration with little sample replication. Thus, errors in any one given sample could have notable impacts on the overall model calibration. Low density of samples temporally also limits calibration and interpretation, particularly

around the start and end of summer stratification. Many of these limitations can be overcome with increased sampling, visits, or methods implemented, which is limited by funding available. That considered, the completed work was a relatively comprehensive and powerful assessment of Twin Lakes given the budget applied.

8.5 Summary of Anthropogenic Influences & Management Action

The Twin Lakes watershed has been impacted by human activity and development. These impacts have been mentioned and discussed to a degree elsewhere throughout this report but are outlined specifically and concisely here. Alongside this discussion are commonly considered management actions for likely specific management goals on Twin Lakes.

8.5.1 Erie-Ontario Mine

The Erie-Ontario Mine, as named by online mine site references, was located in the northern reaches of the Misery River watershed (Diggings, 2022). The mine had at least one, and likely two or more, open, flooded shafts of unknown depth. Downslope of the positively identified shaft was a ~1-meter diameter, 2.5-meter-deep concrete cistern (see figure 8-14).

Figure 8-14: Concrete cistern downslope from flooded shaft of Erie-Ontario Mine

This cistern and the open shaft emitted a sulfurous odor upon disturbance of the water. Sulfate loading has been shown to stimulate phosphate release in wetland soils in some circumstances (Lamers, Tomassen, & Roelofs, 1998); however, the magnitude in this single distal discharge which drains to a long wetland complex is uncertain and may be minimal. The cistern appeared to be fed by groundwater, with only ~2 mm thick ice at the undisturbed open water surface, in weather which had been consistently below -7ºC for greater than a week prior to the visit. The cistern also had water seeping from the concrete base juncture with the ground surface. Conductivity measurements were higher

in cistern water (128.6 μS /cm^2) and seepage pools ~15 meters downstream of the cistern (68.9 μS/cm^2) than in neighboring drainage seeps (16.9 μS/cm^2) or most summer lake water (see conductivity map in figure 8-5). These measurements were taken with substantial snow on the landscape which may influence or obscure results. The mine site was upslope of highway M26, making road salt contamination impacting the site unlikely. Given apparently elevated conductivity in the Misery River, examination of this mine in the future as a contributor to elevated water conductivity is warranted; though, road salt is still an obvious and likely watershed-wide culprit not to be ignored. Additionally, heavy metals contamination is possible and present as a result of mines in the general area, though this was not tested (Klemans, 2015). The mine was reported to the Houghton County Mine Inspector. The mine was not examined further, not being the center of the work performed but was reported here for completeness and as a potential impactor to Twin Lakes water quality.

8.5.2 Summarizing Anthropogenic Influence & Potential Management Actions

A history of human presence on Twin Lakes has left specific traces on the landscape and water quality. Apparent anthropogenic impacts within the Twin Lakes watershed and the lakes include:

A) road salt contamination of soils along highway M26 and Misery River water,

B) Erie-Ontario Mine remnants with unknown impacts to lake water quality,

C) hypolimnetic dissolved oxygen depletion during the summer stratified period,

D) eutrophication of Twin Lakes from oligotrophic to mesotrophic,

E) excess phosphorus loading from anthropogenic sources,

F) lake fishery no longer supporting cold-water fish species,

G) residential development of the lakes' shorelines, and

H) modified water levels with a weir structure at the lakes' outflow.

Many of the listed impacts are linked – some integrally, others distally – while some stand alone. All represent divergence from historically present conditions on Twin Lakes. A value judgement is required to say which of these changes are good or bad.

Anthropogenic sources of excess P loading are particularly relevant as the likely driver of eutrophication, DO deficits, and fishery degradation. This excess P load was assumed to be approximated by the determined "residual load" in the nutrient budget (22% of the budget at 6.6 kg). Shoreline surveys indicated lakeshore residential developments as a possible source of excess P loading. Common sources of P loading from residential shorelines include leaking septic systems, lawn fertilizer application, dumping and decomposition of yard wastes, and increased P running off the developed landscape into the lake (ATSDR, 2016; CDC, 2023; EPA, 2015; Reckhow, 1981). Nutrient loading reductions are a common goal for lake managers on eutrophied lakes; therefore, a summary of common options for this goal is included here.

Despite the impacts associated with development, much of the Twin Lakes watershed remains in a relatively unimpacted state from a water quality standpoint. The watershed contains no agriculture, is largely managed as commercial forest, and supports substantial wetlands. Agriculture is one of the largest causes of excess nutrient pollution broadly,

including P (ATSDR, 2016; CDC, 2023; EPA, 2015; Reckhow, 1981). The Twin Lakes watershed, being void of agriculture and maintaining pre-development landcover (mostly forested in some form), supports a more natural water quality regime. Modern forestry practice, if carried out in accordance with local best management practices, provides buffers around streams and lakes to protect water quality (Ensign & Mallin, 2001; Merino, Balboa, Rodríguez Soalleiro, & González, 2005; Yanai, 1998). The watershed contains ~55 ha of wetland cover (~2% of the watershed per figure 8-7), which is generally indicative of healthy landscape function and unimpacted water quality (NLCD, 2016). The broadly intact natural function of the watershed suggests the bulk of likely anthropogenic influence is focused on the shoreline regions of Twin Lakes.

Treatment of eutrophication is likely a favorable goal by many stakeholders, which might be pursued in various ways. Stakeholders will have varying levels of support for different management actions. The following seeks simply to outline potential actions to address specific components of the human impacts discussed here. This is by no means a complete list, or any requirement on lake managers, residents, or other parties.

Reductions in residential sources of P loading might be achieved through some or all of the following landowner actions. Active septic system maintenance and/or replacement would serve to reduce leakage to the lakes and reduce P contamination (Dersch, 2017; EPA, 2022). Septic ordinances might enable the implementation of these goals. Yard management BMPs which could reduce P loading may include disposal of yard wastes distal to the lakes, implementation of unmown “buffer strips” at the lake edge to catch

runoff, and elimination or reduction of fertilizers (Dorioz, Wang, Poulenard, & Trévisan, 2006; Roberts, Stutter, & Haygarth, 2012). Low phosphorus fertilizer blends would provide benefit over traditional varieties as well (Lehman, Bell, & McDonald, 2009; Qiu, Prato, & Wang, 2014). Dialogue, group effort, and incentivization by stakeholders involved in these steps have also been instrumental in successful efforts elsewhere (Sharpley, Kleinman, Flaten, & Buda, 2011). Additionally, continuing to apply BMPs for forestry practice and new development will prevent excess P in runoff from reaching the lakes (Ensign & Mallin, 2001; Merino et al., 2005).

Treatment of specific symptoms might also be considered for some impacts to the lake. Supplementing DO to the hypolimnion during the stratified period could enable successful stocking of cold-water species (Beutel & Horne, 1999; Kortmann, Knoecklein, & Bonnell, 1994; McCord & Schladow, 2001; Taggart, 1980). Treatment of internal sediment P release with alum or similar might be considered as an immediate P load reduction measure (Huser, 2017; James, 2017b; Kuster, Kuster, & Huser, 2020). Mechanical harvest of aquatic macrophytes, which are present in significant quantities in some areas of the lakes (though this was not a primary focus of the work presented here), might remove a substantial P pool from the lake and provide specifically valued aesthetic improvements to certain stakeholders (Carpenter & Adams, 1978; Li, Wang, Ye, & Ba, 2014). Additional study and planning to assess feasibility and specific application plans for these tools would be required beyond the work presented here before implementation. Further detailed study of the fishery in light of the lake processes revealed here may

reveal practical steps for fishery management to address specific fishery goals or concerns.

8.5.3 Phosphorus Reduction Response & Historical Implications

Application of the P budget forecast model as outlined in section 7.4.5 enables cursory prediction of the response of Twin Lakes to specific changes to P loading. This analysis is carried out at the scale of the full Twin Lakes system because impacts will likely be carried out throughout the watershed, and the connected nature of the basins will make the results felt throughout the system; thus, Twin Lake trophic health as a system in considered. A number of specific reductions to the residual load starting in 2023 were considered and plotted (see figure 8-15). The scenarios are bound by immediate and complete reduction (bottom) as the best-case-scenario for return the lakes to pre-development conditions, and no change to the residual load (top) as the status-quo. Notably, the assumption of status-quo being no change to loading may be flawed. More likely, some degree of continued increased loading could be expected with continued development and aging of existing infrastructure.

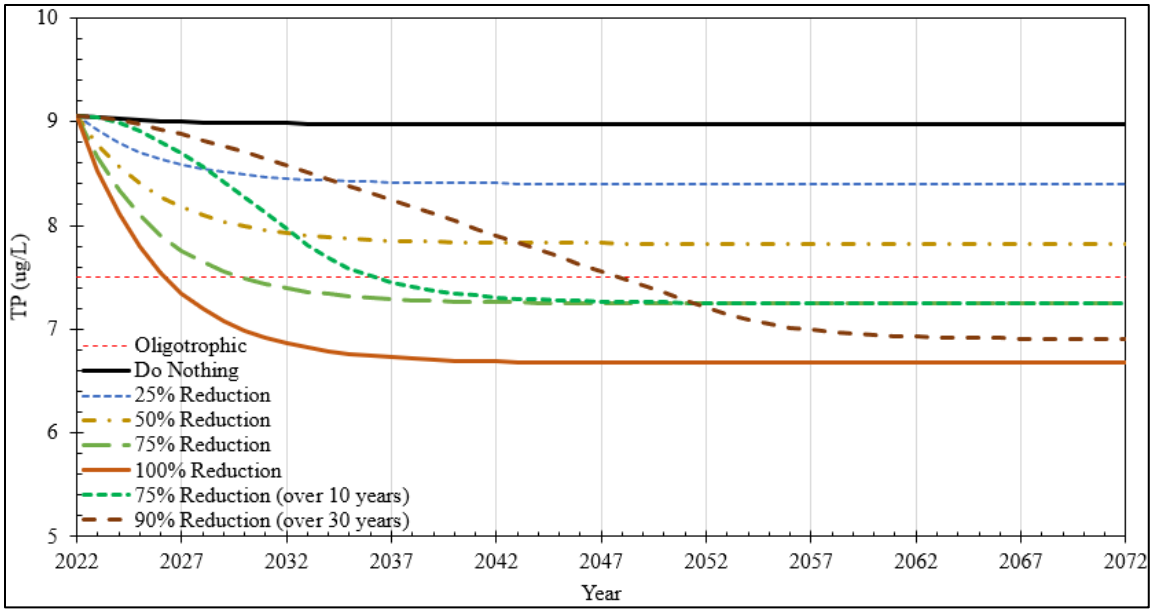

Figure 8-15: Modeled response of Twin Lakes to specific phosphorus residual load reduction scenarios

Load reductions in figure 8-15 carried out over some number of years assume a constant linear reduction in the loading starting in 2023. Complete removal of the residual load results in a steady-state TP level of 6.67 µg/L, taken to be the approximate pre-development TP levels in Twin Lakes. For the steady state TP concentration to reach 7.5 µg/L or less (taken as oligotrophic level), a minimum of a 64% residual load reduction (or 4.24 kg reduction during the stratified period) would be required. The lakes appear relatively responsive to load reductions, with oligotrophic conditions restored in just ~7-8 years following 75% residual loading reduction. More realistically, if a reduction in residual loading of 75-90% could be achieved in the next 10-30 years, Twin Lakes might see oligotrophic conditions restored in the next 15-25 years. This presents a potentially ambitious and challenging reduction goal for lake managers and stakeholders (depending on the true distribution of the "residual" load), but offers very promising results if attained.

A similar application of the forecast model was utilized to speculate a historical account of the Twin Lakes system beginning at the increased development of the early 1900s. Figure 8-16 presents a best estimate of historic TP levels, beginning with the determined pre-development TP level of 6.67 μg/L and constrained by historical documentation of the lakes and current conditions. The beginning of substantial loading was assumed to occur after a short delay following the beginning of significant development identified by historical imagery, and generally following the classification of the lakes as oligotrophic (Madison, 2019; NETRONLINE, 2022). The timeline is further supplemented with fishery and water quality data from the DNR and current work (Madison, 2019, 2022; Urban, 2022; USGS, 2006; Wright, 2015). Walleye introductions were carried out to provide a walleye fishery and/or to support cold-water fish success (like trout, splake, etc.) by reducing perch populations which compete with juvenile cold-water fishes for resources (Madison, 2019, 2022). Cold-water fish are an important indicator species for lake health (see section 8.1.4), and the hypothesized historical trends in trophic level on Twin Lakes go hand in hand with the decline of cold-water fish success in the system. A subset of the potential future scenarios presented in figure 8-15 are also shown in figure 8-16.

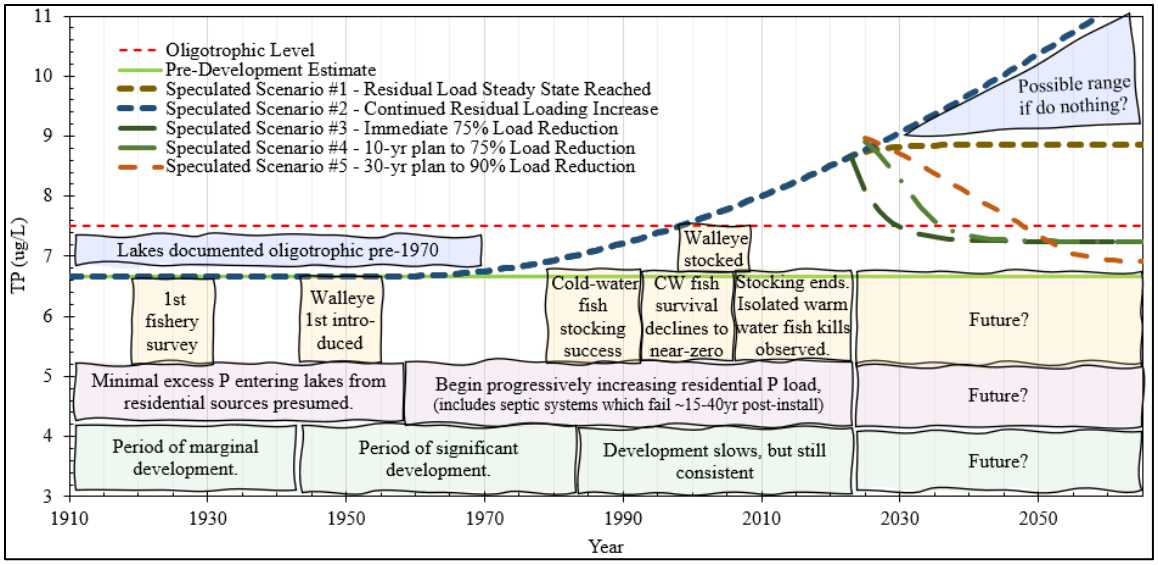

Figure 8-16: Speculated historical TP levels in Twin Lakes alongside potential future conditions

The plotted account of TP (as a metric for lake trophic state) presented in figure 8-16 is admittedly speculative, but provides a best estimated account of changes observed on Twin Lakes which is informed by and corroborative with historical accounts of the lakes. Thus, it helps put perspective to the past and potential-future impacts of the human presence on Twin Lakes. Care should be taken not to take the estimates shown as true values, but as a most likely point within a range of possibility.

8.6 Suggested Future Work

This work on Twin Lakes, as performed, provides conclusions useful for Twin Lakes and informs future lake modeling work. Specific modification to methodology might improve results and utility for Twin Lakes. Similarly, results of this study point to some specific areas in which further research might improve future lake modeling and management efforts.

8.6.1 Twin Lakes Methodology Improvements

Incorporating more information into analysis and examination of Twin Lakes could likely further the accuracy and resolution of conclusions drawn. A better understanding of how residual loading of P moves through the system could be gained by incorporating a septic leakage component in the model. This has been done in other cases, but accurate application requires substantial information about the infrastructure and subsurface conditions; for example, useful data may include detailed soil & groundwater information and documented septic system locations, age, condition, & maintenance records (Nejadhashemi, Woznicki, & Douglas-Mankin, 2011; TetraTech, 2018). Similarly, lawn fertilizer sources might be considered individually, but again would require site-specific insight into how landowners are using them. Residential surveys have been used in other investigations to get at this information, but may not be completely accurate and participation rate of residents may be variable (FB-Environmental-Associates, 2018; Sharpley et al., 2011). Groundwater flow information might be accurately gleaned from use of piezometers in a number of places around the lakes, which would substantially inform how/where septic leakage may be a concern or not and may better improve the

understanding of the lakes' hydrology. Application of each of these measures would take substantial financial resources, so relative value added by each must be weighed. Additionally, a conductivity budget (as a proxy for chloride) would validate the water budget employed and the conductivity gradient observed in the lakes, but would have required conductivity measurements in the contributing tributaries. This would be a very simple, negligible-cost improvement possible on any future work.

For the model framework presented, monitoring and data for future years would prove valuable. This would provide a true validation dataset for the model presented, ideally lending the model far more credibility. Future years of Twin Lakes data would also demonstrate if 2022 was a typical, representative year for the system as was assumed.

Similarly, direct measurement of more items assumed in the model could also improve certainty of results. Gauging of the unnamed tributary and TP measurement at the north end of Lake Roland would be a valuable addition to the study. This tributary was assumed proportional to the Misery River watershed in flow rate, and equal in species concentration, which may or may not be fully true as was seen in section 8.2.3. This would improve the hydrologic model applied to the lakes and better constrain the tributary P load applied. Measurement of atmospheric deposition would be valuable due to broad variability in these values and spotty coverage of literature estimates (Redfield, 2002; Tipping et al., 2014); that said, the estimate used in this analysis is taken with relative confidence. Measurement of internal loading on each lake would be useful in constraining and informing the optimization output examined in sections 7.4.3 and 8.4.2.

Measurement by incubation of sediment cores could provide this information at any time of the year, though variability exists throughout the lakebed (Burnet & Wilhelm, 2021; Holdren Jr & Armstrong, 1980; Orihel et al., 2017). This may provide further backing for the smaller net flux of P into Lake Roland's hypolimnion compared to Lake Gerald (see figure 8-12). This could also better inform considerations around treatment measures like alum application. Examination of sediment cores could reveal historical P deposits which support or inform the historical record of P loading. Further, consideration of vegetation, both in terms of P uptake during the growing season and matter cycling following senescence could better inform the model's assumptions of total P present and what that means for lake residents practically. Again, these improvements would require more field effort, greater study resources, and increased analysis, so their relative impact on the overall conclusions of the work must be weighed. Gauging of a second tributary, additional years of data, or direct measurement of internal loading may be the easiest measure with the greatest and most certain value added of these options by engineering judgement.

Application of a more formal stochastic approach to parameter estimation and to sensitivity analysis could better demonstrate uncertainty in the nutrient budget as a whole. Application of environmental models deterministically are often required for practical use, but may suffer from the stochastic nature of environmental processes being neglected in the utilized output metrics (Farmer & Vogel, 2016). Fitting optimized parameters (settling rates, sediment fluxes, and residual loading rates) to a distribution with known uncertainty would allow for formal and statistically backed estimation of

error in model output, which in turn could better inform and improve conclusions drawn. A formalized Monte Carlo simulation to assess distribution of parameter estimations could achieve this end. Similarly, sensitivity analysis of optimized parameters was rudimentary and bound the realm of possibility (which was wide in some cases), as seen in sections 7.4.3 and 8.4.2. Formal and detailed sensitivity analysis carried out on each estimated or assumed value would not change the best guess at model output but could better support the certainty of the conclusions drawn.

8.6.2 Potential for Future Research

The perceived "sink" effect arising in Lake Roland brings to question whether this is common among other lakes in series, particularly in low-productivity systems. Lake Roland had notably higher productivity than Lake Gerald or Little Lake Gerald (see figures 8-1, 8-2, & 8-5 and tables 8-5 & 8-6). Table 8-7 shows that Lake Roland also had the highest base inflow but the lowest base outflow, indicating relative importance of evaporation to Twin Lakes hydrology and the accumulation of species including nutrient during "normal" summer conditions. Again, this assumes no large groundwater losses from the lake, but nothing in the water budget or well logs examination has shown this to be likely. That said, Lake Roland had both the largest mean inflow and outflow, because high flow events (associated with water release at the outlet weir) dominated the hydrologic dynamics in Lake Roland (and greatly impacted those of the upper lakes). A regional, or broad, investigation of lakes may reveal trends in eutrophication rates or susceptibility related to hydrologic characteristics (i.e. flashiness, evaporative fraction of outflow, etc.) or lake position in a series of basins. This could better inform where

management action priority is placed and how hydrologic controls are applied to lakes. For example, there may be a consistently higher value in *X* quantity of septic improvements in the upper lakes relative to the lower; similarly, best practices in exercise of hydraulic structures (i.e. outlet weir) might be developed to best support lake health.

Shoreline survey heat maps proved a useful tool in assessment of conditions on Twin Lakes and their likely drivers; further work might develop standardized methods for heatmap creation and enable a more quantitative approach to their application on lakes. If a simple, reproducible procedure for shoreline survey and heatmap generation could be correlated to known processes on well-studied lakes, shoreline survey could prove a flexible and cost-effective approach to understanding lake biogeochemistry and health. Here, the spatial part of the shoreline surveys was used largely as a qualitative tool which graphically informed and backed already posed hypotheses and model outputs. This was of great value, but directed work to broaden the utility of the surveys could put a new and powerful tool in the kit of lake managers.

The use of optical brightening agents (OBAs) as tracers and indicators for leaking septic systems should be studied further before widespread adoption. Application in scientific literature is limited to a few studies with non-standard methodology and mixed success (Cao et al., 2009; Curtis, 2012; Dubber & Gill, 2017; Jourdonnais, 1986; Stanford & Jourdonnais, 1985). The OBA:DOC ratio methodology for removing organic matter fluorescence signal should be examined in variable water chemistries; specifically, examination at a range of DOC levels including expected level in natural systems. As

shown in section 8.2.2, fluorescence signal from DOC may not be in direct proportion to DOC levels; thus, DOC impacts may still dominate the simple returned OBA:DOC ratio. The ultraviolet light exposure method for identifying OBA presence or absence (outlined by Cao et al. (2009), Dubber and Gill (2017), & Dixon (2009)) ought to be studied more rigorously for application to natural systems, and again across a range of environmentally relevant organic matter levels. OBAs make a superior indicator of septic leakage over only conductivity, nutrient levels, or bacterial samples, because each of the other metrics may have alternative environmental or anthropogenic sources (Cao et al., 2009; Dubber & Gill, 2017; Kramer et al., 1996). Other indicators like caffeine or *E. Coli* might be useful in the future, though they are generally more intensive to employ and have less specificity to wastewater streams than OBAs. A more rigorously supported methodology for successful OBA identification in environmental systems would prove a valuable a versatile tool to lake managers at large.

8.7 Summarizing Results & Implications for Twin Lakes

Twin Lakes was confirmed to be P-limited, naturally low in nutrients, and historically oligotrophic. The lakes are now mesotrophic, very likely due to anthropogenic P loading from shoreline development which may include septic leakage, lawn fertilizers, yard wastes, and increased nutrient-laden runoff. The largest component P source of the modeled nutrient budget was atmospheric deposition, with watershed loading, internal loading, and the "residual load" also substantial components. Due to low background P levels, the lakes are likely susceptible to eutrophication (as observed), with Lake Roland having higher productivity than Little Lake Gerald and Lake Gerald (which function very similarly). Lake Roland maintains higher productivity than Lake Gerald, and acts as a sort of sink with a typically small outflow. Shoreline surveys of water quality and associated heatmaps provide limited support for these conclusions; however, specific contaminant point sources were not identified. Published OBA detection methods were shown to be limited or non-applicable in at least the Twin Lakes system as employed.

Twin Lakes has been changed as a system by human presence and associated eutrophication. The impacts of these changes to Twin Lakes have been felt with increased nuisance vegetation observed, decline of lake suitability for cold-water fish species, and periodic isolated fish kills. Substantial hypolimnetic DO depletion is likely driving those fishery trends. Elevated conductivity stemming from the Misery River watershed likely points to road salt contamination to the lakes. The presence of the uncapped Erie-Ontario Mine in the watershed may also pose a water quality concern. Historically, Twin Lakes likely has an overall average TP level of ~6.67 μg/L, well within oligotrophic levels.

Without change to the status quo of nutrient loading on Twin Lakes, TP level will likely remain in excess of 9 μg/L, or climb further. A minimum reduction of ~64% of the residual load, taken as the anthropogenic load, would be required to return the lakes to oligotrophic status (taken as <7.5 μg TP/L). The lakes are likely to respond relatively quickly to implemented changes improving nutrient loading.

This study successfully applied a coupled series of two-box models for the Twin Lakes systems to construct a phosphorus budget for the 2022 stratified season. These results were supported and complemented by shoreline surveys and limited historical information on the lakes. Broadly, the results of this work provide substantial insight into the Twin Lakes system, applicable to managers and others who care for the lakes. The work also serves as an interesting case study for a naturally oligotrophic, now-eutrophied system of lakes in series within the Great Lakes region and a relatively undeveloped watershed.

9 WORKS CITED

Albright, E. A. (2022). *Mechanisms of Internal Phosphorus Loading in Lentic Ecosystems.* ProQuest Dissertations Publishing,

ATSDR. (2016). *NITRATE AND NITRITE - POTENTIAL FOR HUMAN EXPOSURE*. Online: CDC Retrieved from https://www.atsdr.cdc.gov/ToxProfiles/tp204-c6.pdf.

Battifarano, O. (2020). *Road Salt Deicers as Contaminants in the Environment.* ProQuest Dissertations Publishing,

Beutel, M. W., & Horne, A. J. (1999). A Review of the Effects of Hypolimnetic Oxygenation on Lake and Reservoir Water Quality. *Lake and Reservoir Management, 15*(4), 285-297. doi:10.1080/07438149909354124

Boardman, E., Danesh-Yazdi, M., Foufoula-Georgiou, E., Dolph, C. L., & Finlay, J. C. (2019). Fertilizer, landscape features and climate regulate phosphorus retention and river export in diverse Midwestern watersheds. *Biogeochemistry, 146*(3), 293-309. doi:10.1007/s10533-019-00623-z

Boehme, J. S., Rachel. Bejankiwar, Raj. (2012). *Atmospheric Deposition of Phosphorus to Freshwater Lakes*. Retrieved from Windsor,

ON: https://legacyfiles.ijc.org/tinymce/uploaded/Atmospheric%20Deposition%20of%20Phosphorus.pdf

Brungs, W. A., & Jones, B. R. (1977). Temperature Criteria for Freshwater Fish: Protocol and Procedures. *Available from the National Technical Information Service, Springfield VA 22161 as PB-270 032, Price codes: A07 in paper copy, A01 in microfiche. Ecological Research Series, Report EPA-600/3-77-061, May 1977, 129 p, 25 tab, 8 fig, 129 ref.*

Burnet, S. H., & Wilhelm, F. M. (2021). Estimates of internal loading of phosphorus in a western US reservoir using 3 methods. *Lake and Reservoir Management, 37*(3), 261-274. doi:10.1080/10402381.2021.1923590

Burres, E. (2011). Measuring Optic Brighteners in Ambient Water Samples Using a Fluorometer. In.

Camarero, L., & Catalan, J. (2012). Atmospheric phosphorus deposition may cause lakes to revert from phosphorus limitation back to nitrogen limitation. *Nature communications, 3*(1), 1118-1118. doi:10.1038/ncomms2125

Cao, Y., Griffith, J. F., & Weisberg, S. B. (2009). Evaluation of optical brightener photodecay characteristics for detection of human fecal contamination. *Water research (Oxford), 43*(8), 2273-2279. doi:10.1016/j.watres.2009.02.020

Carpenter, S. R., & Adams, M. S. (1978). Macrophyte Control by Harvesting and Herbicides: Implications for Phosphorus Cycling in Lake Wingra, Wisconsin. *Journal of Aquatic Plant Management Vol. 16, p 20-23, June 1978. 4 fig, 24 ref. NSF DEB-7519777*.

CDC. (2023). Where Are Nitrates and Nitrites Found? Retrieved from https://www.atsdr.cdc.gov/csem/nitrate-nitrite/where_are.html

Chapra. (2008). *Surface water-quality modeling*. Long Grove, Ill: Waveland Press.

Chapra, & Sonzogni, W. C. (1979). Great Lakes total phosphorus budget for the mid 1970s. *Journal - Water Pollution Control Federation, 51*(10), 2524-2533.
Chapra, S., Dove, A., & Rockwell, D. (2009). Great Lakes Chloride Trends: Long-Term Mass Balance and Loading Analysis. *Journal of Great Lakes Research, 35*, 272-284. doi:10.1016/j.jglr.2008.11.013
Coleman. (2022). *Houghton County Parcel Map* [Map Parcels].
Curtis, L. (2012). *Investigation of Septic Leachate to the Shoreline Area of Whitefish Lake*.
Dersch, E. (2017). *Managing Your Septic System*. Retrieved from Online: https://www.canr.msu.edu/septic_system_education/uploads/E-3350%20Managing%20Septic.pdf
Diggings, T. (2022). Mines Map. Retrieved from https://thediggings.com/usa/michigan/houghton-mi061/map
Dixon, L. K. (2009). *Tracing anthropogenic wastes: Detection of fluorescent optical brighteners in a gradient of natural organic matter fluorescence.* ProQuest Dissertations Publishing,
Dorioz, J. M., Wang, D., Poulenard, J., & Trévisan, D. (2006). The effect of grass buffer strips on phosphorus dynamics—A critical review and synthesis as a basis for application in agricultural landscapes in France. *Agriculture, Ecosystems and Environment, 117*(1), 4-21. doi:10.1016/j.agee.2006.03.029
Dubber, D., & Gill, L. W. (2017). Suitability of fluorescent whitening compounds (FWCs) as indicators of human faecal contamination from septic tanks in rural catchments. *Water research (Oxford), 127*, 104-117. doi:10.1016/j.watres.2017.10.005
PART 4. WATER QUALITY STANDARDS, (2006).
EGLE. (2022a). *EGLE Open Data* [GIS]. Retrieved from: https://gis-egle.hub.arcgis.com/search
EGLE. (2022b). WellLogic Viewer. Retrieved from https://www.deq.state.mi.us/geowebface/
Engel, B. (2016). Long Term Hydrologic Impact Analysis (L-THIA). *Purdue University Department of Agricultural Biological Engineering*.
Ensign, S. H., & Mallin, M. A. (2001). Stream water quality changes following timber harvest in a coastal plain swamp forest. *Water research (Oxford), 35*(14), 3381-3390. doi:10.1016/S0043-1354(01)00060-4
EPA, U. (2015). Contaminant Candidate List (CCL) and Regulatory Determination. Retrieved from https://www.epa.gov/ccl/chemical-contaminants-ccl-4
EPA, U. (2022). SepticSmart. Retrieved from https://www.epa.gov/septic/septicsmart#:~:text=Follow%20these%20SepticSmart%20quick%20tips,Don't%20Strain%20Your%20Drain!
Farmer, W. H., & Vogel, R. M. (2016). On the deterministic and stochastic use of hydrologic models: DETERMINISTIC AND STOCHASTIC MODEL USE. *Water resources research, 52*(7), 5619-5633. doi:10.1002/2016WR019129
FB-Environmental-Associates. (2018). *Spofford Lake Management Plan*. Retrieved from Online: https://www.des.nh.gov/documents/spofford-lake-watershed-management-plan

Fox, P. M., LaPerriere, J. D., & Carlson, R. F. (1979). Northern lake modeling: A literature review. *Water resources research, 15*(5), 1065-1072. doi:10.1029/WR015i005p01065

Garmin. (2022). Navionics ChartViewer Web App. Retrieved from https://webapp.navionics.com/

Graham, L. (2022). Michigan's lack of septic system regulations is causing problems for some of its most pristine lakes. Retrieved from https://www.michiganradio.org/environment-climate-change/2022-05-04/michigans-lack-of-septic-system-regulations-is-causing-problems-for-some-of-its-most-pristine-lakes

Han, H., Bosch, N., & Allan, J. D. (2011). Spatial and temporal variation in phosphorus budgets for 24 watersheds in the Lake Erie and Lake Michigan basins. *Biogeochemistry, 102*(1-3), 45-58. doi:10.1007/s10533-010-9420-y

Hanson, L. (2022, February, 2022). ["Lidar"].

Holdren Jr, G. C., & Armstrong, D. E. (1980). Factors affecting phosphorus release from intact lake sediment cores. *Environmental science & technology, 14*(1), 79-87. doi:10.1021/es60161a014

Hoverson, D. (2008). *Phosphorus Release from Sediments in Shawano Lake, Wisconsin.* (MS in Natural Resources (Water Resources)), University of Wisconsin Stevens Point, Retrieved from https://minds.wisconsin.edu/bitstream/handle/1793/81234/Hoverson.pdf?sequence=1&isAllowed=y

Huser, B. J. (2017). Aluminum application to restore water quality in eutrophic lakes: maximizing binding efficiency between aluminum and phosphorus. *Lake and Reservoir Management, 33*(2), 143-151. doi:10.1080/10402381.2016.1235635

James, W. F. (2017a). Internal phosphorus loading contributions from deposited and resuspended sediment to the Lake of the Woods. *Lake and Reservoir Management, 33*(4), 347-359. doi:10.1080/10402381.2017.1312647

James, W. F. (2017b). Phosphorus binding dynamics in the aluminum floc layer of Half Moon Lake, Wisconsin. *Lake and Reservoir Management, 33*(2), 130-142. doi:10.1080/10402381.2017.1287789

James, W. F., Barko, J. W., Eakin, H. L., & Sorge, P. W. (2002). Phosphorus Budget and Management Strategies for an Urban Wisconsin Lake. *Lake and Reservoir Management, 18*(2), 149-163. doi:10.1080/07438140209354145

Jourdonnais, J. H. S., J. A.; Hauer, R. F.; Noble, R. A. (1986). *Investigation of Septic Contaminated Groundwater Seepage as a Nutrient Source to Whitefish Lake, Montana*. Retrieved from

Kelly, V. R., Findlay, S. E., Hamilton, S. K., Lovett, G. M., & Weathers, K. C. (2019). Seasonal and Long-Term Dynamics in Stream Water Sodium Chloride Concentrations and the Effectiveness of Road Salt Best Management Practices. *Water, air, and soil pollution, 230*(1), 1-9. doi:10.1007/s11270-018-4060-2

Klemans, D. (2015). *Site-Specific Modifications to the Chronic Water Quality Values for Copper in Select Upper Peninsula Water Bodies*. Michigan Department of Environment, Great Lakes, and Energy Retrieved from https://www.michigan.gov/egle/-

/media/Project/Websites/egle/Documents/Programs/WRD/SWAS/Rule-57-site-specific-Cu-Aquatic-Life-values.pdf?rev=422f6ff0a2c04cb7bd6dc07155f3a1ea&hash=D400505A953BEE7069A0335CF0A47D62.

Koopal, M. (2022, July 25, 2022). [Whitefish Lake Septic Leachate Study Methods].

Kortmann, R. W., Knoecklein, G. W., & Bonnell, C. H. (1994). Aeration of Stratified Lakes: Theory and Practice. *Lake and Reservoir Management, 8*(2), 99-120. doi:10.1080/07438149409354463

Kramer, J. B., Canonica, S., Hoigné, J., & Kaschig, J. (1996). Degradation of Fluorescent Whitening Agents in Sunlit Natural Waters. *Environmental science & technology, 30*(7), 2227-2234. doi:10.1021/es950711a

Kuster, A. C., Kuster, A. T., & Huser, B. J. (2020). A comparison of aluminum dosing methods for reducing sediment phosphorus release in lakes. *Journal of environmental management, 261*, 110195-110195. doi:10.1016/j.jenvman.2020.110195

Lamers, L. P. M., Tomassen, H. B. M., & Roelofs, J. G. M. (1998). Sulfate-Induced Eutrophication and Phytotoxicity in Freshwater Wetlands. *Environmental science & technology, 32*(2), 199-205. doi:10.1021/es970362f

Larson, J. H., James, W. F., Fitzpatrick, F. A., Frost, P. C., Evans, M. A., Reneau, P. C., & Xenopoulos, M. A. (2020). Phosphorus, nitrogen and dissolved organic carbon fluxes from sediments in freshwater rivermouths entering Green Bay (Lake Michigan; USA). *Biogeochemistry, 147*(2), 179-197. doi:10.1007/s10533-020-00635-0

Lehman, J. T., Bell, D. W., & McDonald, K. E. (2009). Reduced river phosphorus following implementation of a lawn fertilizer ordinance. *Lake and Reservoir Management, 25*(3), 307-312. doi:10.1080/07438140903117217

Li, C.-h., Wang, B., Ye, C., & Ba, Y.-x. (2014). The release of nitrogen and phosphorus during the decomposition process of submerged macrophyte (Hydrilla verticillata Royle) with different biomass levels. *Ecological engineering, 70*, 268-274. doi:10.1016/j.ecoleng.2014.04.011

Madison, G. (2019). *Lake Roland & Lake Gerald ("Twin Lakes") Status of the Fishery Report*. Retrieved from https://www.michigan.gov/dnr/-/media/Project/Websites/dnr/Documents/Fisheries/Status/2020/SFR2020-301.pdf?rev=24597cb507824a939d02826388a090df&hash=14D5455EA4AC03A6B9975B5A66C633B5

Madison, G. (2022, March 31, 2022). [Twin Lakes Fisheries].

Malecki, L. M., White, J. R., & Reddy, K. R. (2004). Nitrogen and phosphorus flux rates from sediment in the Lower St. Johns River estuary. *Journal of environmental quality, 33*(4), 1545-1555. doi:10.2134/jeq2004.1545

MathWorks. (2022a). ode45. Retrieved from https://www.mathworks.com/help/matlab/ref/ode45.html

MathWorks. (2022b). simulannealbnd. Retrieved from https://www.mathworks.com/help/gads/simulannealbnd.html?searchHighlight=simulannealbnd&s_tid=srchtitle_simulannealbnd_1

Mays, L. W. (2019). *Water Resources Engineering* (Third Edition ed.): John Wiley & Sons, Inc.
McCord, S. A., & Schladow, S. G. (2001). Design Parameters for Artificial Aeration of Ice-Covered Lakes. *Lake and Reservoir Management, 17*(2), 121-126. doi:10.1080/07438140109353980
McCrackin, M. L., Muller-Karulis, B., Gustafsson, B. G., Howarth, R. W., Humborg, C., Svanbäck, A., & Swaney, D. P. (2018). A Century of Legacy Phosphorus Dynamics in a Large Drainage Basin. *Global biogeochemical cycles, 32*(7), 1107-1122. doi:10.1029/2018GB005914
McGuire, K. M., & Judd, K. E. (2020). Road salt chloride retention in wetland soils and effects on dissolved organic carbon export. *Chemistry and ecology, 36*(4), 342-359. doi:10.1080/02757540.2020.1735376
MDNR (Cartographer). (1937). Lake Roland and Lake Gerald Bathymetirc Maps
MDNR. (2022). *MDNR Open GIS Data* [GIS]. Retrieved from: https://gis-midnr.opendata.arcgis.com/
Merino, A., Balboa, M. A., Rodríguez Soalleiro, R., & González, J. G. Á. (2005). Nutrient exports under different harvesting regimes in fast-growing forest plantations in southern Europe. *Forest Ecology and Management, 207*(3), 325-339. doi:10.1016/j.foreco.2004.10.074
Mosner, M., & Aulenbach, B. (2003). COMPARISON OF METHODS USED TO ESTIMATE LAKE EVAPORATION FOR A WATER BUDGET OF LAKE SEMINOLE, SOUTHWESTERN GEORGIA AND NORTHWESTERN FLORIDA.
Nejadhashemi, A. P., Woznicki, S. A., & Douglas-Mankin, K. R. (2011). Comparison of four models (STEPL, PLOAD, L-THIA, AND SWAT) in simulating sediment, nitrogen, and phosphorus loads and pollutant source areas. *Transactions of the ASABE, 54*(3), 875-890. doi:10.13031/2013.37113
NETRONLINE. (2022). Historic Aerials. Retrieved from https://www.historicaerials.com/
NLCD. (2016). *National Land Cover Dataset* [GIS]. Retrieved from: https://www.mrlc.gov/data/nlcd-land-cover-conus-all-years
NOAA. (2022). *Daily Summaries Station Details - HANCOCK HOUGHTON CO AIRPORT* [Weather]. Retrieved from: https://www.ncei.noaa.gov/cdo-web/datasets/GHCND/stations/GHCND:USW00014858/detail
NRCS. (2022). Web Soil Survey. Retrieved from https://websoilsurvey.sc.egov.usda.gov/App/HomePage.htm
Nshimyimana, J. P., Martin, S. L., Flood, M., Verhougstraete, M. P., Hyndman, D. W., & Rose, J. B. (2018). Regional Variations of Bovine and Porcine Fecal Pollution as a Function of Landscape, Nutrient, and Hydrological Factors. *Journal of environmental quality, 47*(5), 1024-1032. doi:10.2134/jeq2017.11.0438
Orihel, D. M., Baulch, H. M., Casson, N. J., North, R. L., Parsons, C. T., Seckar, D. C. M., & Venkiteswaran, J. J. (2017). Internal phosphorus loading in Canadian fresh waters: a critical review and data analysis. *Canadian journal of fisheries and aquatic sciences, 74*(12), 2005-2029. doi:10.1139/cjfas-2016-0500

Pelletier, G. J., & Welch, E. B. (1987). PHOSPHORUS LOADING AND DIVERSION FOR PINE LAKE, WASHINGTON. *Lake and Reservoir Management, 3*(1), 38-47. doi:10.1080/07438148709354758

Qiu, Z., Prato, T., & Wang, H. (2014). Assessing long-term water quality impacts of reducing phosphorus fertilizer in a US suburban watershed. *Water policy, 16*(5), 917-929. doi:10.2166/wp.2014.163

Reckhow, K. H. (1981). *Lake data analysis and nutrient budget modeling*. Corvallis, Or: Corvallis Environmental Research Laboratory, Office of Research and Development, U.S. Environmental Protection Agency.

Redfield, G. W. (2002). Atmospheric deposition of phosphorus to the everglades: concepts, constraints, and published deposition rates for ecosystem management. *TheScientificWorld, 2*, 1843-1873. doi:10.1100/tsw.2002.813

Roberts, W. M., Stutter, M. I., & Haygarth, P. M. (2012). Phosphorus Retention and Remobilization in Vegetated Buffer Strips: A Review. *Journal of environmental quality, 41*(2), 389-399. doi:10.2134/jeq2010.0543

Schlesinger, W. H., & Bernhardt, E. S. (2013). *Biogeochemistry*.

Sharpley, A. N., Kleinman, P. J. A., Flaten, D. N., & Buda, A. R. (2011). Critical source area management of agricultural phosphorus: Experiences, challenges and opportunities. *Water science and technology, 64*(4), 945-952. doi:10.2166/wst.2011.712

Snodgrass, W. J., & Dillon, P. J. (1983). A test of two models of different levels of complexity for predicting changes of phosphorus concentration in a lake's outflow. *Ecological modelling, 19*(3), 163-187. doi:10.1016/0304-3800(83)90052-2

SOLARGIS. (2023). Global Solar Atlas. Retrieved from https://globalsolaratlas.info/map?c=46.935495,-88.858795,11&s=46.894455,-88.840256&m=site

Sperling, E. V. (1992). *Determination of the settling velocity of phosphorus in an aerated lake* (Vol. 26).

Stanford, J. A., & Jourdonnais, J. H. (1985). Verification of Shoreline Sewage Leachates in Flathead Lake, Montana. *Available from the National Technical Information Service, Springfield VA 22161 as PB85-230118/AS, Price codes: A03 in paper copy, A01 in microfiche. Montana Water Resources Research Center Bozeman completion report no. 148, Bozeman, February, 1985. 38 p, 7 fig, 13 tab, 11 ref. USGS G853-04. 14-08-0001-G853*.

Sturm, T. W. (2001). *Open Channel Hydraulics* (E. M. Munson Ed. First ed.). Print: Thomas E. Casson.

Taggart, C. T. (1980). *Ecological effects of hypolimnetic aeration of a eutrophic kettle lake.* ProQuest Dissertations Publishing,

TetraTech. (2018). User's Guide - Spreadsheet Tool for the Estimation of Pollutant Load In. Online: US EPA.

Tipping, E., Benham, S., Boyle, J. F., Crow, P., Davies, J., Fischer, U., . . . Toberman, H. (2014). Atmospheric deposition of phosphorus to land and freshwater. *Environmental science--processes & impacts, 16*(7), 1608-1617. doi:10.1039/c3em00641g

Turnipseed, D. P. S., V. B. (2010). *Discharge Measurements at Gaging Stations*. Online: USGS Retrieved from https://pubs.usgs.gov/tm/tm3-a8/tm3a8.pdf.

Urban, N. (2022). *Limnology Labratory Course Measurements of Twin Lakes Bog* [Water Quality Data].

USDA. (2022). *Title 210 – National Engineering Handbook*. Online: USDA NRCS Retrieved from https://directives.sc.egov.usda.gov/OpenNonWebContent.aspx?content=48557.wba.

USGS. (2006). *LAKE ROLAND AT TWIN LAKES, MI* [Water Quality Data]. Retrieved from: https://waterdata.usgs.gov/monitoring-location/465303088510701/#period=P1Y

USGS. (2022). *TNM Download (v2.0)* [GIS]. Retrieved from: https://apps.nationalmap.gov/downloader/#/

Verhougstraete, M. P., Martin, S. L., Kendall, A. D., Hyndman, D. W., & Rose, J. B. (2015). Linking fecal bacteria in rivers to landscape, geochemical, and hydrologic factors and sources at the basin scale. *Proceedings of the National Academy of Sciences - PNAS, 112*(33), 10419-10424. doi:10.1073/pnas.1415836112

WI-DNR. (2022). Inland lakes (group). Retrieved from https://dnr.wi.gov/topic/EndangeredResources/Communities.asp?mode=detail&Code=c5

Wisconsin, S. L. (2022). Chapter NR 102: WATER QUALITY STANDARDS FOR WISCONSIN SURFACE WATERS.

Wright, S. M., Michael. (2015). *Lake Level Study for Twin Lakes*. Retrieved from http://elmrivertownship.com/Study/Lake%20Study%202015.pdf

Wunderground. (2022). *Houghton, MI Weather History* [Historical Weather]. Retrieved from: https://www.wunderground.com/history/daily/KCMX

Yanai, R. D. (1998). The effect of whole-tree harvest on phosphorus cycling in a northern hardwood forest. *Forest Ecology and Management, 104*(1), 281-295. doi:10.1016/S0378-1127(97)00256-9

Zhang, X., Liu, Y., & Guo, H. (2016). Cross-lake comparisons of physical and biological settling of phosphorus: A phosphorus budget model with Bayesian hierarchical approach. *Ecological modelling, 337*, 231-240. doi:10.1016/j.ecolmodel.2016.07.011

10 APPENDICES:

10.1 APPENDIX A – Twin Lakes Development Map

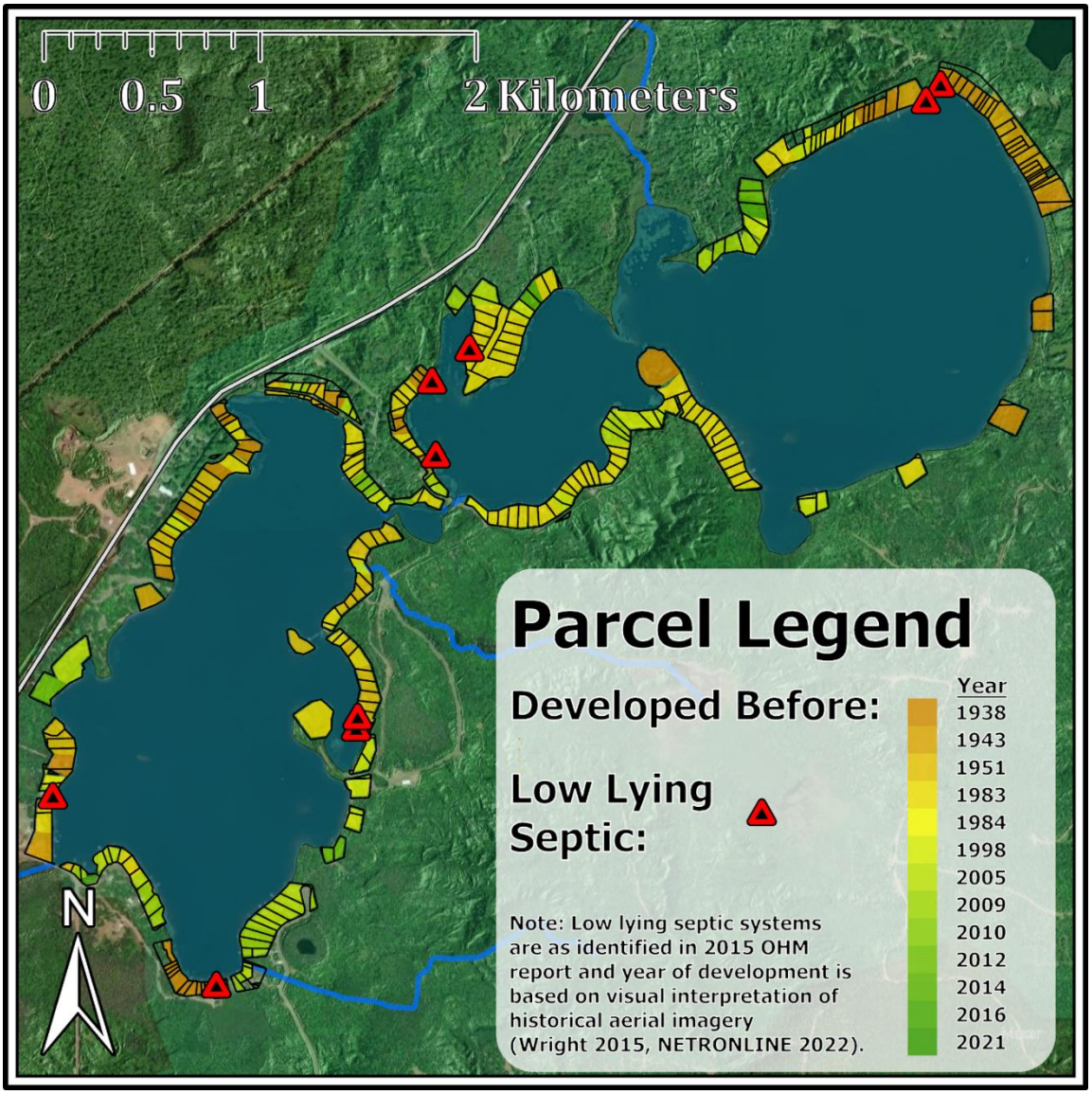

Figure A1: Developed parcel map of Twin Lakes system, with color of parcel indicating development year and notable low elevation septic systems prone to flooding shown as identified by the OHM lake level study (2015).

10.2 APPENDIX B – Twin Lakes Bathymetry

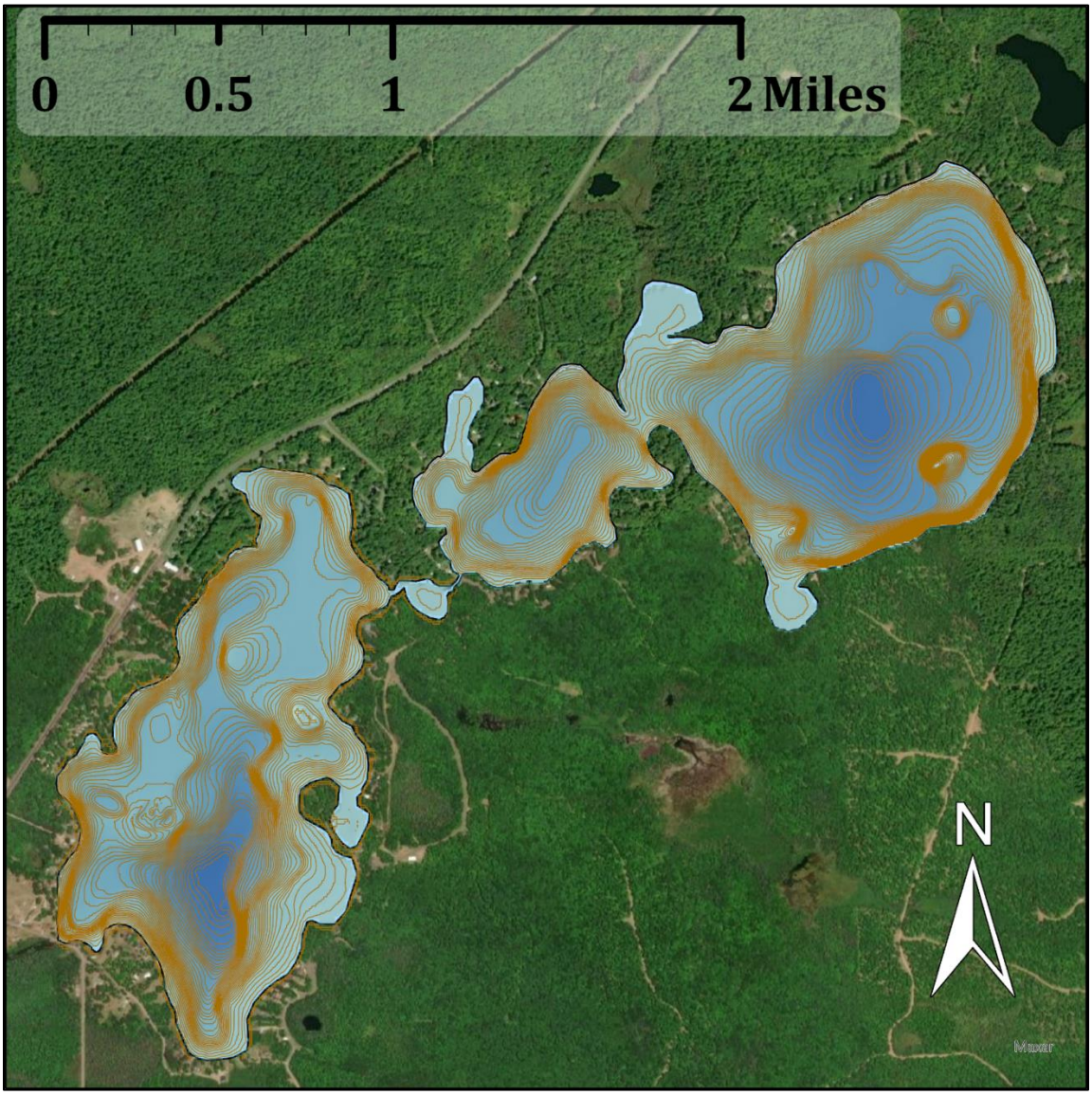

Figure B1: Bathymetric map of Twin Lakes with 0.305-meter (1-foot) generated contours

Table B1: Depth-Area-Volume Relationships for Lake Gerald (Little Lake Gerald excluded)

Depth (m)	Area (m^2)	Cumulative Volume (m^3)
0	1147640.22	6956408.724
1	997898.36	5883639.434
2	912170.98	4928604.764
3	852184.28	4046427.134
4	795773.07	3222448.459
5	737753.16	2455685.344
6	670650.97	1751483.279
7	532119.24	1150098.174
8	411128.6	678474.254
9	271976.5	336921.704
10	134642.6	133612.154
11	59053.62	36764.04396
12	12143.01	1165.72896
12.192	0	0

Table B2: Depth-Area-Volume Relationships for Little Lake Gerald

Depth (m)	Area (m^2)	Cumulative Volume (m^3)
0	327897.61	1185117.855
1	259374.17	891481.965
2	220789.45	651400.155
3	184240.9	448884.98
4	151206.9	281161.08
5	113827.34	148643.96
6	68750.63	57354.975
7	22979.66	11489.83
8	0	0

Table B3: Depth-Area-Volume Relationships for Little Lake Roland

Depth (m)	Area (m^2)	Cumulative Volume (m^3)
0	1112705.437	4701700.504
1	924302.937	3683196.317
2	811570.737	2815259.48
3	727986.087	2045481.068
4	597033.987	1382971.031
5	340345.987	914281.0435
6	237191.687	625512.2065
7	180445.427	416693.6495
8	128271.427	262335.2225
9	97493.947	149452.5355
10	65342.007	68034.55851
11	32501.237	19112.93651
12	4802.547	461.044512
12.192	0	0

Table B4: Depth-Area-Volume Relationships for all of Twin Lakes

Depth (m)	Area (m^2)	Cumulative Volume (m^3)
0	2588243.267	12843227.08
1	2181575.467	10458317.72
2	1944531.167	8395264.398
3	1764411.267	6540793.181
4	1544013.957	4886580.569
5	1191926.487	3518610.347
6	976593.287	2434350.46
7	735544.327	1578281.653
8	539400.027	940809.4765
9	369470.447	486374.2395
10	199984.607	201646.7125
11	91554.857	55876.98047
12	16945.557	1626.773472
12.192	0	0

10.3 APPENDIX C – Weir Leakage Corrections

Correction for variable leakage in the weir was examined in relation to both depth and discharge at the weir at a given time. The variability of the size or presence of the leak lends error to the considered methods; thus, a baseline leakage rate was applied uniformly through the season (0.002 CMS). The alternative methods and their associated success are tabulated in table B1 below.

Table C1: Summary of corrections considered for application to the flowrate of the leaking weir outlet of Twin Lakes.

Comparing Solver Leakage Corrections			
Scale Factor	**Formulation**	**RMSE**	**Correction Equation**
Discharge	Linear	0.083936355	$Q_{adjust} = Q_{calc} + Q_{calc} * f_{correction}$
	Squared Linear	0.084303678	$Q_{adjust} = Q_{calc} + Q_{calc}^2 * f_{correction}$
	Exponential	0.084973083	$Q_{adjust} = Q_{calc} + Q_{calc}^{f_{correction}}$
	Linear Offset	0.084036203	$Q_{adjust} = Q_{calc} + Q_{calc} * f_{correction} + y$
Depth	Linear	0.081873139	$Q_{adjust} = Q_{calc} + Z_{weir} * f_{correction}$
	Squared Linear	0.082885389	$Q_{adjust} = Q_{calc} + Z_{weir}^2 * f_{correction}$
	Exponential	0.084972053	$Q_{adjust} = Q_{calc} + Z_{weir}^{f_{correction}}$
	Linear Offset	0.078332884	$Q_{adjust} = Q_{calc} + Z_{weir} * f_{correction} + y$
Control	None	0.084973083	None

Where Q_{adjust} is the corrected value of discharge, Q_{calc} is the discharge value given by equations 7.2A and 7.2B, z_{weir} is the depth of water at the upstream face of the weir, $f_{correction}$ is a empirically fit value of linear correction, and y is an empirically fit scalar adjustment factor. Both y and $f_{correction}$ were obtained by minimizing the root mean square error (RMSE) between measured and calculated flowrates (n=15). Excel's Data Analysis GRG Nonlinear Solver tool was applied for this analysis. Notably, only marginal improvements in RMSE were obtained (<0.007) by any correction method. The "best" corrections (RMSE < 0.83) poorly fit either high or low data points. The depth-based correction, "Linear Offset," yielded the best RMSE, but with a y value of about 0.12 CMS and negative $f_{correction}$ value. This was discarded as not mechanistically sound, theoretically yielding a flow of 0.12 CMS with no water present at the weir; for perspective, this is larger than the season's average discharge (0.11 CMS).

10.4 APPENDIX D – Phosphorus Model Framework:

Thermal Mixing across the Thermocline:

Vertical Mixing [ºC /10min]: $$\frac{dT_h}{dt} = \frac{v_t A_t (T_e - T_h)}{V_h} \quad (1)$$

Where: T_e = Average epilimnetic temperature [ºC] - *Observed*
T_h = Average hypolimnetic temperature [ºC] - *Observed*
A_t = Thermocline area [m^2] - *Measured*
V_h = Hypolimnetic volume [m^3] - *Measured*
V_t = Rate of mixing across thermocline $\left[\frac{m}{10min}\right]$ – *Optimized via simulated annealing*

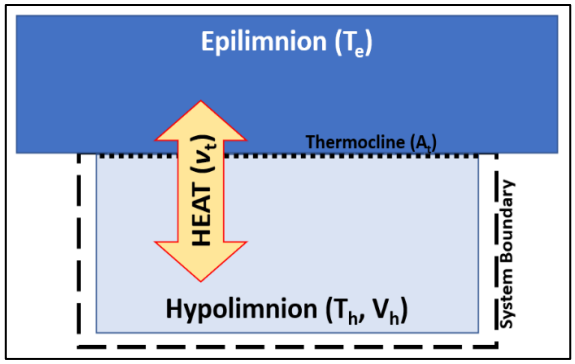

Figure D1: Box model of thermal transfer across the thermocline. A 10-minute heat balance was performed on the hypolimnion calibrated to 7 observed temperature profiles. Constants defined

Phosphorus Mass Balance:

Epilimnion [mg/10min]:

$$\frac{dP_{epi}}{dt} = +External\ Load - D/S\ \ Transport +/- Hypolimnetic\ Diffusion - Settling$$
$$\frac{dP_{epi}}{dt} = \frac{W_{ext} - (Q_{out} * P_{epi} * 1000) + (V_t * A_t * (P_{hyp} - P_{epi}) * 1000) - (v_s * A_t * P_{epi} * 1000)}{V_e} \quad (2)$$

With:

$$W_{ext} = +U/S\ Lake\ Load + Direct\ Watershed\ Load + Atmospheric\ Deposition + Residual\ Load$$
$$W_{ext} = (Q_{out-U/S} * P_{epi-U/S}) + ((Q_{Misery} * \frac{A_{WS}}{A_{Misery}}) * P_{Misery}) + (P_{atm} * SA) + (W_{ant} * Per) \quad (3)$$

Hypolimnion [mg/10min]:

$$\frac{dP_{hyp}}{dt} = +/- Epilimnetic\ Diffusion +/- Internal\ Load\ \&\ Burial + Epilimnetic\ Settling$$
$$\frac{dP_{hyp}}{dt} = \frac{(V_t * A_t * (P_{epi} - P_{hyp}) * 1000) - (v_b * A_t) + (v_s * A_t * P_{epi} * 1000)}{V_h} \quad (4)$$

Where: P_{epi} = Phosphorus Concetration in epilimnion $[\frac{mg}{L}]$ - *Observed*

P_{hyp} = Phosphorus Concetration in hypolimnion $[\frac{mg}{L}]$ - *Observed*

$P_{epi-U/S}$ = Phosphorus Concetration in epilimnion of upstream lake $[\frac{mg}{L}]$ - *Observed*

P_{Misery} = Phosphorus Concetration in Misery River inflow $[\frac{mg}{L}]$ - *Observed*

P_{atm} = Atmopheric depositional phosphorus loading rate $[\frac{mg}{m^2 * 10min}]$ – *Lit. value*

Per = Shoreline length [km] - *Measured*

W_{ant} = Residual shore phosphorus load $[\frac{mg}{km * 10min}]$ – *Optimized simulated annealing*

W_{ext} = Phosphorus load including runoff & depositional sources $[\frac{mg}{10min}]$ -*Calc'd*

Q_{out} = Lake outflow $\left[\frac{m^3}{10min}\right]$ – *Observed / Calculated from Water Budget*

$Q_{out-U/S}$ = Outflow of upstream lake $\left[\frac{m^3}{10min}\right]$; - *zero for Lake Gerald*

Q_{Misery} = Discharge of Misery River at stream gauge $\left[\frac{m^3}{10min}\right]$ - *Observed*

A_{WS} = Watershed area; w/o lake surface & U/S lake watershed $[m^2]$ – *Meas.*

A_{Misery} = Watershed area of Misery River at stream gauge $[m^2]$ - *Measured*

A_t = Thermocline area $[m^2]$ – *assumed approx. equal to hypolimnion lakebed*

V_t = Rate of mixing across thermocline $\left[\frac{m}{10min}\right]$ – *From eq. 1 optimization*

v_s = Net settling & burial rate $[\frac{m}{10min}]$ – *Optimized via simulated annealing*

SA = Surface area of lake $[m^2]$ - *Measured*

v_b = Burial rate $\left[\frac{m}{10min}\right]$ – *Optimized via simulated annealing*

V_e = Epilimnetic volume $[m^3]$ - *Measured*

V_h = Hypolimnetic volume $[m^3]$ - *Measured*

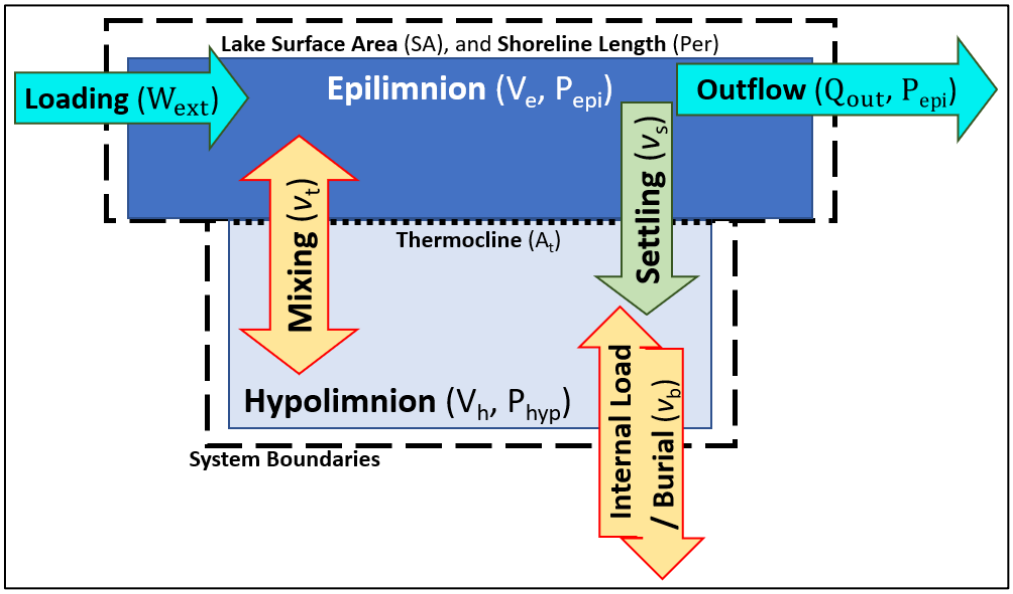

Figure D2: Two box model of phosphorus cycling in Twin Lakes. Separate mass balances were carried out for the epilimnion and hypolimnion.

10.5 APPENDIX E – Model Calibration Iterations & Relationships

Linear relationships arose among model calibration iteration endpoints between the optimized parameters. These relationships are presented graphically here between settling rate (v_s), burial and internal loading rate (v_b), and residual load (W_ant). All values would simultaneously be either on the low end of their optimized range (not their bounding ranges), or on the the high end, or somewhere linearly between those points. The chosen claibration minimized model error.

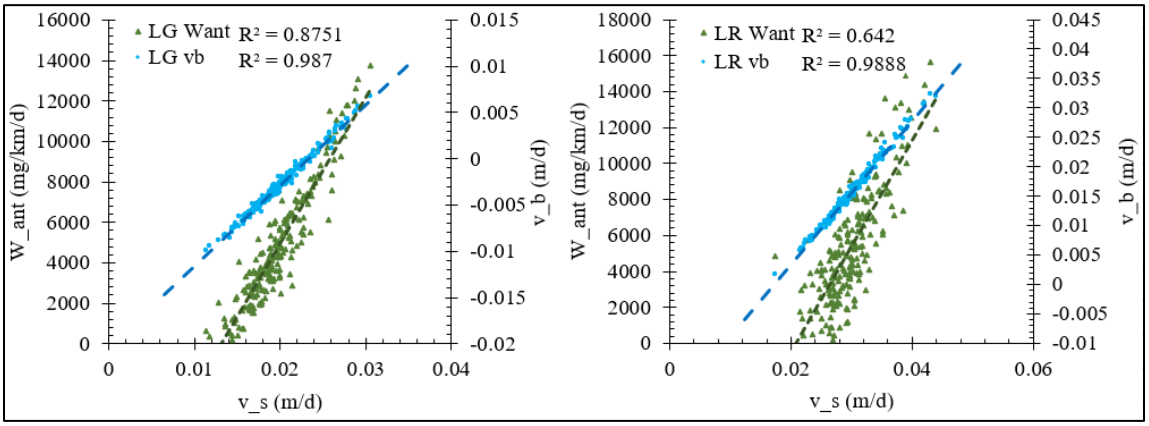

Figure E1: Linear relationships of residual load and sediment flux to optimized settling rate.

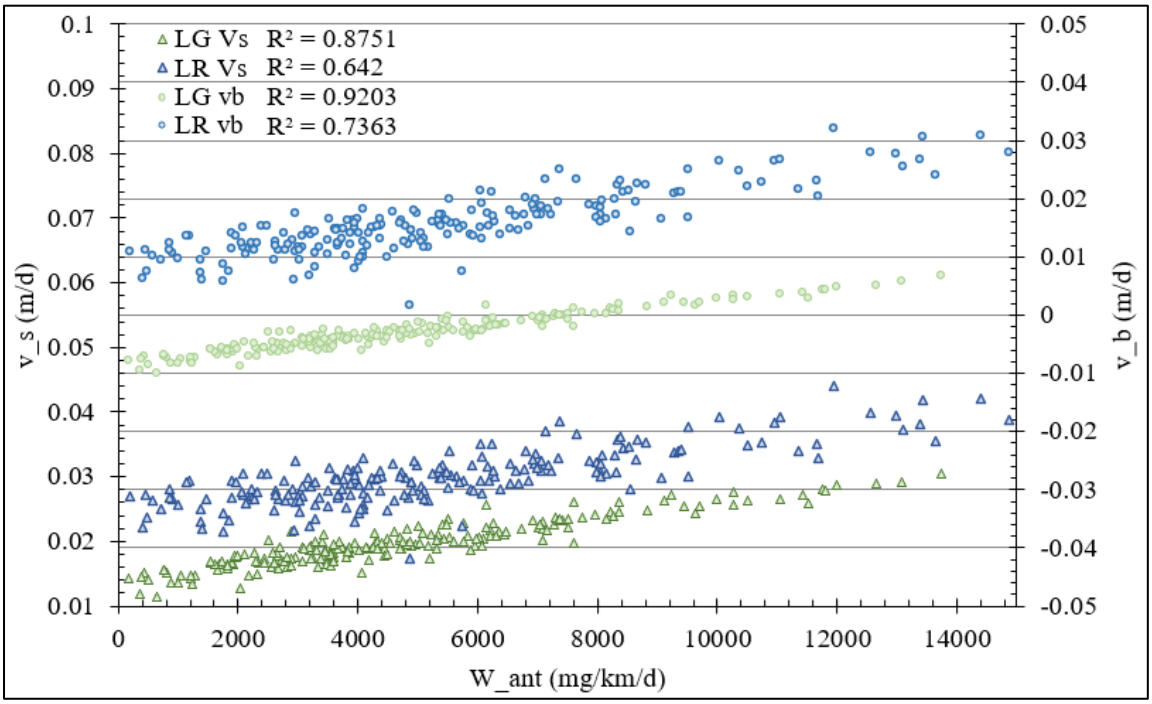

Figure E2: Linear relationships of settling rate and sediment flux to optimized residual load.

10.6 APPENDIX F – Water Quality Profiles

All full profile measurements taken are presented here in greater detail. Additionally included are profile measurements of pH and conductivity not specifically addressed in the main body discussion of profiles.

Table F1: 2022 Twin Lakes temperature profiles (ºC); red corresponds to high temperatures, while green corresponds to low temperatures.

Date:	17-May	7-Jun	6-Jul	18-Jul	2-Aug	23-Aug	27-Sep	4-Oct	19-Oct
Depth (m)	**Lake Gerald**								
0	13.23	17.34	21.03	25.15	22.39	23.24	15.67	15.11	8.99
1	13.10	17.65	20.89	25.08	22.23	23.15	15.69	15.11	9.05
2	12.41	17.33	20.74	23.32	22.02	22.96	15.69	15.11	9.04
3	11.87	16.07	20.65	22.29	21.96	22.47	15.69	15.08	9.05
4	10.92	15.62	20.57	21.64	21.92	22.15	15.69	14.87	9.05
5	8.60	15.04	19.50	20.48	21.40	21.34	15.69	14.77	9.09
6	7.80	12.92	18.59	16.55	18.43	19.54	15.67	14.72	9.09
7	7.10	9.95	12.80	12.33	13.52	14.87	15.66	14.70	9.00
8	6.90	8.20	9.94	10.30	10.98	11.79	15.63	14.43	8.99
9	6.79	7.94	9.27	9.62	10.03	10.56	15.15	14.43	8.97
10	6.72	7.73	9.08	9.38	9.78	10.08	10.50	11.10	8.92
11	6.64	7.66	8.80	9.05	9.50	9.90	10.17	10.70	8.87
~11.5	6.53		8.00	9.04	9.46				
Depth (m)	**Little Lake Gerald**								
0	14.71	18.39	21.68	25.20	22.90	23.23	15.26	14.84	7.84
1	14.26	18.25	21.51	25.17	22.72	23.09	15.30	14.84	7.85
2	12.94	17.16	21.05	23.59	22.48	23.03	15.31	14.50	7.86
3	9.10	16.33	20.78	22.17	22.10	22.48	15.31	14.74	7.89
4	7.52	13.38	19.07	18.65	20.20	21.05	15.32	14.53	7.88
5	6.79	8.49	12.20	13.11	14.18	16.63	15.32	14.41	7.88
6	6.50	7.71	9.91	10.97	12.01	13.55	15.32	14.31	7.89
~6.4	6.43	7.61	9.53	10.52	11.50	13.23	15.33	14.29	8.04
Depth (m)	**Lake Roland**								
0	14.05	18.30	21.78	25.36	22.52	23.10	15.15	14.46	7.90
1	13.87	18.26	21.40	25.22	22.34	23.09	15.17	14.42	7.91
2	13.65	18.13	21.34	23.00	22.22	22.66	15.17	14.35	7.91
3	13.56	16.62	20.85	21.76	21.89	22.10	15.16	14.27	7.91
4	9.50	15.77	20.15	20.36	21.21	21.33	15.15	14.16	7.91
5	8.49	13.07	18.14	17.42	18.57	20.00	15.14	14.09	7.91
6	7.80	10.06	13.23	13.32	14.35	16.00	15.13	14.05	7.91
7	7.43	8.20	9.96	10.07	10.32	11.26	15.13	13.88	7.91
8	7.20	7.77	8.42	8.65	8.73	9.55	13.00	13.74	7.91
9	6.99	7.44	8.11	8.00	8.27	8.65	9.22	11.14	7.90
10	6.84	7.25	7.64	7.69	7.92	8.29	8.46	9.19	7.90
11	6.78	7.15	7.49	7.61	7.80	8.04	8.23	8.32	7.87
~11.75	6.72	7.07	7.53	7.46	7.75	7.93	8.17	8.23	7.86

Table F2: 2022 Twin Lakes dissolved oxygen (DO) profiles (mg O_2/L); red corresponds to low DO values, while blue corresponds to high values.

Date:	17-May	7-Jun	6-Jul	18-Jul	2-Aug	23-Aug	27-Sep	4-Oct	19-Oct
Depth (m)	**Lake Gerald**								
0	10.23	9.19	8.49	8.08	8.16	8.34	8.79	9.64	10.83
1	10.26	9.21	8.52	8.17	8.15	8.36	8.83	9.67	10.78
2	10.29	9.21	8.51	8.50	8.15	8.36	8.84	9.67	10.77
3	10.32	9.25	8.49	8.37	8.11	8.25	8.86	9.64	10.76
4	10.17	9.15	8.46	8.05	8.04	8.06	8.86	9.45	10.76
5	9.90	8.99	7.40	7.09	7.34	7.21	8.86	9.29	10.75
6	9.70	8.39	6.97	4.17	3.70	3.60	8.87	9.24	10.75
7	9.39	7.62	4.30	2.06	0.82	0.38	8.87	9.19	10.75
8	9.29	6.57	2.93	1.31	0.43	0.29	8.87	8.98	10.75
9	9.21	6.20	2.13	0.89	0.35	0.26	8.27	8.41	10.76
10	9.14	5.95	1.91	0.71	0.32	0.24	0.80	0.88	10.77
11	8.74	1.10	0.80	0.27	0.27	0.20	0.40	0.47	10.51
~11.5	1.30		0.46	0.24	0.29				
Depth (m)	**Little Lake Gerald**								
0	9.82	9.45	8.21	7.98	8.07	8.27	8.71	9.75	10.96
1	9.85	9.47	8.23	8.00	8.07	8.29	8.82	9.76	10.94
2	10.02	9.65	8.25	8.16	8.05	8.28	8.84	9.76	10.92
3	9.90	9.40	8.13	8.03	7.92	8.16	8.86	9.71	10.90
4	9.30	8.91	7.18	5.85	5.20	6.35	8.87	9.63	10.89
5	8.39	4.81	2.13	0.76	0.72	0.72	8.87	9.53	10.88
6	6.62	2.45	0.64	0.37	0.46	0.28	8.84	8.92	10.86
~6.4	2.05	0.70	0.37	0.27	0.30	0.22	6.90	1.60	7.00
Depth (m)	**Lake Roland**								
0	9.76	9.28	8.14	8.05	7.79	8.13	8.60	9.83	11.17
1	9.78	9.27	8.14	8.16	7.94	8.13	8.77	9.87	11.16
2	9.78	9.27	8.13	8.17	7.88	8.08	8.81	9.88	11.16
3	9.75	8.90	7.83	6.90	7.40	7.44	8.86	9.84	11.15
4	9.50	8.57	7.02	5.07	6.10	6.50	8.87	9.69	11.15
5	9.38	7.83	5.25	2.58	1.42	4.26	8.87	9.67	11.14
6	9.25	7.17	3.36	1.53	0.42	0.80	8.87	9.69	11.14
7	9.22	6.97	3.52	1.99	0.59	0.43	8.86	9.30	11.13
8	9.19	6.78	3.41	1.69	0.36	0.36	2.72	9.01	11.13
9	9.02	6.44	2.99	0.77	0.30	0.32	1.10	2.84	11.13
10	8.61	6.29	2.02	0.31	0.28	0.30	0.56	0.98	11.13
11	8.25	5.86	0.51	0.26	0.27	0.28	0.43	0.62	11.12
~11.75	0.60	0.60	0.33	0.22	0.22	0.24	0.36	0.50	4.95

Table F3: 2022 Twin Lakes conductivity profiles (µS/cm^2); red corresponds to high conductivity values, while blue corresponds to low values.

Date:	17-May	7-Jun	6-Jul	18-Jul	2-Aug	23-Aug	27-Sep	4-Oct	19-Oct
Depth (m)	**Lake Gerald**								
0	44.20	49.30	54.40	60.70	57.70	59.60	50.60	50.00	42.90
1	44.00	49.30	53.90	60.60	57.60	59.90	50.70	50.10	43.00
2	43.30	49.30	53.80	58.10	57.30	59.20	50.60	50.10	43.00
3	42.70	47.80	53.70	56.70	57.10	58.50	50.60	50.10	43.00
4	42.00	47.40	53.50	55.90	57.10	58.50	50.60	50.00	43.00
5	39.20	46.90	57.90	54.90	56.60	57.00	50.60	49.80	43.00
6	38.50	44.70	55.00	50.70	53.50	55.40	50.60	49.80	43.00
7	37.70	41.30	45.40	45.80	48.20	53.80	50.60	49.80	43.00
8	37.50	39.30	42.60	44.00	46.50	52.40	50.60	49.80	43.00
9	37.40	39.00	42.00	43.80	46.50	52.10	51.30	49.90	42.90
10	37.30	38.80	41.90	43.90	47.00	52.30	61.00	63.50	43.00
11	37.30	40.40	49.50	56.40	49.20	62.20	63.40	67.10	43.00
~11.5	44.50		49.20	58.30	58.20				
Depth (m)	**Little Lake Gerald**								
0	49.20	53.10	56.10	61.80	58.90	60.10	49.80	49.20	40.10
1	48.50	52.90	56.00	61.80	58.70	59.90	49.90	49.10	40.40
2	46.80	51.30	55.30	59.60	58.40	59.80	49.80	49.10	40.40
3	42.90	50.60	55.00	57.70	58.00	59.10	49.80	49.00	40.50
4	41.20	47.40	54.60	54.50	57.00	58.10	49.80	48.80	40.50
5	40.60	43.60	49.40	52.40	55.10	60.40	49.80	48.70	40.50
6	40.50	43.40	49.30	52.70	58.70	70.80	49.80	48.60	40.50
~6.4	40.60	43.90	50.60	72.60	79.10	81.60	52.00	45.00	39.90
Depth (m)	**Lake Roland**								
0	37.20	41.10	44.30	49.40	46.70	48.10	39.80	38.90	32.50
1	37.00	41.10	44.20	49.10	46.60	48.00	39.80	38.90	32.50
2	36.80	40.90	44.20	46.80	46.50	47.50	39.80	38.90	32.50
3	36.80	39.60	43.90	45.90	46.30	47.00	39.80	38.80	32.50
4	32.70	39.00	43.40	44.90	46.10	46.30	39.80	38.70	32.50
5	31.80	36.40	42.30	42.50	44.50	45.20	39.80	38.70	32.50
6	31.10	33.60	37.90	38.40	40.50	46.40	39.80	38.70	32.50
7	30.80	31.80	33.90	35.40	36.60	41.20	39.80	38.50	32.50
8	30.50	31.50	32.70	34.20	36.10	40.60	43.20	38.50	32.50
9	30.30	31.20	32.80	34.40	36.10	42.20	46.30	42.30	32.50
10	30.30	31.00	33.10	35.20	40.10	42.40	47.70	49.50	32.50
11	30.40	31.20	45.90	44.60	41.90	45.10	49.90	52.70	32.40
~11.75	39.70	51.00	47.30	59.60	50.70	54.90	55.80	54.20	36.90

Table F4: 2022 Twin Lakes pH profiles; Green corresponds to more basic pH values, while yellow corresponds to more acidic values.

Date:	17-May	7-Jun	6-Jul	18-Jul	2-Aug	23-Aug	27-Sep	4-Oct	19-Oct
Depth (m)	**Lake Gerald**								
0	7.23	6.69	9.11	8.13	8.52	8.63	7.29	6.39	7.04
1	7.03	6.83	8.60	8.02	8.21	8.52	7.35	6.61	7.07
2	6.95	6.93	8.31	8.14	8.14	8.45	7.27	6.69	7.13
3	6.95	6.94	8.20	8.12	8.05	8.36	7.27	6.73	7.16
4	6.84	6.90	8.11	7.84	7.97	8.16	7.25	6.75	7.19
5	6.65	6.82	7.82	7.44	7.79	7.98	7.25	6.75	7.21
6	6.48	6.70	7.68	7.02	7.45	7.52	7.24	6.75	7.26
7	6.38	6.63	7.70	6.98	7.46	7.16	7.25	6.74	7.33
8	6.37	6.25	7.55	6.91	7.39	7.29	7.22	6.72	7.35
9	6.37	6.14	7.22	6.75	7.25	7.27	6.93	6.63	7.36
10	6.31	6.05	7.04	6.65	7.12	7.21	6.67	6.35	7.36
11	6.25	5.86	6.63	6.66	6.81	7.13	6.78	6.38	7.12
~11.5	6.05		6.76	6.67	6.89				
Depth (m)	**Little Lake Gerald**								
0	7.15	7.41	9.70	7.77	7.79	8.43	7.53	6.63	7.21
1	6.98	7.49	8.77	7.73	7.78	8.32	7.72	6.69	7.24
2	6.84	7.51	8.43	7.79	7.77	8.26	7.39	6.73	7.25
3	6.66	7.41	8.20	7.68	7.76	8.16	7.36	6.76	7.27
4	6.50	7.20	7.91	7.22	7.41	7.62	7.34	6.78	7.27
5	6.38	6.48	7.46	6.65	7.11	7.32	7.32	6.78	7.28
6	6.25	6.24	6.95	6.60	7.00	6.97	7.31	6.71	7.29
~6.4	6.06	6.16	7.12	6.49	6.80	6.95	6.55	5.92	6.87
Depth (m)	**Lake Roland**								
0	6.90	7.21	7.65	7.82	7.54	7.70	7.51	6.87	7.90
1	6.79	7.19	7.63	7.83	7.52	7.73	7.39	6.95	7.85
2	6.70	7.17	7.62	7.81	7.50	7.64	7.39	6.92	7.81
3	6.65	7.02	7.58	7.52	7.42	7.47	7.32	6.93	7.78
4	6.49	6.90	7.44	7.18	7.25	7.31	7.29	6.92	7.74
5	6.25	6.54	7.25	6.96	6.71	6.96	7.25	6.89	7.70
6	6.17	6.34	7.31	6.84	6.71	6.90	7.22	6.86	7.66
7	6.15	6.23	7.23	6.76	6.78	7.18	7.19	6.82	7.64
8	6.14	6.20	7.05	6.66	6.73	7.14	6.47	6.74	7.62
9	6.11	6.14	6.90	6.55	6.68	6.98	6.56	6.14	7.59
10	6.08	6.12	6.79	6.44	6.63	6.91	6.67	6.32	7.57
11	6.03	6.09	6.73	6.37	6.62	6.86	6.70	6.44	7.56
~11.75	5.85	6.09	6.77	6.37	6.55	6.82	6.67	6.42	6.72

10.7 APPENDIX G – Statistical Comparison of Shoreline Survey Sites

Comparison of statistical difference between subsets of shoreline survey data was carried out using upper and lower 95% confidence intervals (CIs). A normal distribution of the data is assumed for the confidence intervals presented here. A student's t-test for 95% CIs and a log-normal distribution for 95% CIs were also considered and yielded identical results with regard to distinctness of subsets of data, so those CIs are not presented. Bolded CIs indicate statistical difference between the intervals. Lake abbreviations are Lake Gerald (LG) and Lake Roland (LR).

Table G1: Statistical comparison of site subsets for OBA:DOC ratio (RFU / mg/L)

Subset of Sites	count	mean	median	min	max	standard deviation	Lower 95% CI	Upper 95% CI
All Sites	60	409.9	407.0	295.2	708.6	76.8	390.4	429.3
Developed Sites	34	403.4	408.7	296.9	498.3	56.6	384.3	422.4
Undeveloped Sites	26	418.4	405.4	317.2	708.6	97.6	380.9	455.9
LG Developed	14	356.1	346.3	296.9	444.0	42.7	333.7	378.4
LG Undeveloped	15	400.0	364.7	317.2	708.6	114.4	342.1	457.9
LR Developed	18	445.2	449.3	398.3	498.3	29.7	431.5	459.0
LR Undeveloped	11	440.9	423.8	396.9	626.5	65.7	402.1	479.8
All LG Sites	29	378.8	352.2	296.9	708.6	88.8	**346.5**	**411.1**
All LR Sites	29	443.6	428.2	396.9	626.5	45.6	**427.0**	**460.2**

Table G2: Statistical comparison of site subsets for dissolved nitrogen (mg/L)

Subset of Sites	count	mean	median	min	max	standard deviation	Lower 95% CI	Upper 95% CI
All Sites	57	0.305	0.262	0.182	0.588	0.102	0.279	0.332
Developed Sites	34	0.305	0.265	0.198	0.588	0.107	0.270	0.341
Undeveloped Sites	26	0.290	0.260	0.182	0.458	0.078	0.260	0.320
LG Developed	15	0.308	0.274	0.203	0.588	0.106	0.254	0.362
LG Undeveloped	15	0.277	0.257	0.199	0.430	0.068	0.243	0.311
LR Developed	18	0.324	0.265	0.198	0.588	0.129	0.265	0.384
LR Undeveloped	11	0.308	0.277	0.182	0.458	0.092	0.254	0.362
All LG Sites	30	0.293	0.258	0.199	0.588	0.089	0.261	0.324
All LR Sites	29	0.318	0.268	0.182	0.588	0.115	0.276	0.360

Table G3: Statistical comparison of site subsets for dissolved organic carbon (mg/L)

Subset of Sites	count	mean	median	min	max	standard deviation	Lower 95% CI	Upper 95% CI
All Sites	58	6.38	5.58	4.15	24.89	3.84	5.39	7.37
Developed Sites	34	6.95	5.86	4.19	24.89	4.83	5.33	8.57
Undeveloped Sites	26	5.51	4.98	4.15	10.45	1.36	4.99	6.04
LG Developed	14	4.66	4.56	4.19	5.32	0.30	4.50	4.81
LG Undeveloped	15	5.17	4.56	4.35	10.45	1.63	4.35	6.00
LR Developed	18	8.99	6.48	5.83	24.89	5.98	6.23	11.75
LR Undeveloped	11	5.95	6.17	4.15	6.75	0.70	5.53	6.36
All LG Sites	29	4.92	4.56	4.19	10.45	1.20	**4.49**	**5.36**
All LR Sites	29	7.84	6.41	4.15	24.89	4.91	**6.05**	**9.63**

Table G4: Statistical comparison of site subsets for conductivity (µS/cm^2)

Subset of Sites	count	mean	median	min	max	standard deviation	Lower 95% CI	Upper 95% CI
All Sites	60	50.3	50.0	14.8	108.4	12.2	47.2	53.4
Developed Sites	34	47.8	48.4	14.8	67.0	10.7	44.2	51.4
Undeveloped Sites	26	53.5	50.4	40.7	108.4	13.5	48.3	58.7
LG Developed	14	55.3	56.2	49.9	63.2	3.6	53.4	57.2
LG Undeveloped	15	60.0	56.2	49.6	108.4	15.5	52.2	67.8
LR Developed	18	41.2	42.3	14.8	67.0	10.6	36.3	46.1
LR Undeveloped	11	45.8	46.4	40.7	53.9	3.8	43.5	48.1
All LG Sites	30	57.5	56.2	49.6	108.4	10.9	**53.6**	**61.4**
All LR Sites	30	43.0	43.6	14.8	67.0	8.7	**39.9**	**46.1**

10.8 APPENDIX H – OBA Normalization to DOC

Variations upon the referenced OBA:DOC ratio methodology for fluorescence signal correction and identification of OBAs were attempted. Performance of various methods was assessed with remaining correlation of the corrected value to DOC levels site by site. Correlation was assessed in MS Excel with Pearson's correlation coefficients (CORREL function). The critical correlation coefficient above which a correlation was deemed significant was 0.2542 (see section 8.2.2) All corrections were deemed still significantly correlated to DOC, with the exception of the bolded correlation coefficient in Table G1; this methodology is discussed at greater length in section 8.2.2.

Table H1: Considered methods of OBA signal correction for DOC fluorescence interference.

Normalization Method	**Correlation Coefficient**
DOC : OBA (i.e. none)	0.9648
logDOC : logOBA	0.9478
logDOC : OBA	0.9719
1/DOC : OBA	-0.8993
sqrt(DOC) : OBA	0.9777
logDOC : logOBA	0.9478
DOC : OBA/sqrtDOC	0.8372
DOC : OBA/DOC	0.3256
DOC : OBA/DOC^1.178	**-2.43E-08**
DOC : OBA/DOC2	-0.7419
DOC : OBA/logDOC	0.8822
DOC : logOBA/logDOC	-0.8862

10.9 APPENDIX I – Landcover breakdown by NLCD

Landcover data for Twin Lakes watershed is shown here, as classified in the NLCD (NLCD, 2016). No simplification of groupings for practical viewing is included. Tributaries #1-5 correspond to the watersheds areas 173 ha, 1104 ha, 238 ha, 320 ha, & 81 ha respectively as shown in figure 5-8.

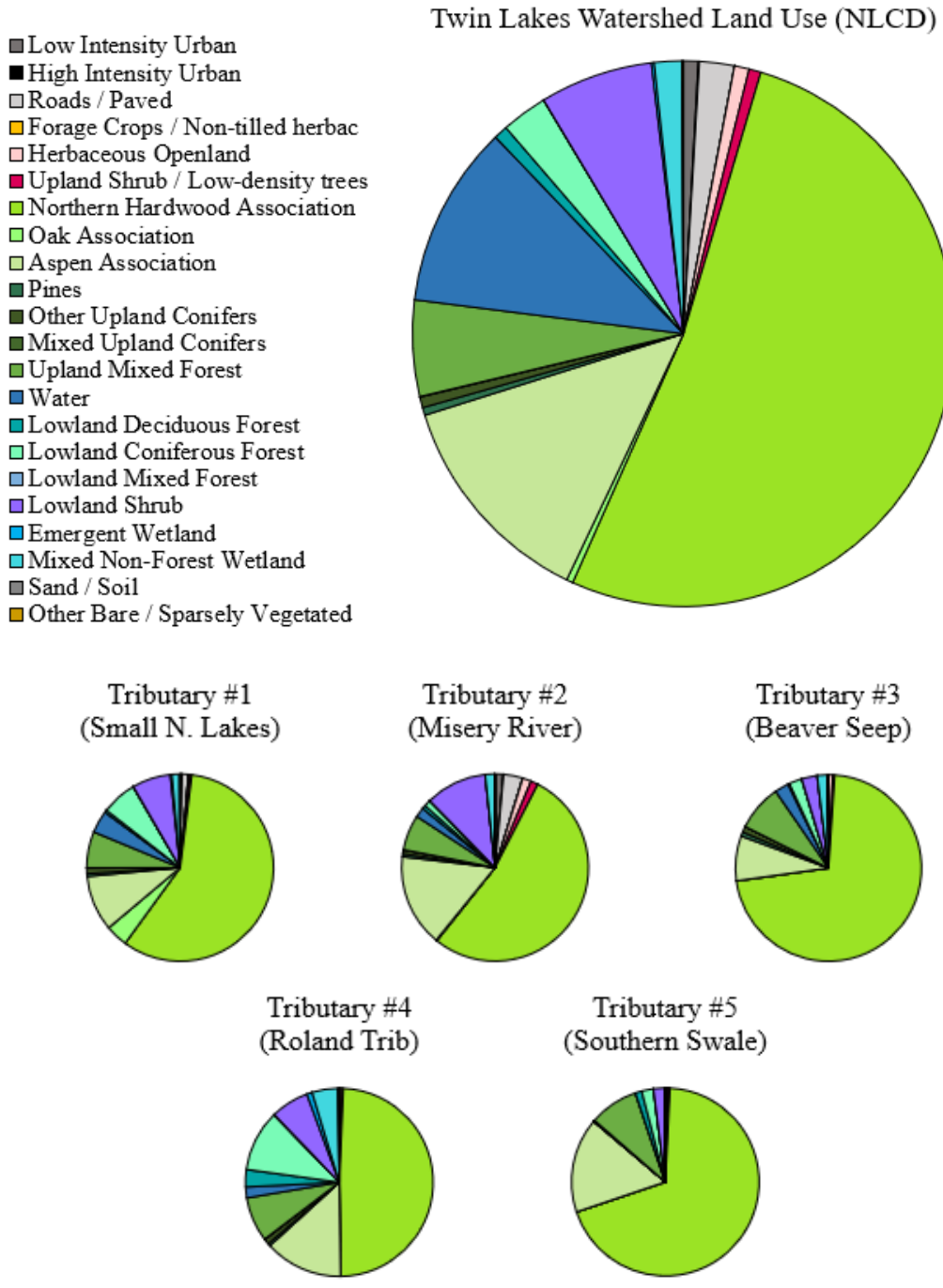

10.10 APPENDIX J – Graphical Presentation of Twin Lakes Nutrient Budget

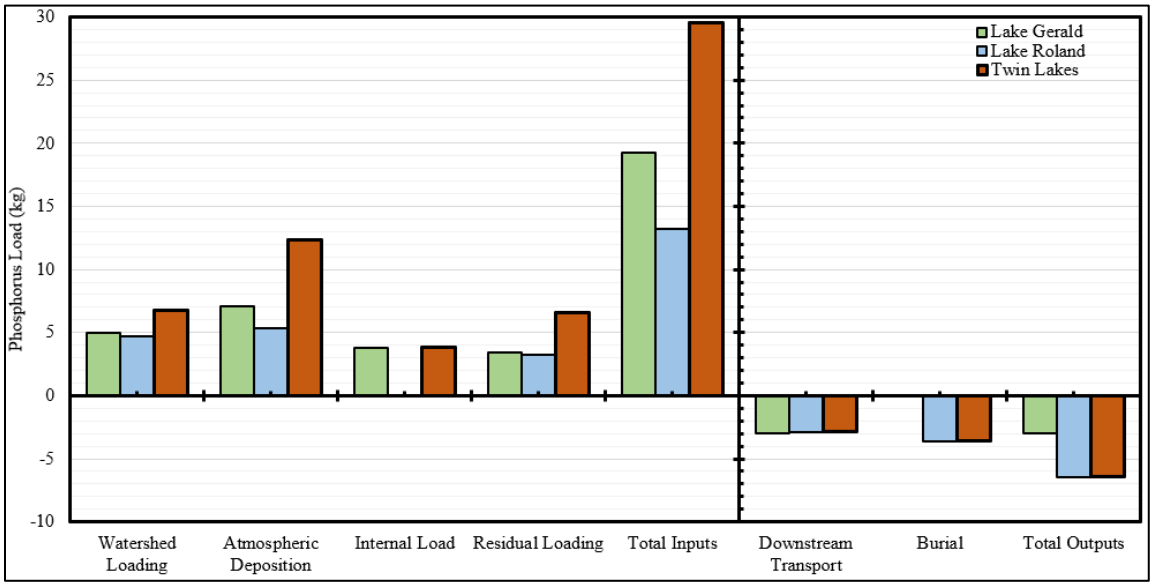

Figure J1: Twin Lakes 2022 stratified period nutrient budget shown by each lake broken up by component processes.

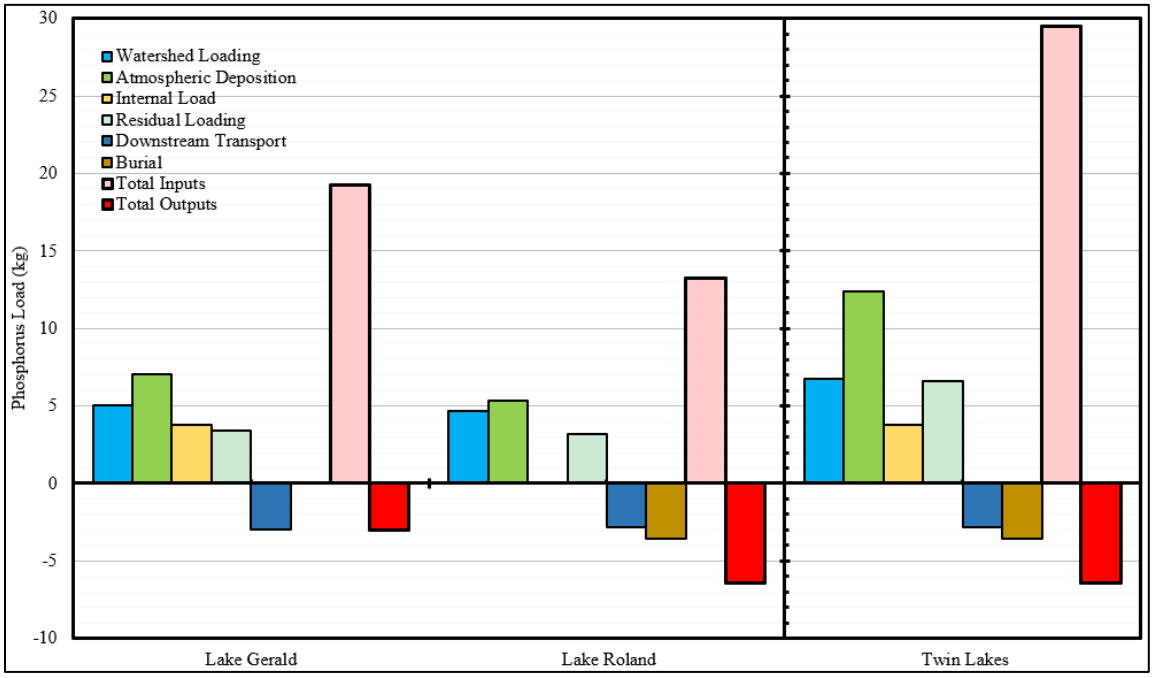

Figure J2: Twin Lakes 2022 stratified period nutrient budget shown by each component process broken up by each lake.